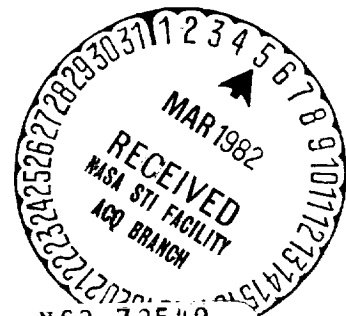REPORT

ON

A STUDY OF THE

HEAT TRANSFER CHARACTERISTICS

OF A PCM THERMAL CAPACITOR

Reporting Period

October 1971 - October, 1972

NASA-AD-S GRANT

MSFC - Monitor
Mr. W. R. Humphries
S&E - ASTN - PLA

Edwin I. Griggs
Department of Mechanical Engineering
Tennessee Technological University
Cookeville, Tennessee 38501

*Pages 35 & 69 are missing*

# TABLE OF CONTENTS

## I.  INTRODUCTION

This report describes a continuing investigation of the heat transfer
characteristics of a PCM thermal capacitor undertaken by the author at
Tennessee Technological University.  The work reported herein is for the
time period from October, 1971 to October, 1972.  There was, however,
no active involvement at the University during the summer months of June
through August since the author returned to Marshall Space Flight Center
to participate in the 1972 NASA/ASEE Summer Faculty Fellowship Program.
The possibility for such participation was recognized at the beginning of
the overall study by the author and the MSFC monitor, and they mutually
agreed upon appropriate scheduling of the work and its objectives to
accommodate the author's involvement in the NASA/ASEE program.

The goals of an overall thermal capacitor study were recognized at the
outset to encompass a multitude of problems.  It was reasoned that
certain of these were capable of resolution without extensive work while
others could be dealt with properly only by an in-depth experimental or
analytical program or even both in some cases.  Consequently, a meeting
was held at Tennessee Tech in November, 1971, by the author and the MSFC
monitor for the purpose of defining objectives and establishing priorities
for this work.  A subsequent meeting was held at MSFC in March, 1972, which
was attended by several others including Dr. Golden from the Colorado
School of Mines who was also doing research on PCM technology under
contract to Space Sciences Laboratory at MSFC.  At this latter meeting,
the status of this work was discussed and the objectives were reevaluated.
A status report covering the effort through the time of this latter

meeting was submitted in April, 1972.

Generally stated, the objectives of the overall program were to conduct some fundamental tests involving a PCM and to explore a numerical scheme for predicting the thermal behavior within a single cell typical of one found in a finned PCM capacitor. As an outgrowth of the meetings mentioned above, some specific tasks that were identified to be pursued by the author under the auspices of the AD-S grant included:

1. independent evaluation of a portion of some in-house test data in order to corroborate in-house conclusions,

2. performance of some basic tests aimed at examination of the effects of cell geometry and cell wall material on the transient temperatures occurring during phase change within a paraffin filled enclosure,

3. consideration of apparent changes in the fusion temperature,

4. examination of the influence of heating rate on interfacial temperature levels,                    '

5. documentation of computer runs made of the single cell model for pure conduction and those made with convective effects included,

6. description and explanation of the computer program used to numerically study a single PCM cell and to further consider its modification relative to the following:

   (a) investigation of methods of changing the effective area at the interface to obtain agreement between data and numerical predictions for freeze tests,

   (b) modification of the single cell model so that it is compatible with using only one vertical column of nodes,

   (c) further consideration of methods of incorporating convective coefficients in the single cell model,

It was believed that task 2 should yield data that would provide considerable insight into tasks 3 and 4. In addition to the aforementioned tasks,

some attention was also devoted to an examination of the influence of metallic fillers on the performance of a total capacitor unit. Some comparable tests using no filler, aluminum fins, and aluminum honeycomb were conducted. Numerical study was limited to the cases with an without fins.

Tasks 1, 3, 4, 5 and major parts of 2 and 6 were completed in the first half of this work, and the results were reported in a status report submitted in April, 1972. Since that time, completion of task 2, a continuing effort on task 6, and the additional study on the influence of fillers on a complete unit have constituted the work. However, since this report covers the total effort, some of the results reported in the earlier status report are also included here for completeness.

In both aspects of the overall study, the phase change material which was studied was nonadecane ($C_{19}H_{40}$). This was utilized in the experimental tests because of its availability and the fact that the fusion temperature is above normal room temperature. The properties, which were incorporated in the numerical studies, are listed in Appendix A.

Part II of this report pertains to several basic experiments and the relationship of the results to tasks 2, 3, and 4. Part III outlines the experimental tests relative to the influence of filler materials on a total unit. The numerical study, as outlined by task 6, is described in Part IV and some representative results are presented. Finally, some conclusions and recommendations are listed in Part V.

## II. SOME BASIC SINGLE CELL EXPERIMENTS

During the course of this investigation, a number of basic experiments were conducted on several types of paraffin-filled enclosures. These were undertaken to study certain aspects of the thermal behavior of the PCM during phase change in support of tasks 2, 3, and 4 as outlined in the introduction. These basic experiments were performed with two primary objectives in mind. First, it was desired to compare the responses of a thermocouple embedded in the PCM during melting and solidification for cases of different enclosure material and geometry. The second objective was to examine the influence of these factors on the melting rate. In all tests, an effort was made to suddenly change the temperature of the surface of the enclosure and maintain it constant thereafter. Two different techniques were tried, and these are discussed below.

Cylindrical Cells Having Different Wall Conductivities:

For the objective concerning the influence of wall material, two cylindrical cells were constructed with the same inside dimensions. One was constructed using copper and the other using plexiglass. The copper cell is depicted in Figure 1 and the plexiglass cell is shown in Figure 2. A structure was constructed upon which each cell could be mounted. The supporting structure is also shown in Figure 2 with the plexiglass cell shown in position. Five one-half inch diameter aluminum rods having a length of 5.50 inches were attached to an aluminum plate. The cells were mounted on top of the aluminum plate. A copper-constantan thermo-
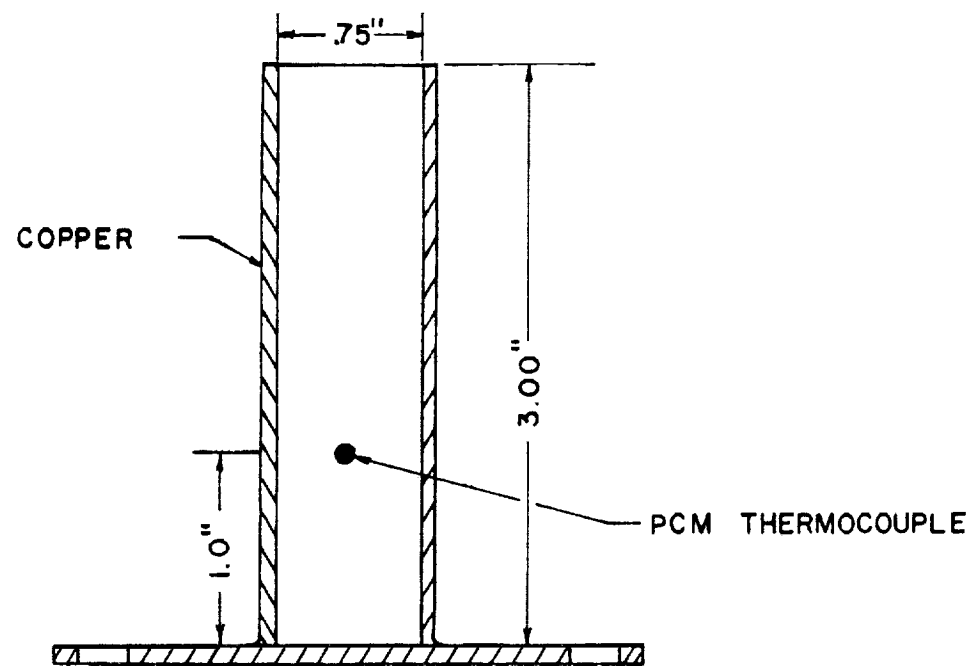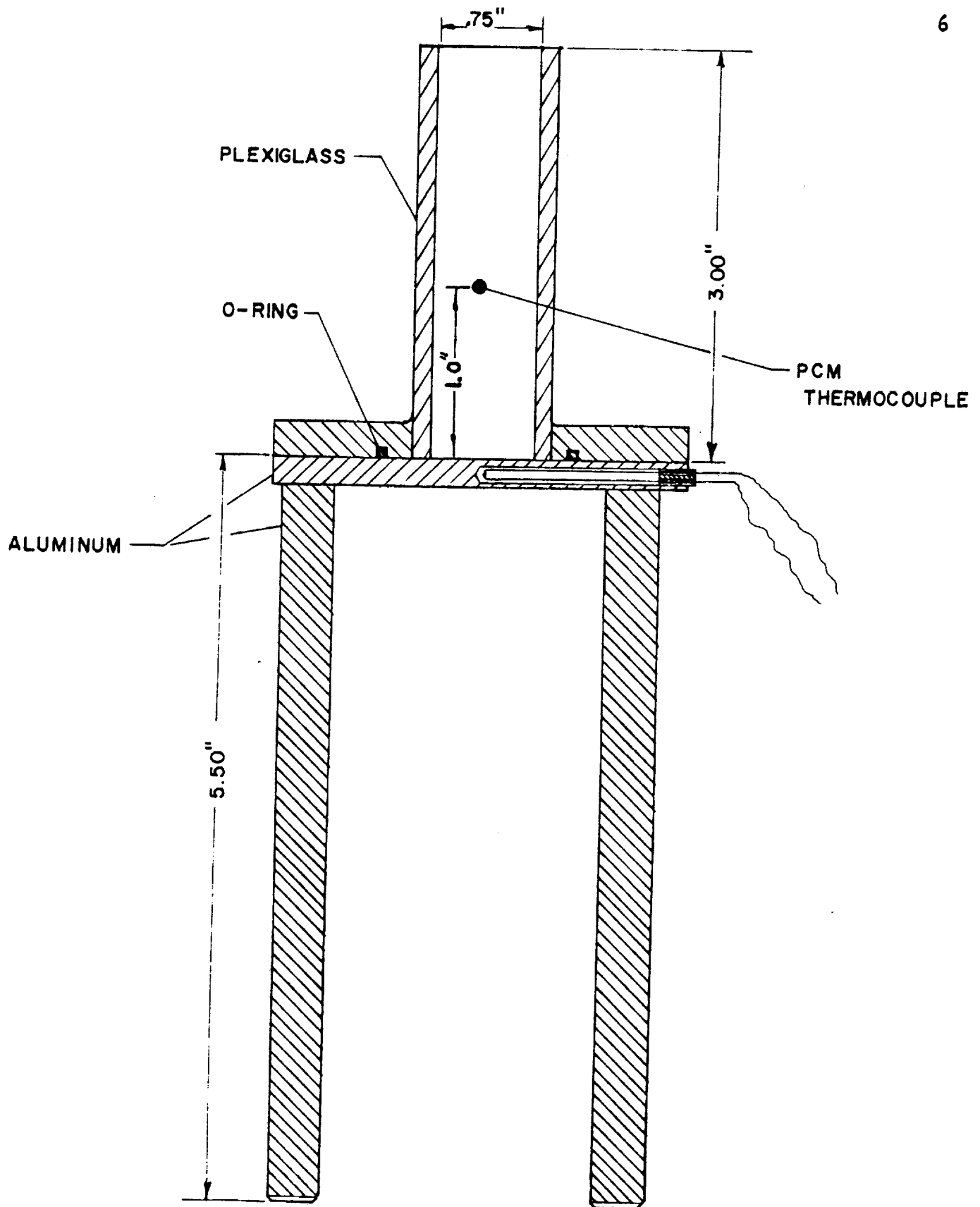
Figure 1. Copper Cell

Figure 2. Plexiglass Cell and Supporting Structure

couple was located in the center of the aluminum plate to provide a temperature measurement of the bottom surface. In each case, a copper-constantan thermocouple (0.005 inch diameter wire) was located in the PCM along the centerline of the cell at a height of 1 inch above the bottom surface. The cells were filled with nonadecane. Heating was achieved by inserting the supporting structure into a water bath which was maintained at constant temperature by a thermostatically controlled electric heater. For solidification runs, the structure was immersed in a bath of cold water.

Several melting and solidification runs were conducted with the arrangements described above. Some representative temperature responses for melting are shown in Figures 3 through 5. In each of these figures, the curves are grouped in pairs by the type of marking used. For each pair, the high-temperature curve corresponds to the bottom plate temperature while its counterpart corresponds to the temperature indicated by the thermocouple located in the PCM. The curves are faired tracings of the recorded thermocouple output in millivolts. Consequently, the vertical scale is not precisely linear in temperature. After the PCM thermocouple had become totally exposed to liquid in the melting tests, its output exhibited a relatively high frequency variation, a feature not revealed by the faired tracings in the figures. This variation is indicative of the convective currents in the liquid. Figure 3 shows results for the plexiglass cell for two different bottom plate temperatures. Figure 4 shows three pairs of results obtained using the plexiglass cell for cases having approximately the same base temperature. The curves identified by dark circles corresponds to a case where the cell was
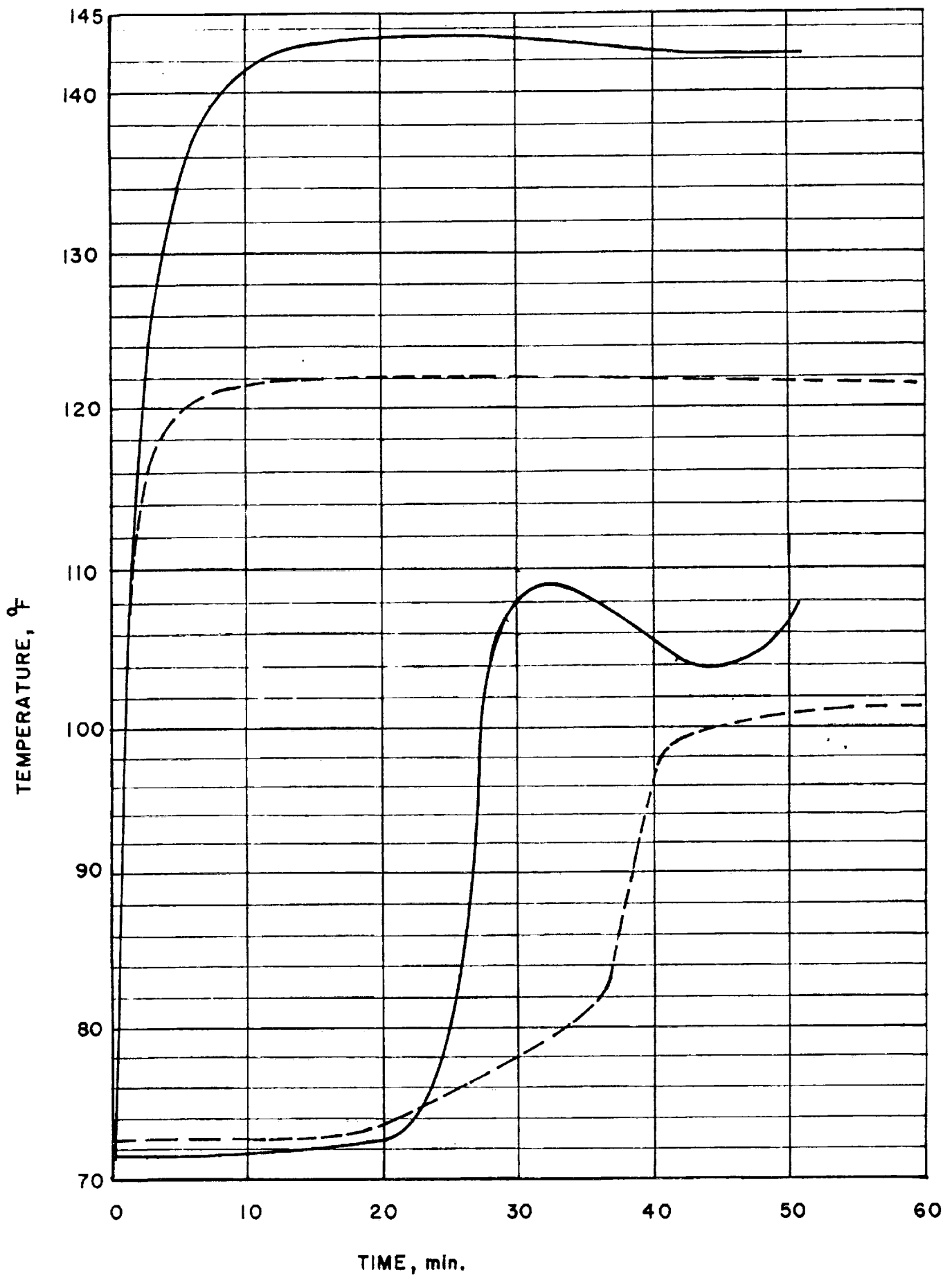
Figure 3. Transient Temperature Response for Plexiglass Cell with Two Different Base Plate Temperatures.
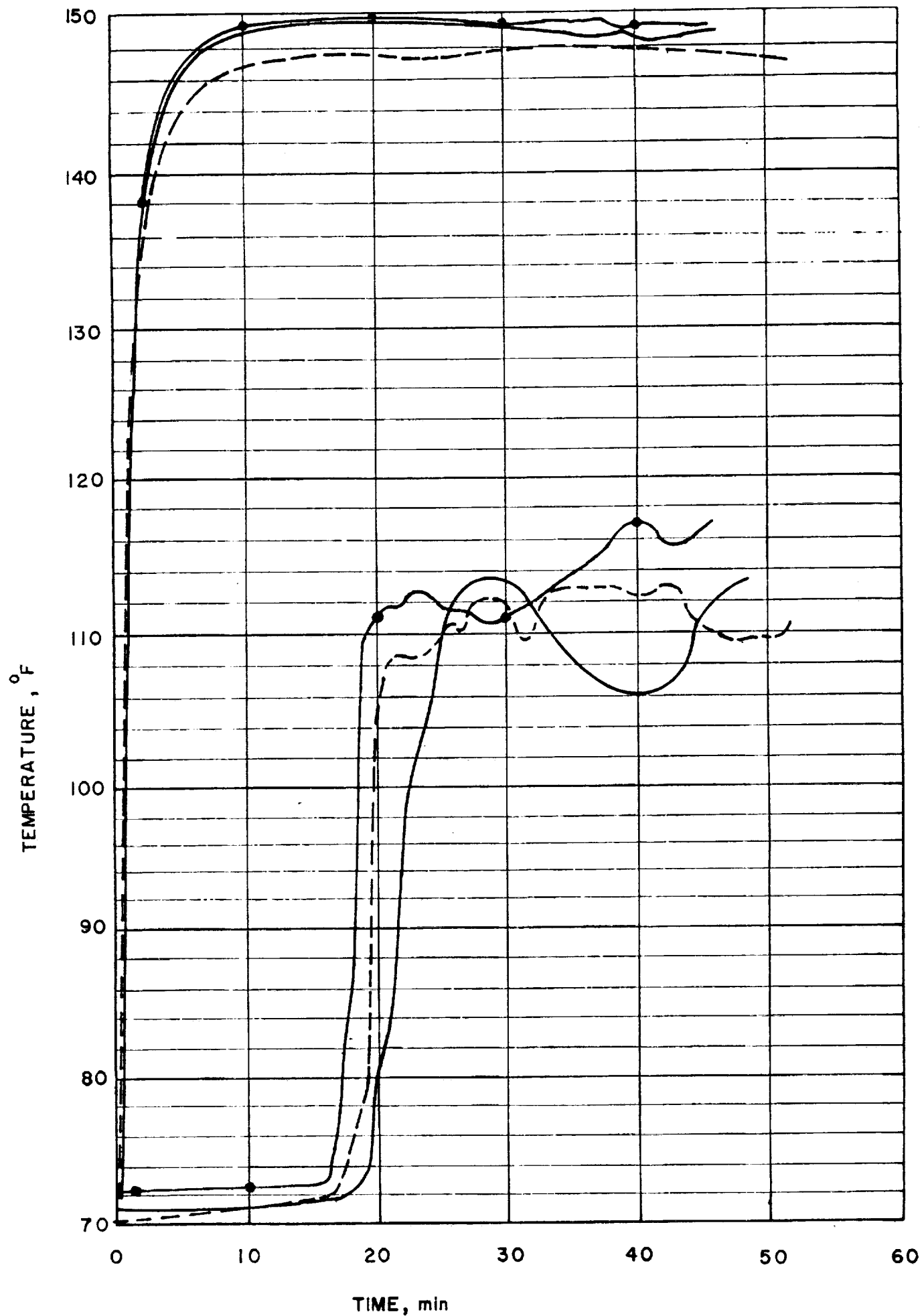
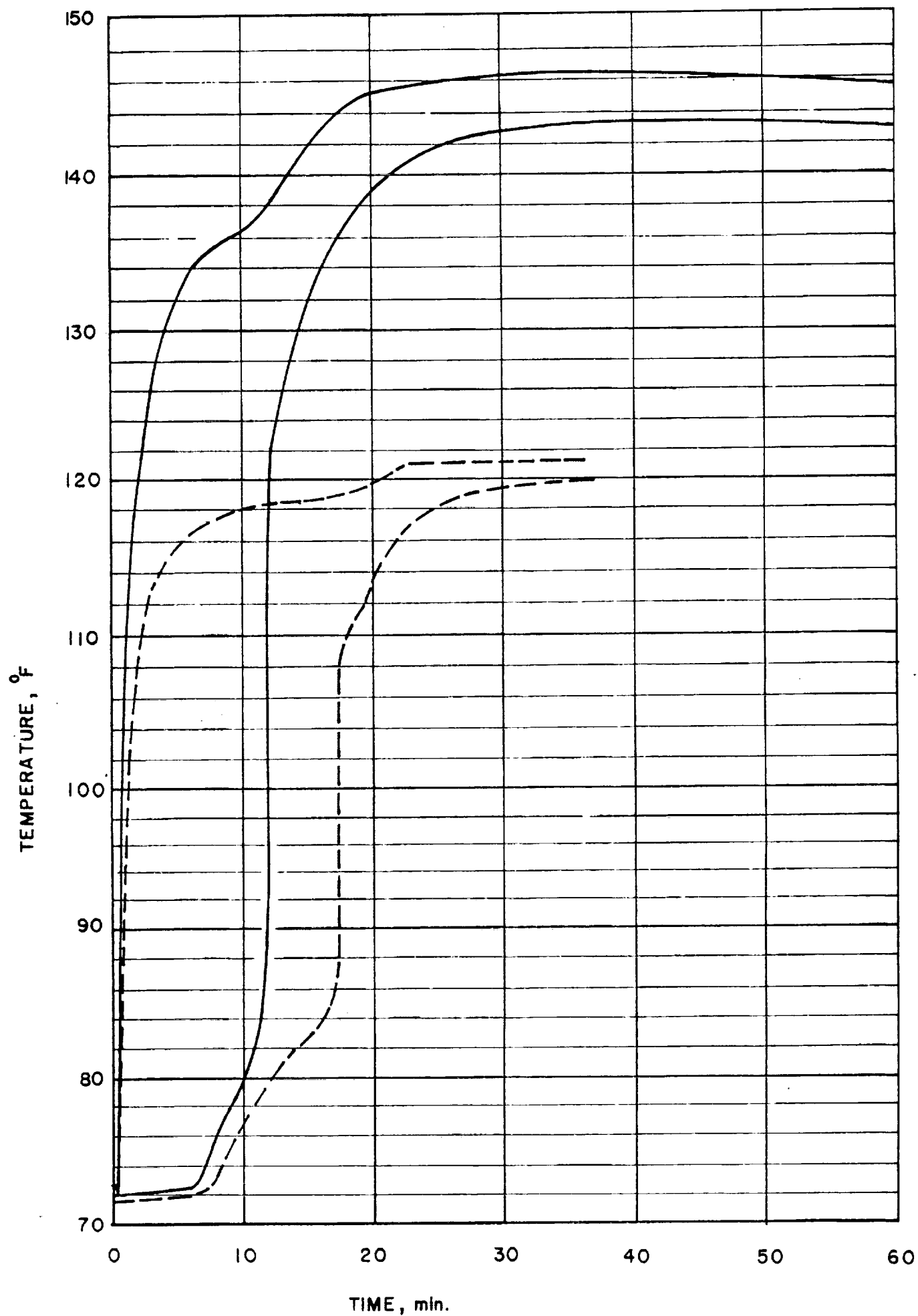Figure 4. Transient Temperature Responses for Plexiglass Cell.

Figure 5.   Transient Temperature Response for Copper Cell.

insulated around its periphery while the other two correspond to cases
where the outside of the cell was left exposed to room air. In all cases
involving the plexiglass cell, the temperature indicated by the PCM
thermocouple, as the interface passed it, was approximately 88°F. The
word approximately is used here since visible recognition that the interface
was exactly at the thermocouple was questionable in some cases. In some
tests gas bubbles collected at the interface which tended to interfere
with the visibility needed in determining exactly when the interface
reached the thermocouple bead. However, no significant variation of the
temperature at the time the PCM thermocouple was near the interface was
detected. Two pairs of results for the copper cell are shown in Figure 5
corresponding to two different base temperatures. There is a notable
difference in the PCM thermocouple response for these cases than those
corresponding to the plexiglass cell for the same base temperature. The
temperature level at which the PCM thermocouple output began to rise
rapidly was at about 88°F. In the copper cell cases, visible observation
of the interface was not possible.

Several solidification runs were made also using the two cells
described above. In each case the results were similar. The PCM thermo-
couple indication dropped from its initial value to 88°F and remained at
that level for a relatively long period of time. This plateau occurred
consistently with the copper cell and with the plexiglass cell for different
base temperatures. In comparing runs with different base temperatures,
a couple of runs when the base plate was at its lowest temperature (i.e.,
the supporting structure was immersed in an ice bath) showed this plateau
level to be slightly lower than the other cases. However, within the
accuracies of the measurements, it is not considered that a significant

point can be made about this trait at this time. No visible detection

of interfacial position during solidification runs was possible even with

the plexiglass because early solidification on the walls blurred visibility.

Plexiglass Cells with Different Geometry:

For the objective relative to the influence of enclosure geometry, four

plexiglass cells were constructed and mounted on a copper base plate. The

inside height of all cells was 2.5 inches. Two were cylindrical with

inside diameters of 0.75 and 1.50 inches, respectively. The other two

were square in cross section with inside dimensions of 0.75 and 1.50 inches,

respectively. The copper base plate was 5 inches square and 1/8 inch

thick. The cells were insulated around their periphery except for a

narrow slot which was provided through the insulation to facilitate

visual observation of interfacial position. The base plate was electrically

heated. Power to the heater was controlled by a Honeywell Electr-O-Volt

control unit which served to maintain the base plate temperature constant

throughout the test except for an initial transient at the beginning of

a run. The position of the interface was observed with the aid of a

Gaertner cathetometer. The procedure required setting the cathetometer

at a certain level and then recording the time when the interface reached

that level. Results of interfacial position versus time for all four cells

for the cases of two different base plate temperatures are shown in

Figures 6 through 13. In each of these figures a solid curve is shown

for comparison purposes. These solid curves were plotted from predictions

obtained by using the steady state convective correlations of O'Toole and

Silveston (1). (See Part V of this report for a discussion of these

predictions.) In plotting these, the assumption was made that all heat

Figure 6.  Liquid Depth versus Time for 0.75 inch Square with Base Plate
at 130°F.

Figure 7. Liquid Depth versus Time for 1.50 inch Square with Base Plate
at 130°F.

Figure 8. Liquid Depth versus Time for 0.75 inch Cylinder with Base Plate at 130°F.

Figure 9.  Liquid Depth versus Time for 1.50 inch Cylinder with Base Plate at 130°F.
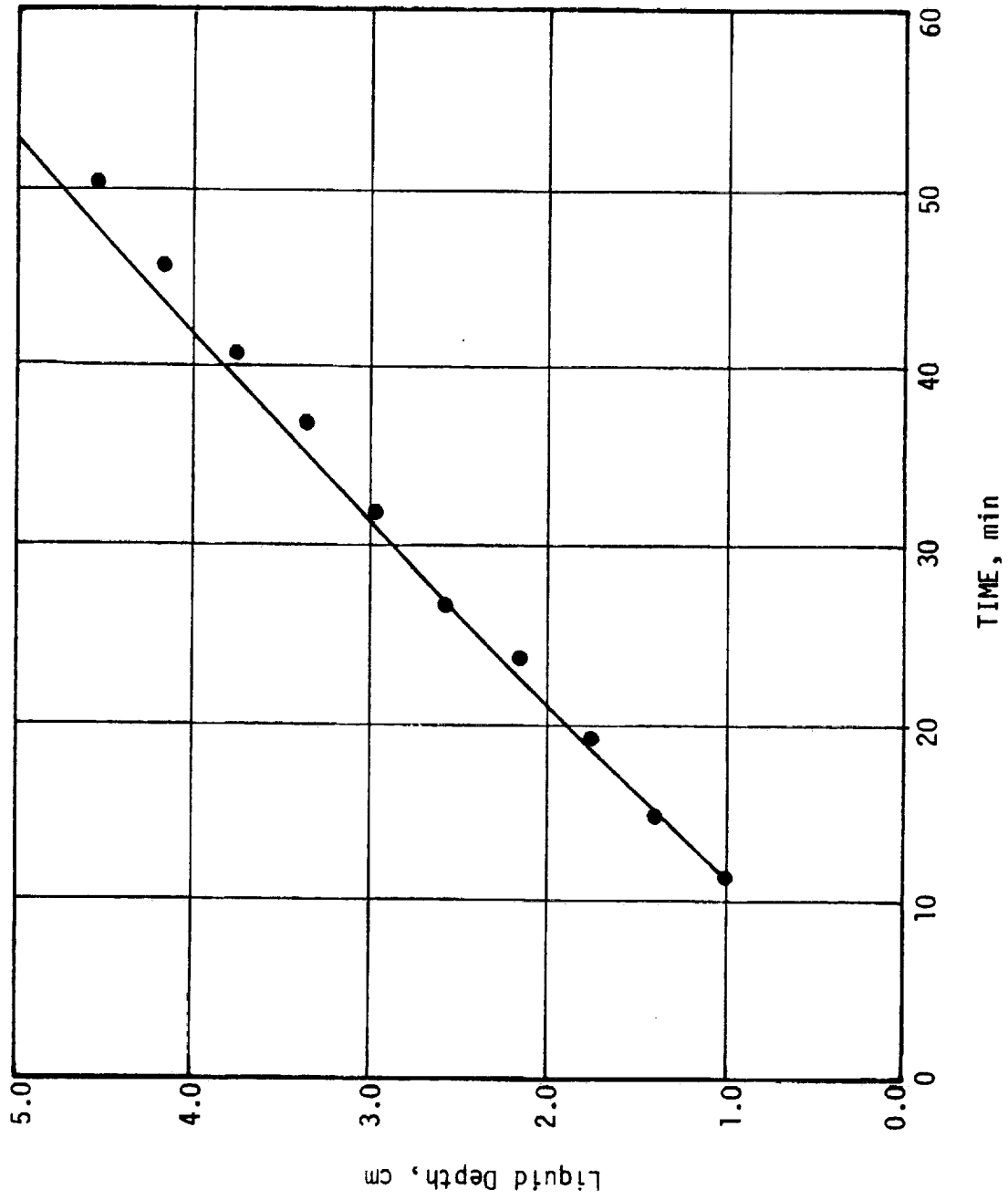
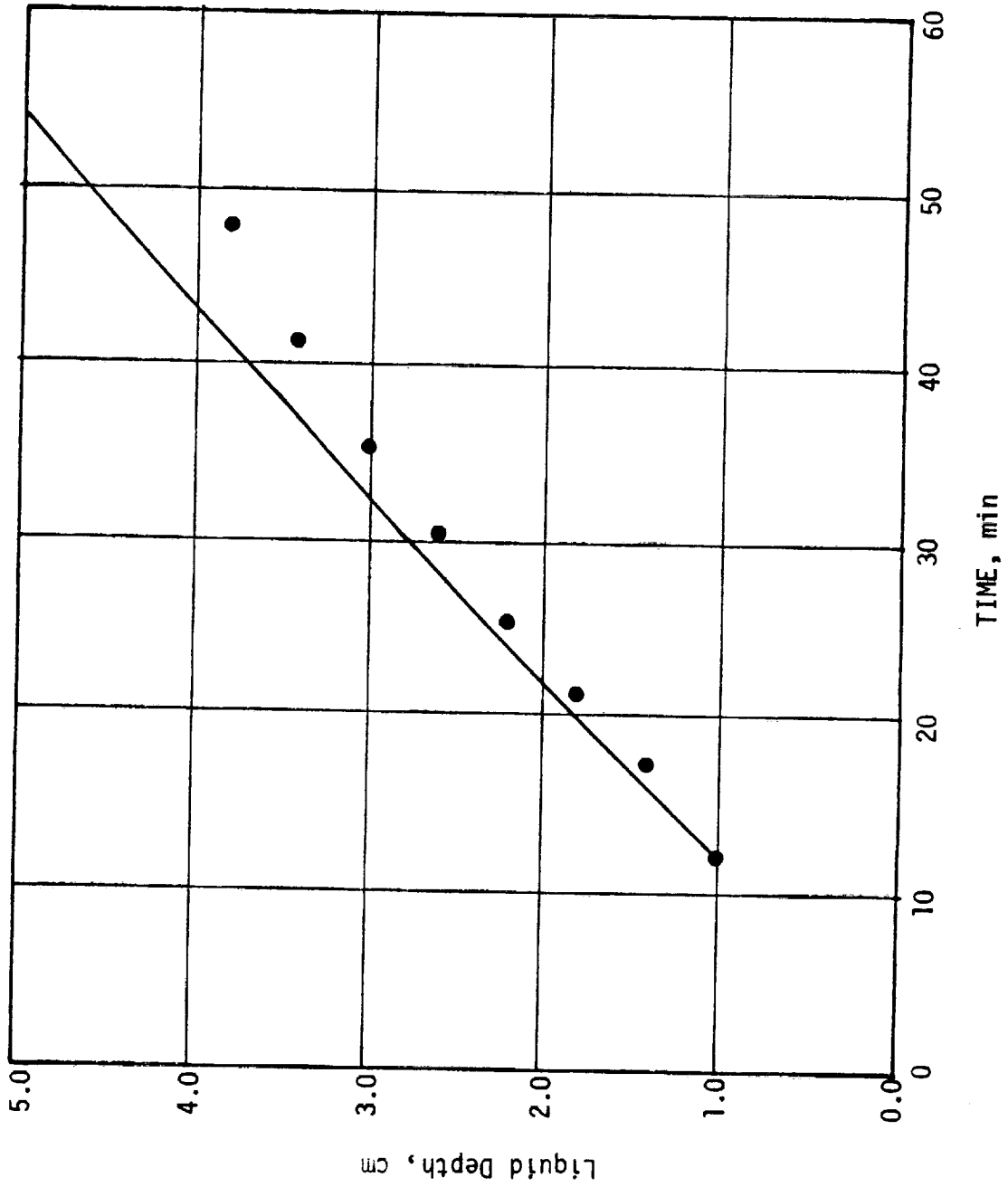Figure 10. Liquid Depth versus Time for 0.75 inch Square with Base Plate at 150°F.

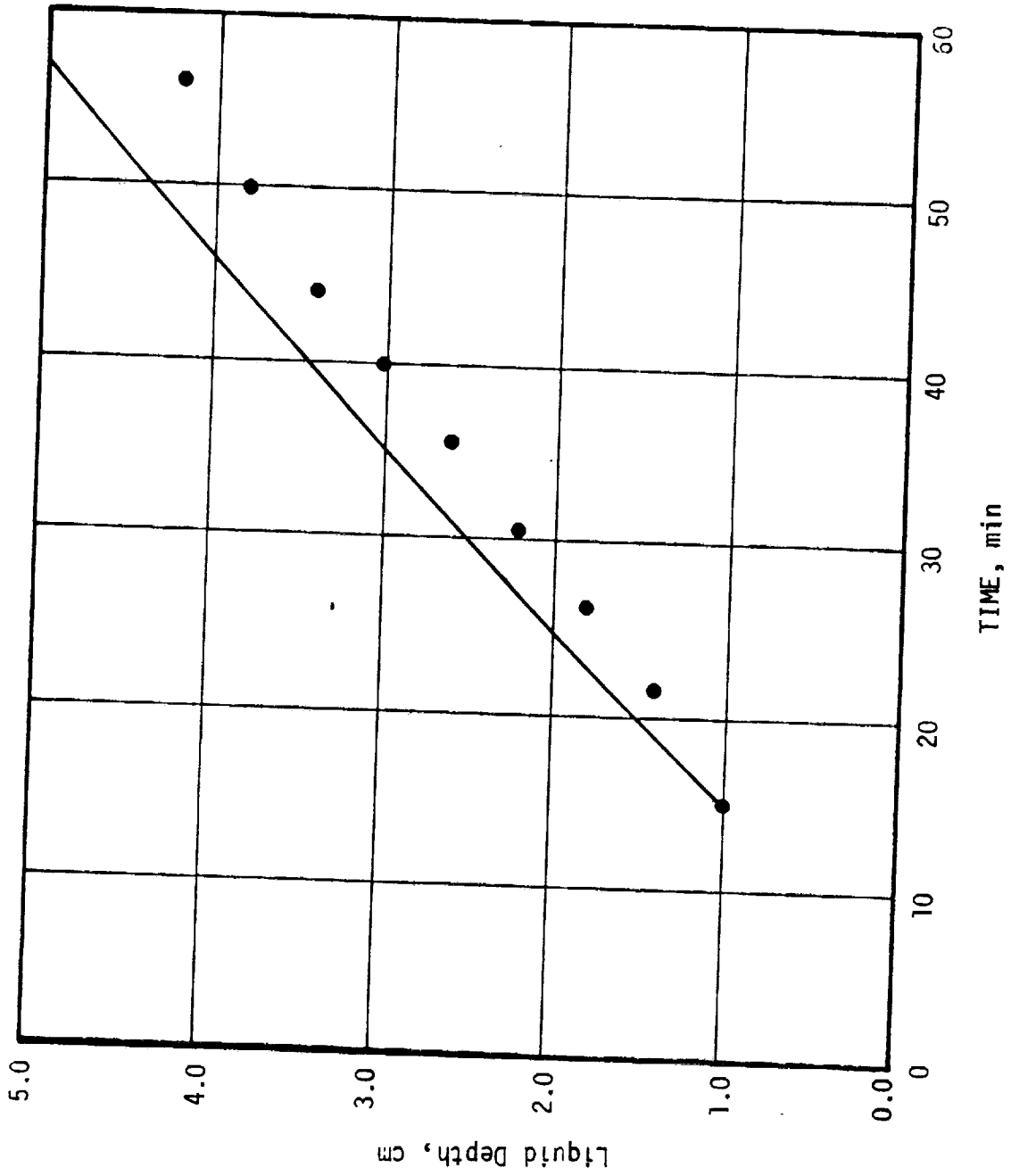Figure 11. Liquid Depth versus Time for 1.50 inch Square with Base Plate at 150°F.
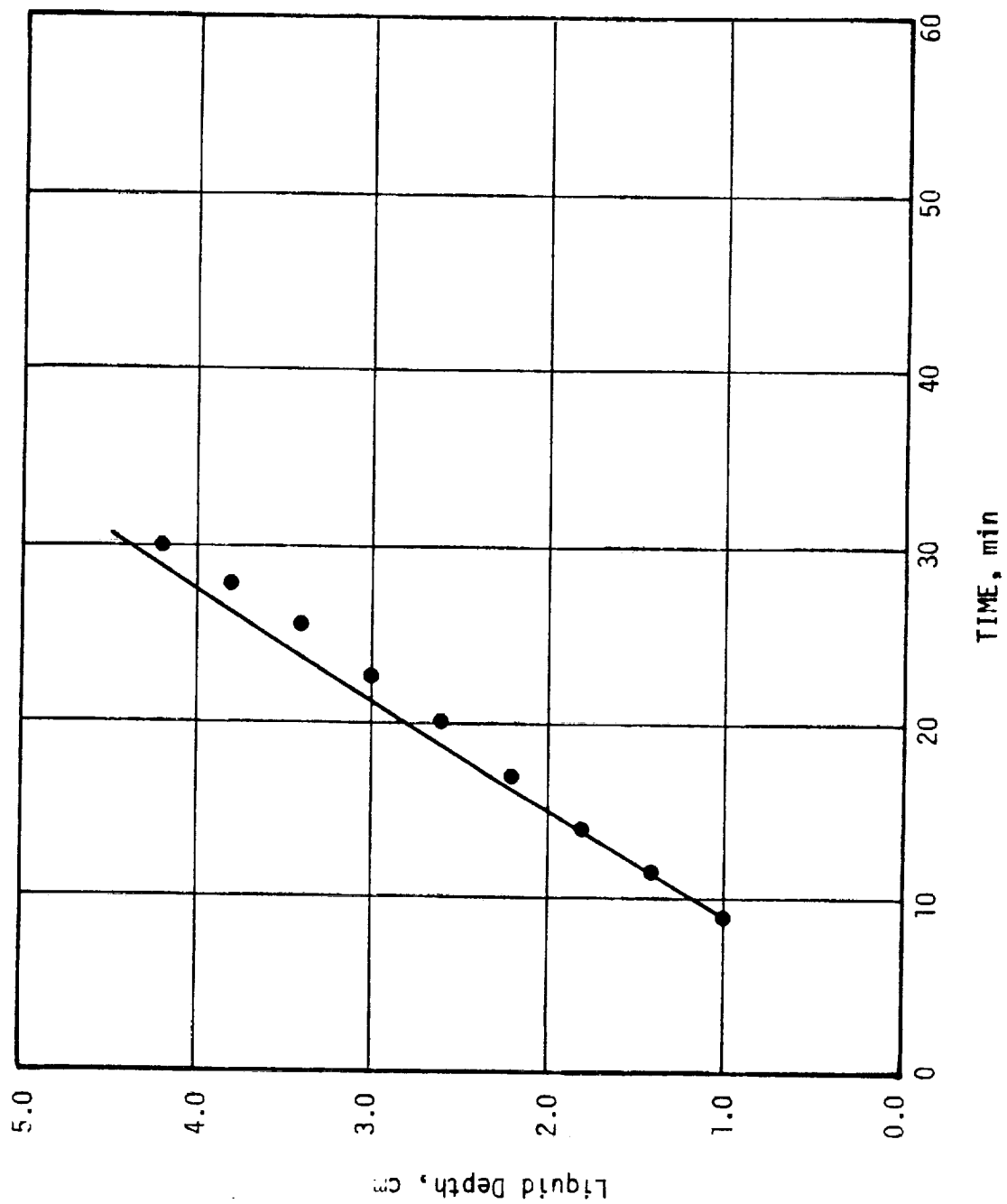
Figure 12.  Liquid Depth versus Time for 0.75 inch Cylinder with Base Plate at 150°F.
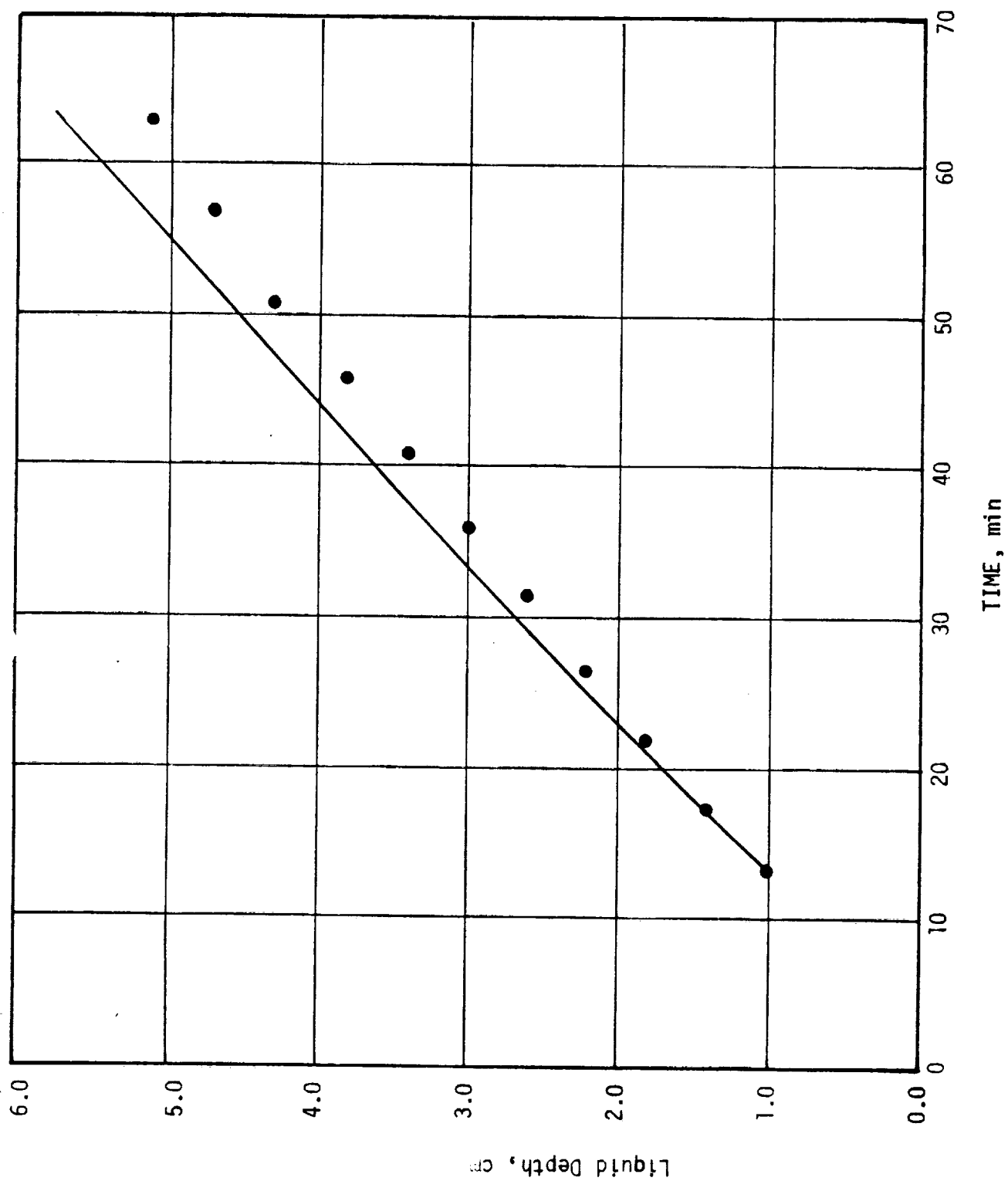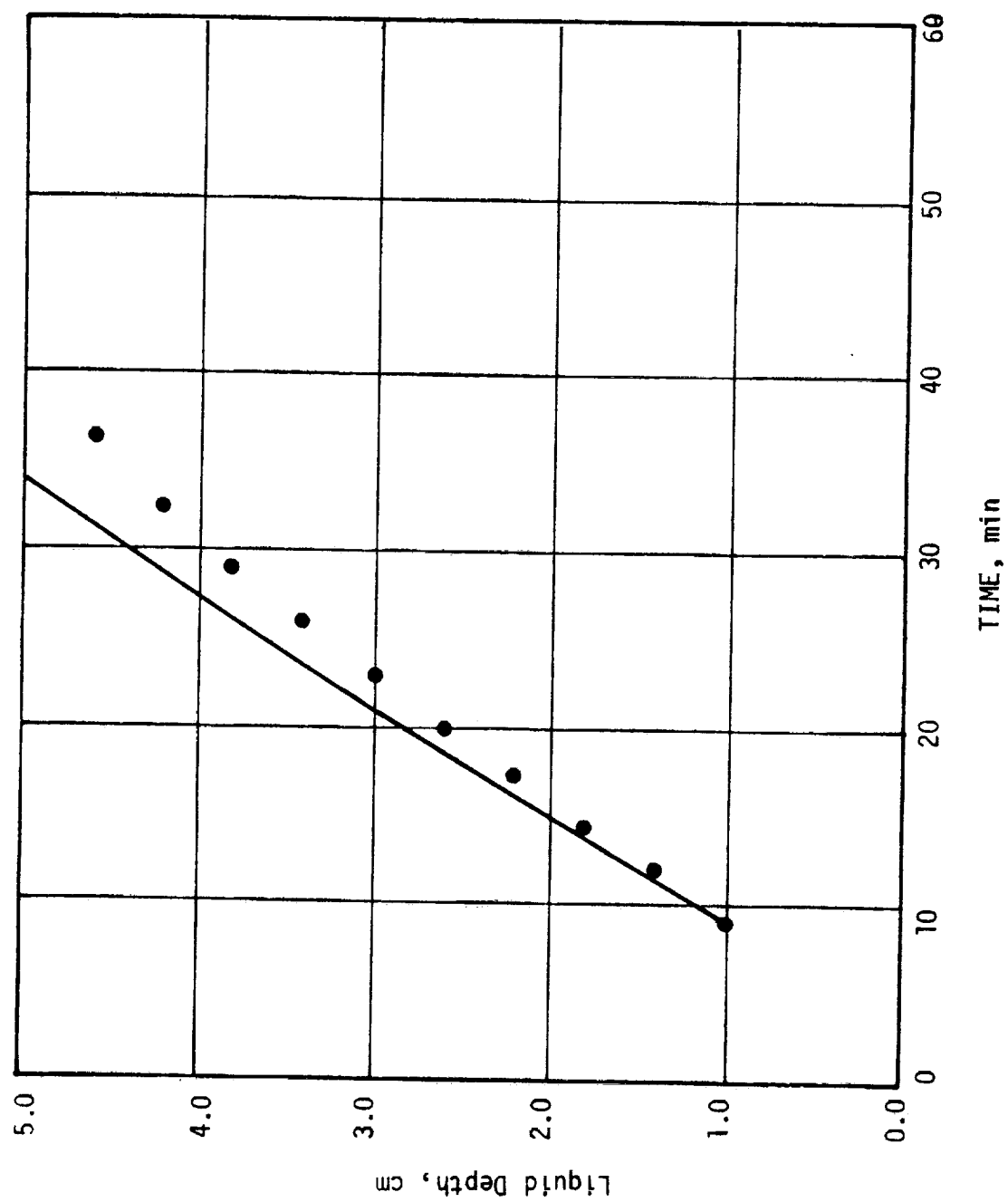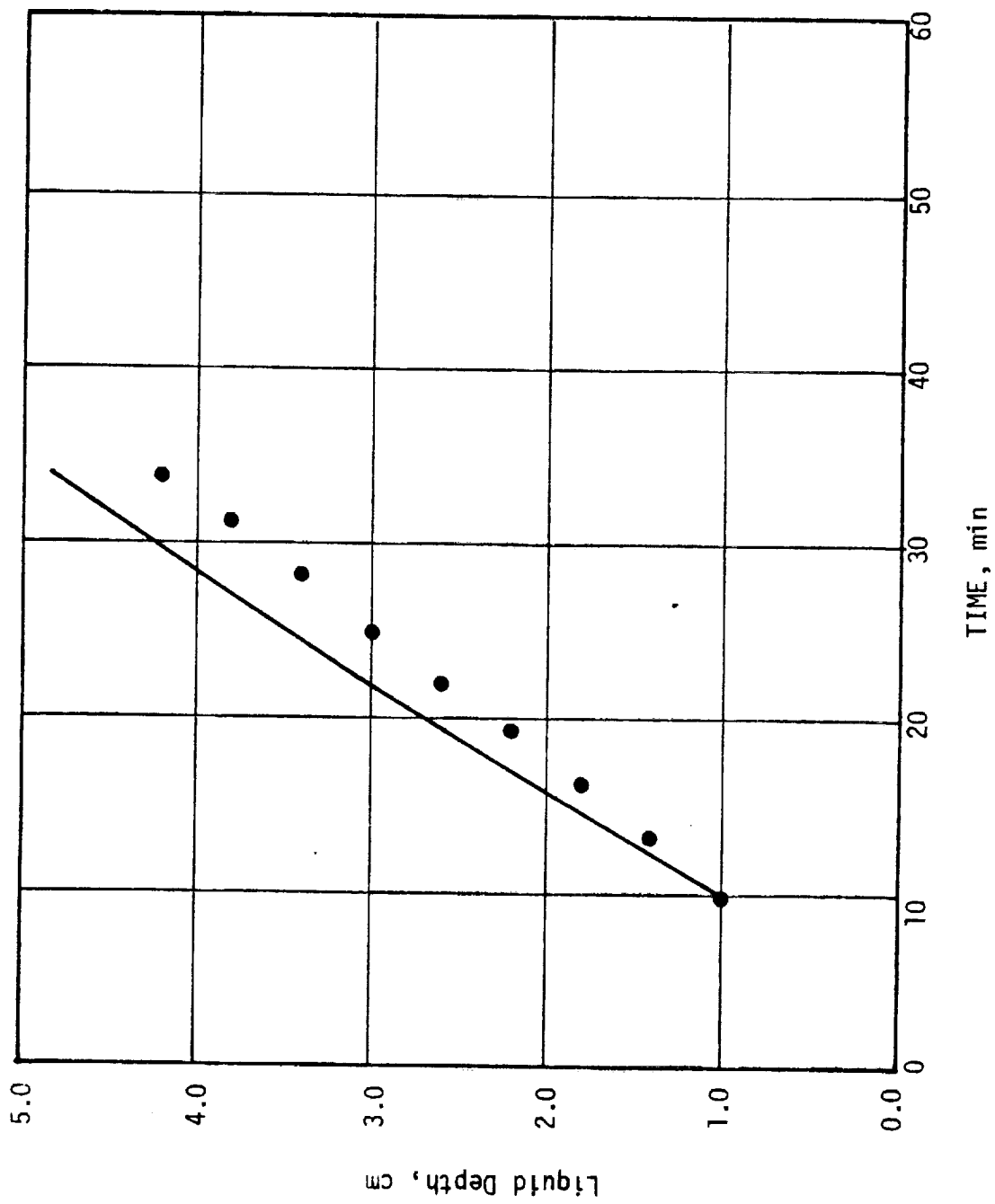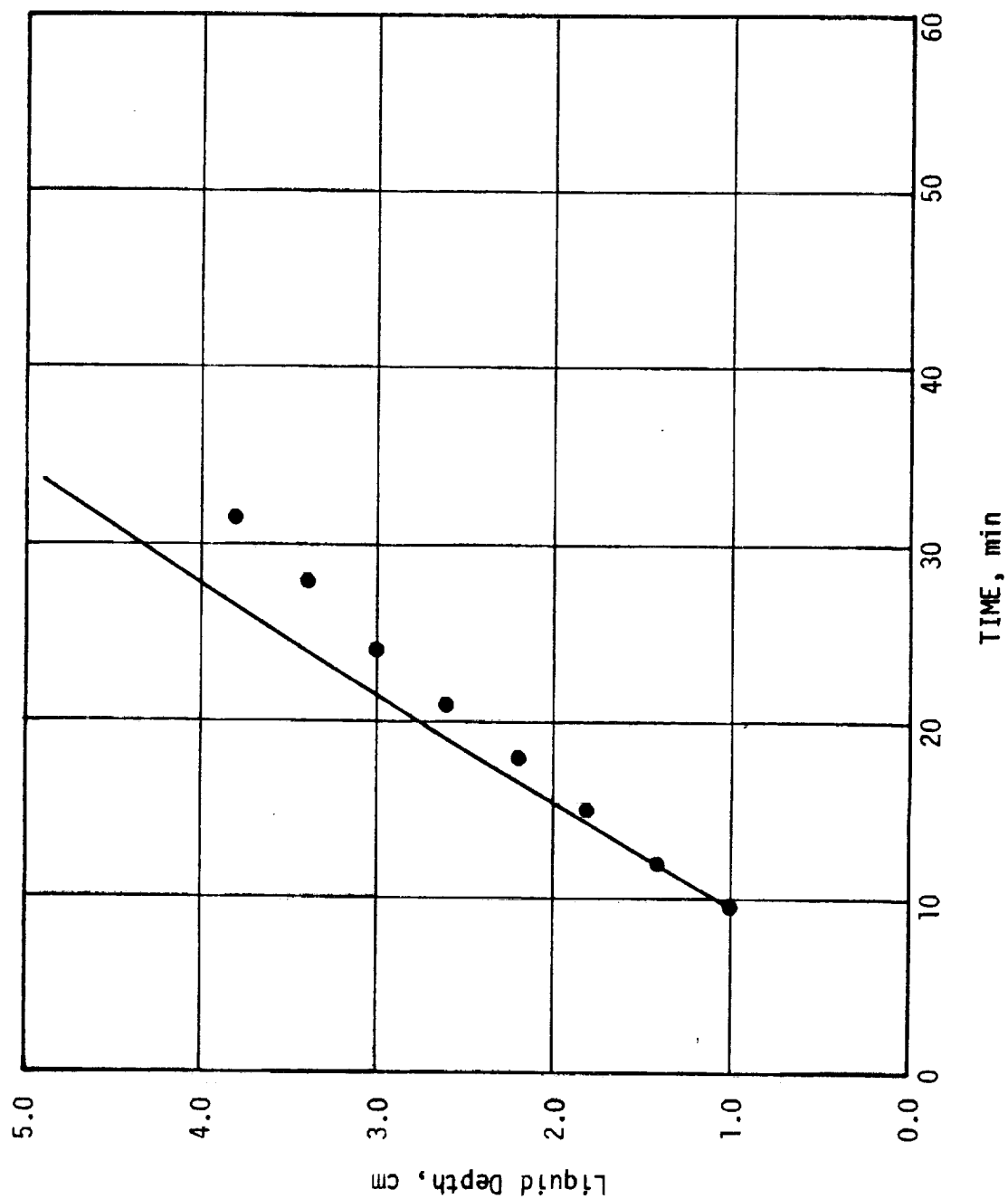
Figure 13. Liquid Depth versus Time for 1.50 inch Cylinder with Base Plate at 150°F.

transfer produces phase change, and the predictions were made to match the first data point. In each case, the data fall below the predictions in the late stages of melting indicating a slightly lower melting rate than that predicted. Two possible factors could partially explain the difference. In these runs, gas bubbles were again noticed on the interface. At times these would agglomerate and make interfacial definition difficult. Their presence could also tend to reduce the heat transfer which would account for a slower rate. Secondly, the rate predicted by the convective correlation is property dependent. Some variation in the liquid properties from those used in the calculation may well be a reality. Accounting of sensible heating of the solid phase would also tend to lower the predictions.

Rectangular Enclosure with Fins:

The objective of the experimental study of the rectangular enclosure was to examine the influence of fins upon melting and freezing of nonadecane. The rectangular enclosure was constructed using one inch thick plexiglass. The inside dimensions were 4 inches long x 2-3/4 inches wide x 2-1/2 inches deep. A copper plate 10 x 9 x 1/8 inches served as the bottom surface. Because of its high thermal conductivity, copper was used in trying to provide an isothermal base. After several attempts with electrical heating, it was decided that a near step change in base temperature could be better achieved by suddenly bringing the base into thermal contact with a liquid bath. Consequently, heating was accomplished by using a bath of water whose temperature was controlled with a thermostatically controlled heater. Cooling was obtained by using a bath of cold water. For the larger cooling rates, a mixture of crushed ice and liquid water was used. Five

aluminum plates were attached to the bottom of the copper base to facilitate improved thermal communication between the bath and the base plate. The fin arrangements were constructed using 0.035 inch thick copper. The fins were 2-1/2 inches high x 4 inches long. They were soldered to a base 2-1/2 inches x 4 inches. Arrangements for both 1/4 inch and 3/4 inch spacing were built. The finned arrangements could be interchanged as well as removed since they were firmly held to the base of the enclosure by eight screw studs that were permanently soldered in the main base. Schematic cross-sections of the enclosure are given in Figure 14.

Temperatures were measured using copper-constantan thermocouples. Four were mounted in the base of the enclosure and wired in parallel to provide a spatial average base temperature measurement. A fifth thermocouple was located within the paraffin in the center of the cell and approximately one inch above the base. The transient responses of the thermocouples were recorded using a Honeywell Electronik 194 recorder. The position of the interface at the center of the cell was observed with the aid of a Gaertner cathetometer. The procedure involved adjusting the level of the cathetometer in certain increments and then recording the time at which the interface reached the set level. In this manner, a transient record of the interface position was obtained. In addition a series of photographs were made for a few of the tests.

Several tests were conducted. In the early stages considerable difficulty was encountered in obtaining a seal between the base plate and the plexiglass housing. Consequently, many tests were terminated prematurely. Overall, however, tests were conducted for melting and freezing for both the 1/4 inch and 3/4 inch fin separations. For each

6.0"

PCM HOUSING

COPPER
BOTTOM PLATE

PLEXIGLASS TOP

COPPER FINS

1/8"

6-3/4"

4-3/4"

4"
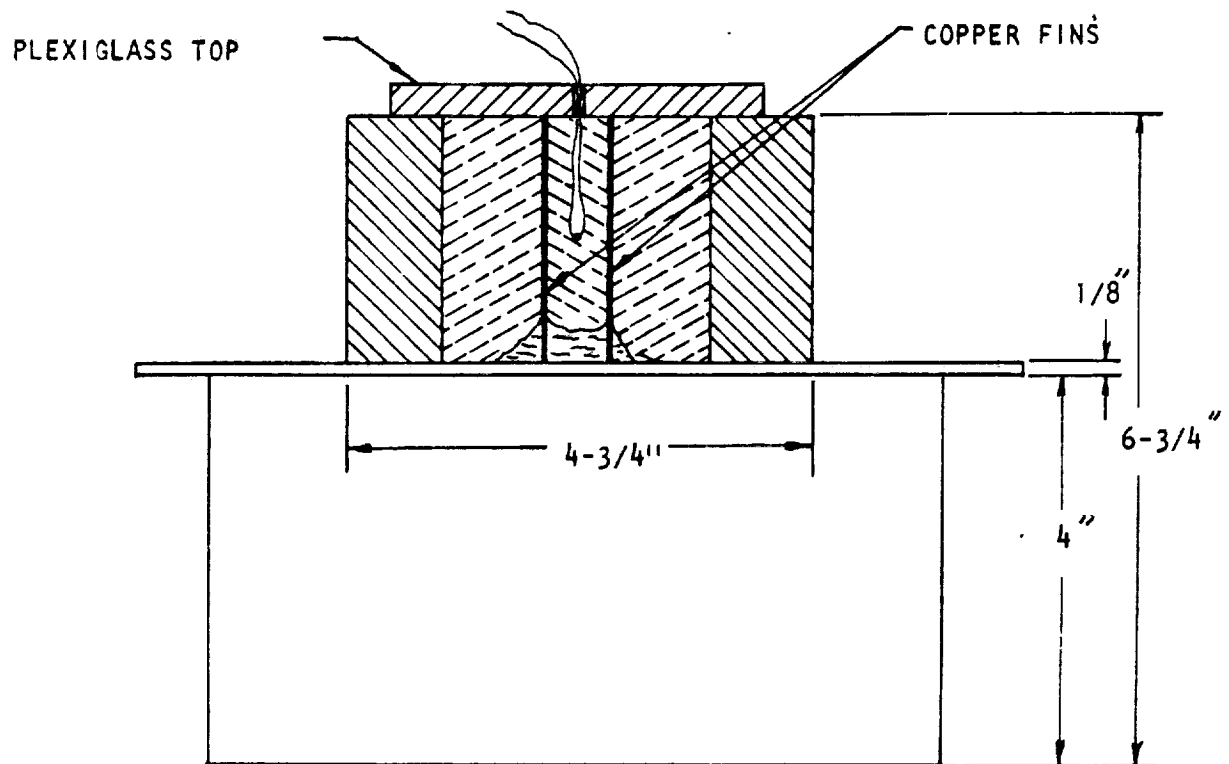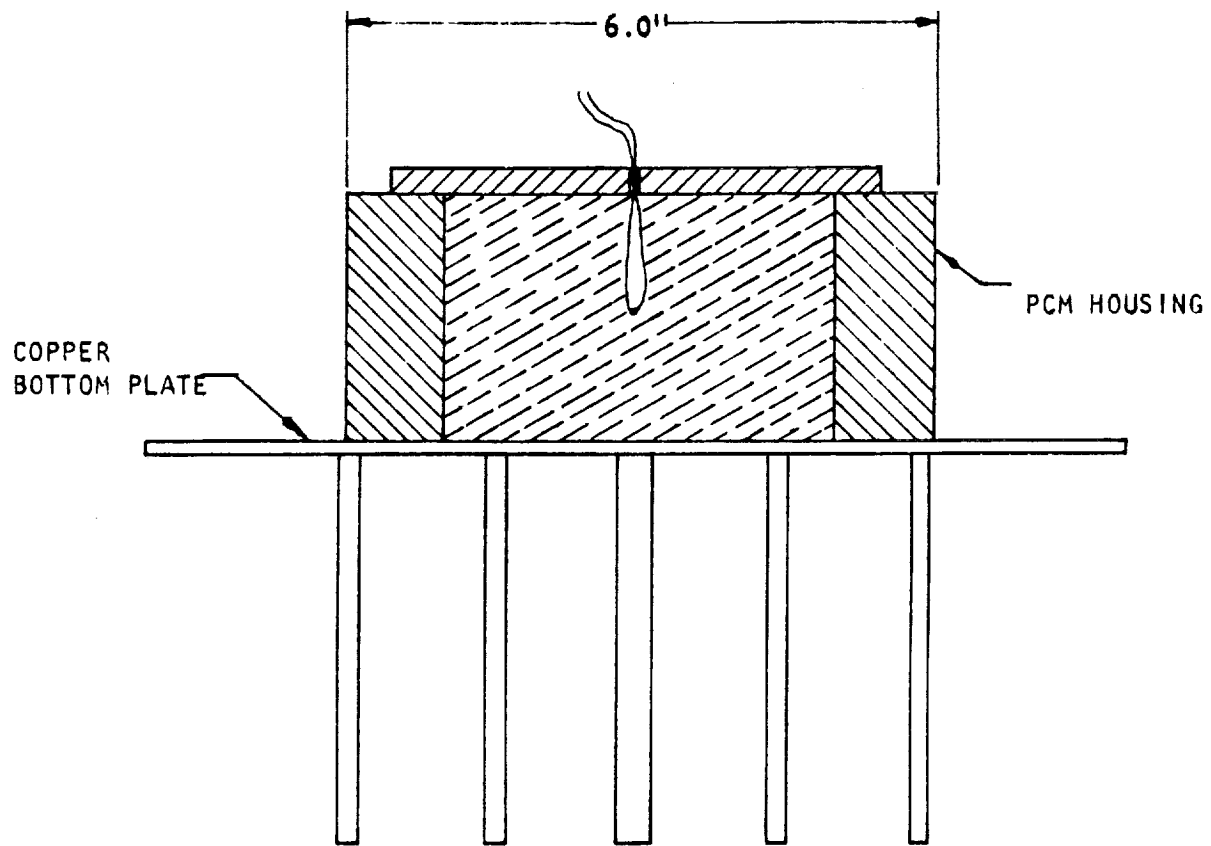
Figure 14. Schematic Cross Section of Rectangular Enclosure
with Fins

melting run, tests were conducted at two different bath temperatures in order to cover different heating rates. Most freeze runs were conducted using only one bath temperature obtained by using a mixture of ice and water.

For the high heating rates, a bath temperature of about 160°F was used while for the lower heating rates a bath temperature of approximately 110 to 115°F was used. Transient temperature data for melting tests with the bath at approximately 160°F are shown for no fins, 1/4 inch spaced fins, and 3/4 inch spaced fins in Figures 15 through 17, respectively. Corresponding data of the interfacial position are given in Figures 18 through 20. For melting tests run with the lower base temperature, transient temperature data for the case of no fins, 1/4 inch spaced fins, and 3/4 inch spaced fins are given in Figures 21 through 23, respectively. The corresponding data of interfacial positions are shown in Figures 24 through 26. Data for the freezing tests are presented in the same sequence in Figures 27 through 31 with the exception of interfacial data for the 1/4 inch spacing. In all cases, interfacial position data correspond to the center of the cell. Temperature data denoted by solid circles represent measurements within the PCM while the other data represent the average base temperature.

Two photographs of melting in the absence of fins are shown in Figures 32 and 33. The camera was inclined for the shot shown in Figure 33 in order to show the presence of bubbles at the interface. The scales shown in these figures are for reference only. Interfacial position measurements were made with the cathetometer as mentioned earlier. Figures 34(a) through 34(d) and 35(a) through 35(d) represent
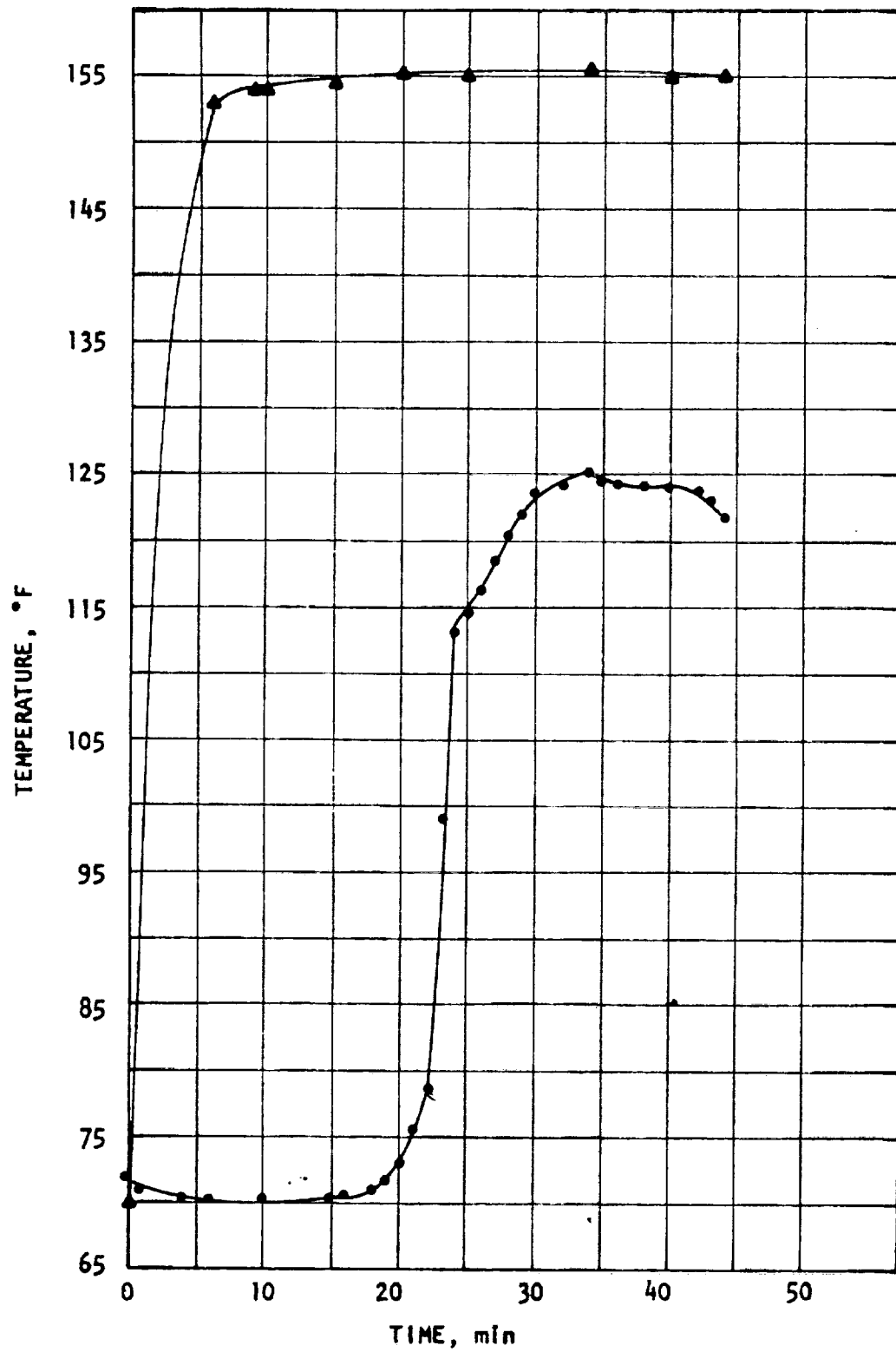
Figure 15.  Transient Temperature Data for Melting using
160°F Bath and No Fins
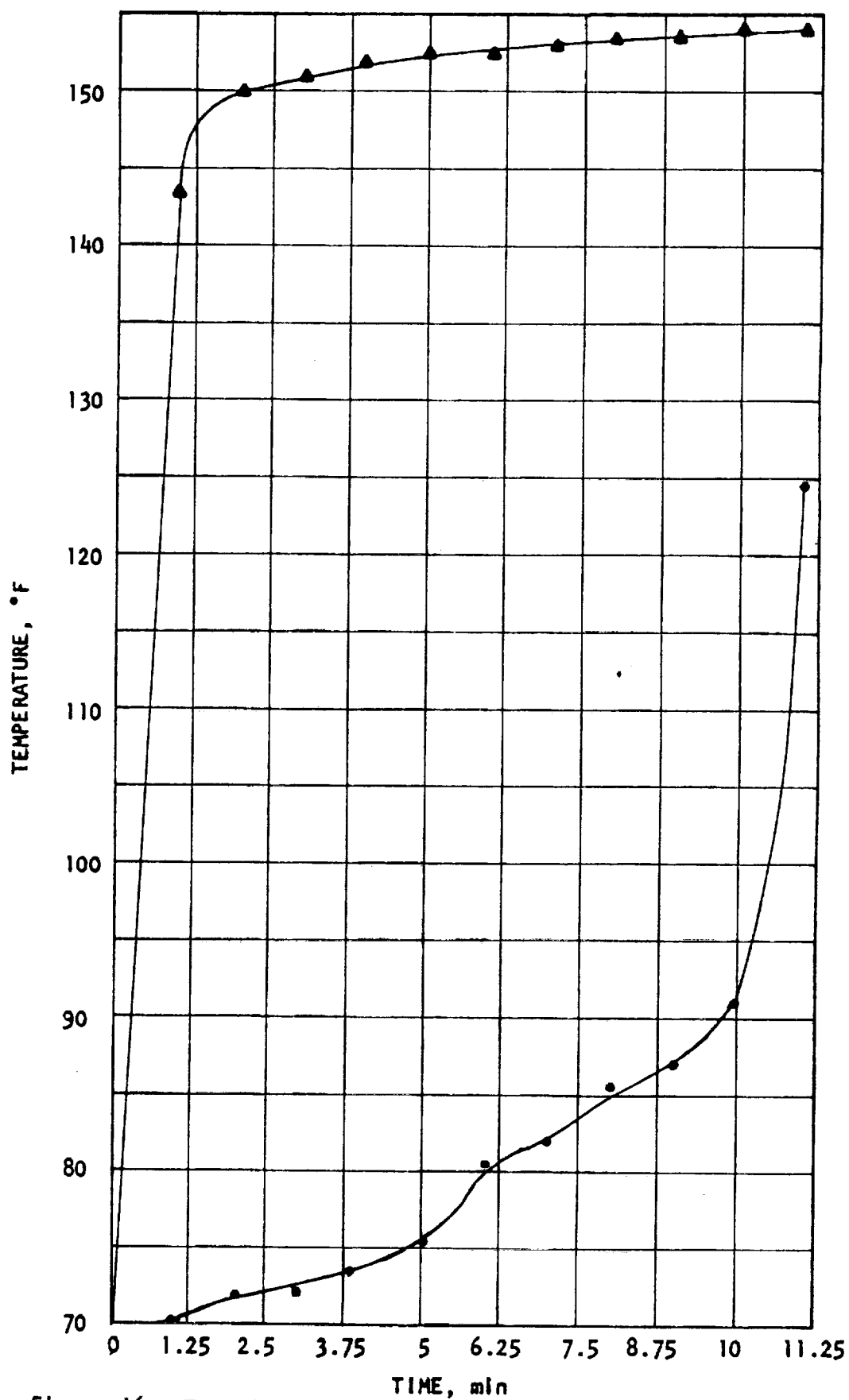
Figure 16.  Transient Temperature Data for Melting using 160°F
Bath and 1/4 Inch Spaced Fins
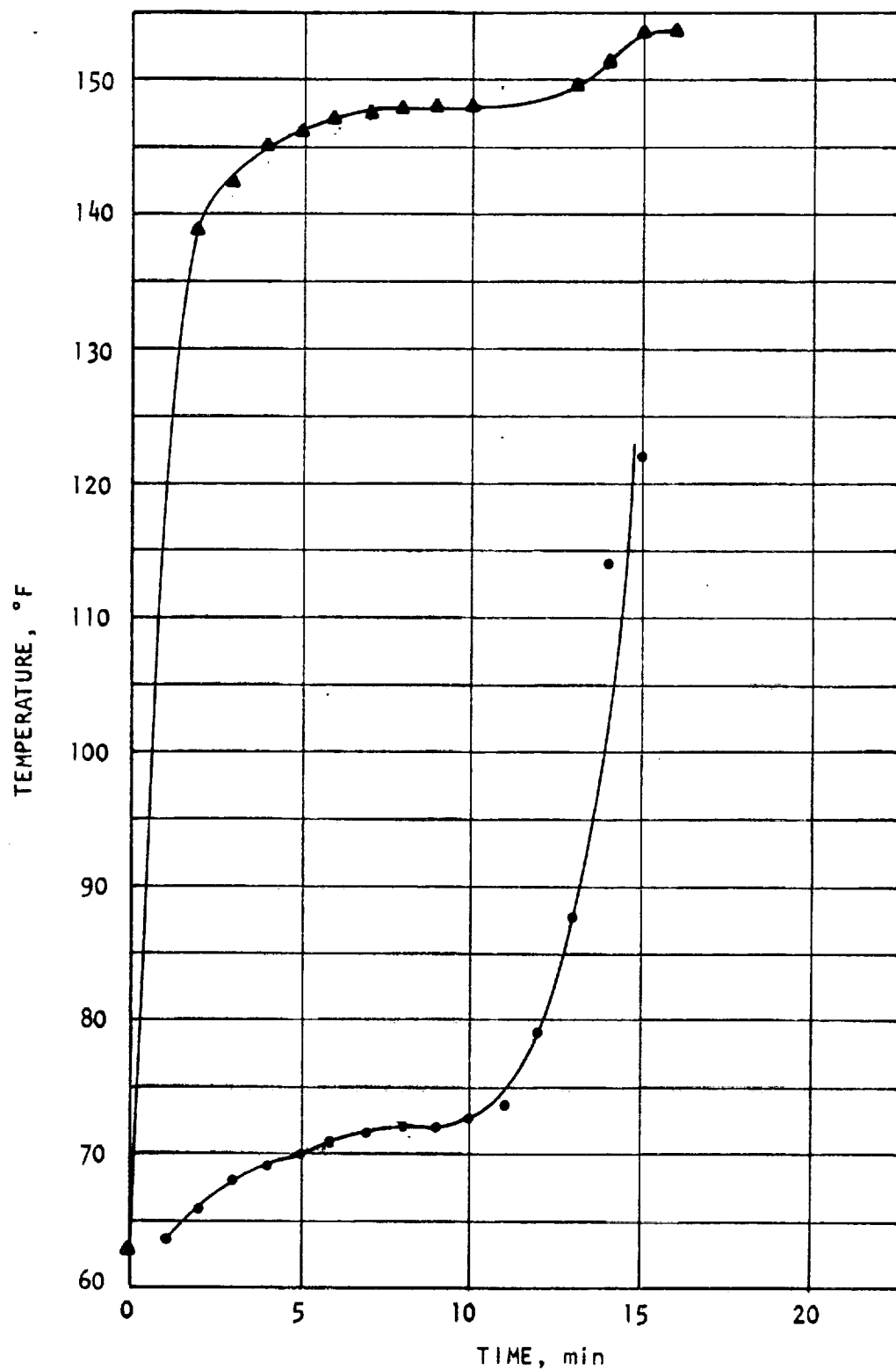
Figure 17. Transient Temperature Data for Melting using 160°F
Bath and 3/4 Inch Spaced Fins
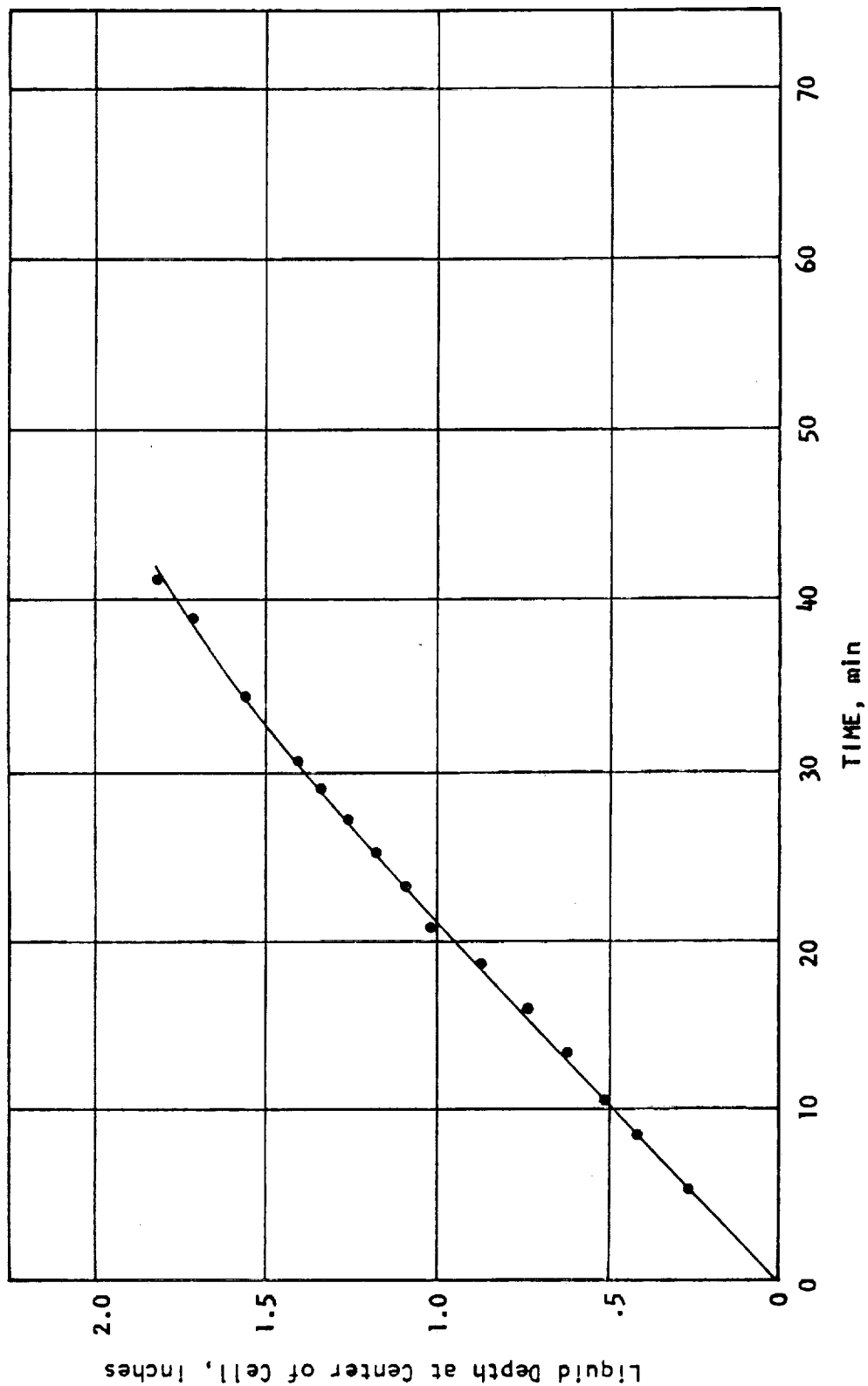
Figure 18.    Interfacial Data for Melting Using 160°F Bath and No Fins
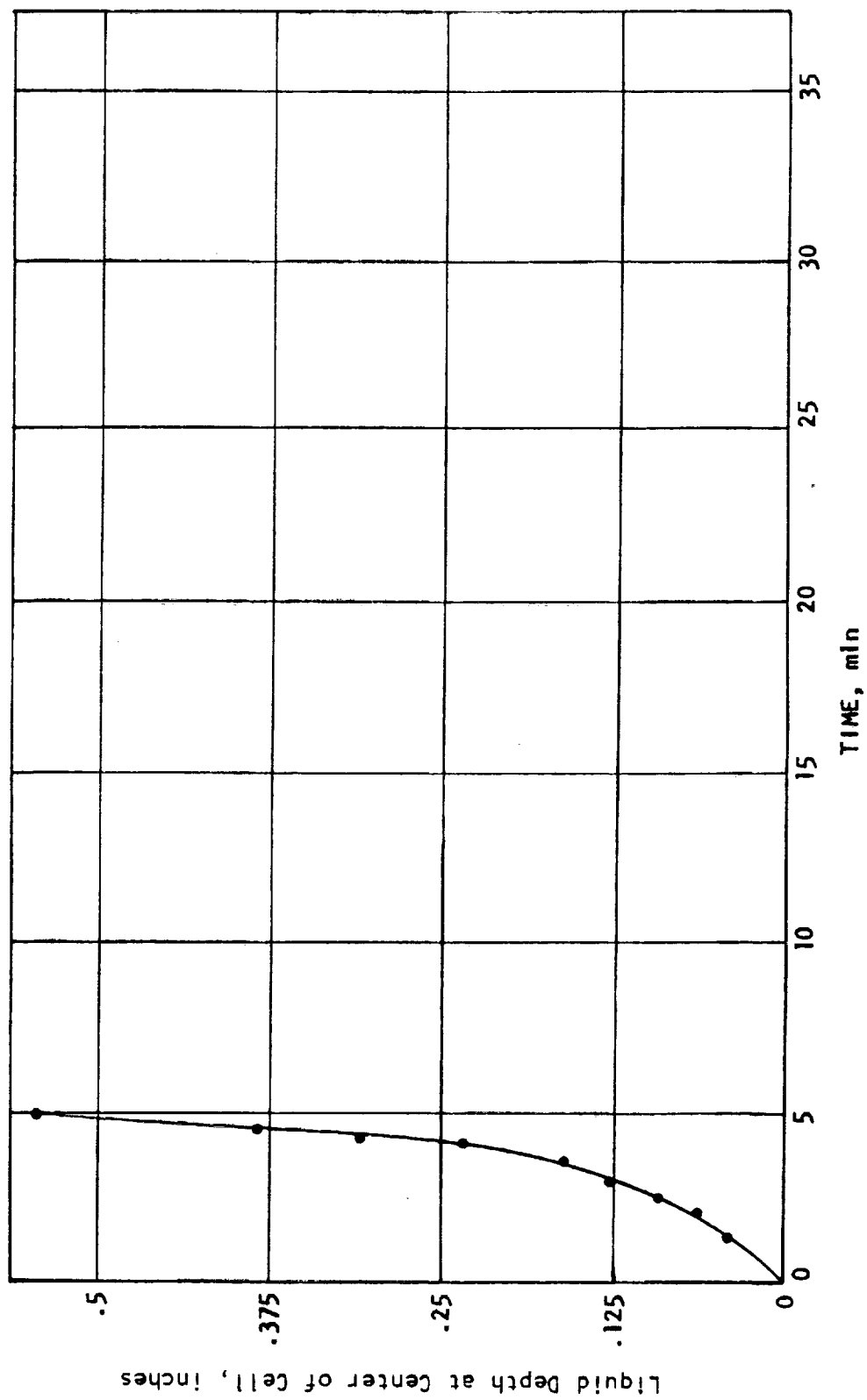
Figure 19.    Interfacial Data for Melting using 160°F Bath and 1/4 Inch
Spaced Fins
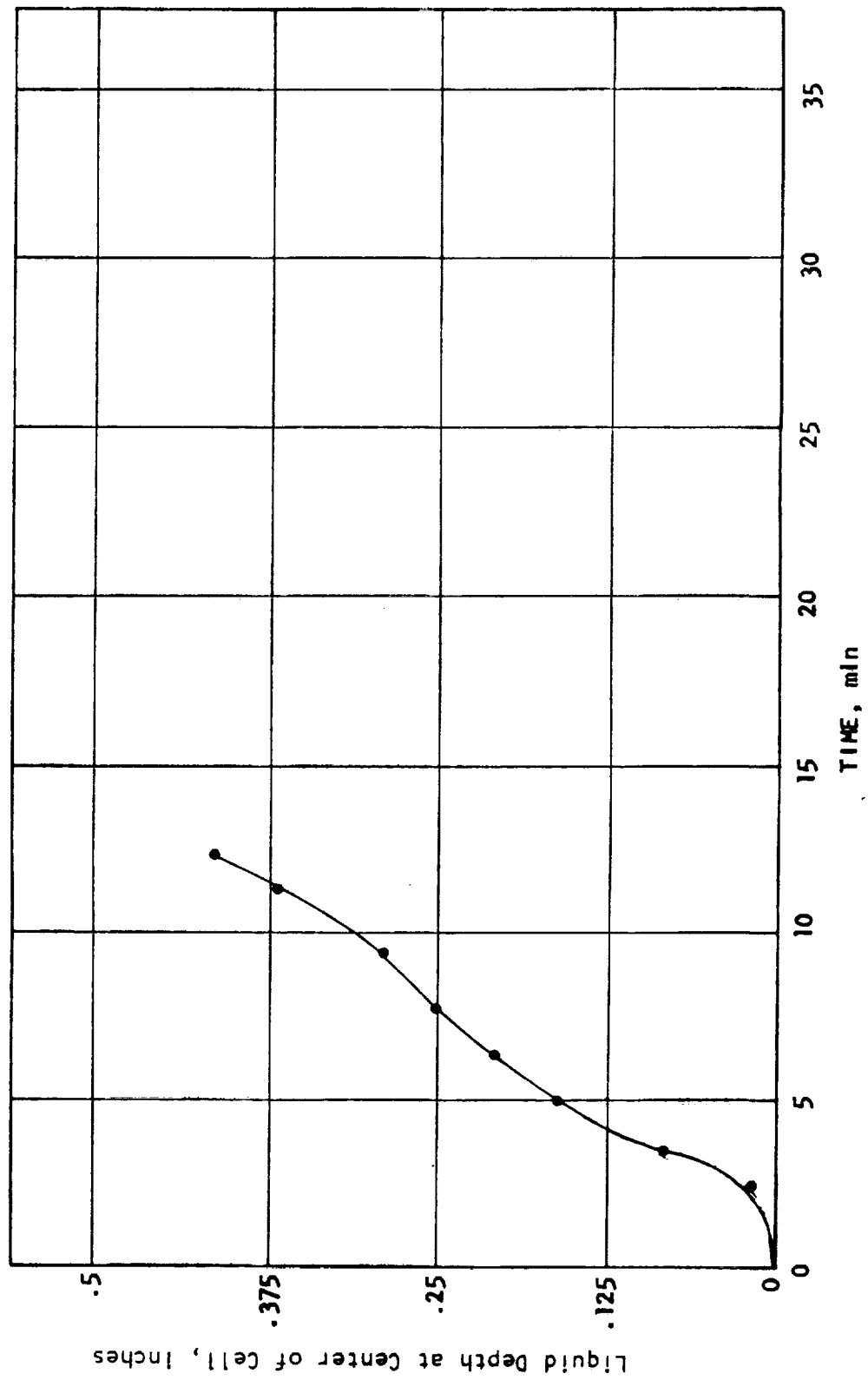
Figure 20. Interfacial Data for Melting using 160°F Bath and 3/4 Inch Spaced Fins
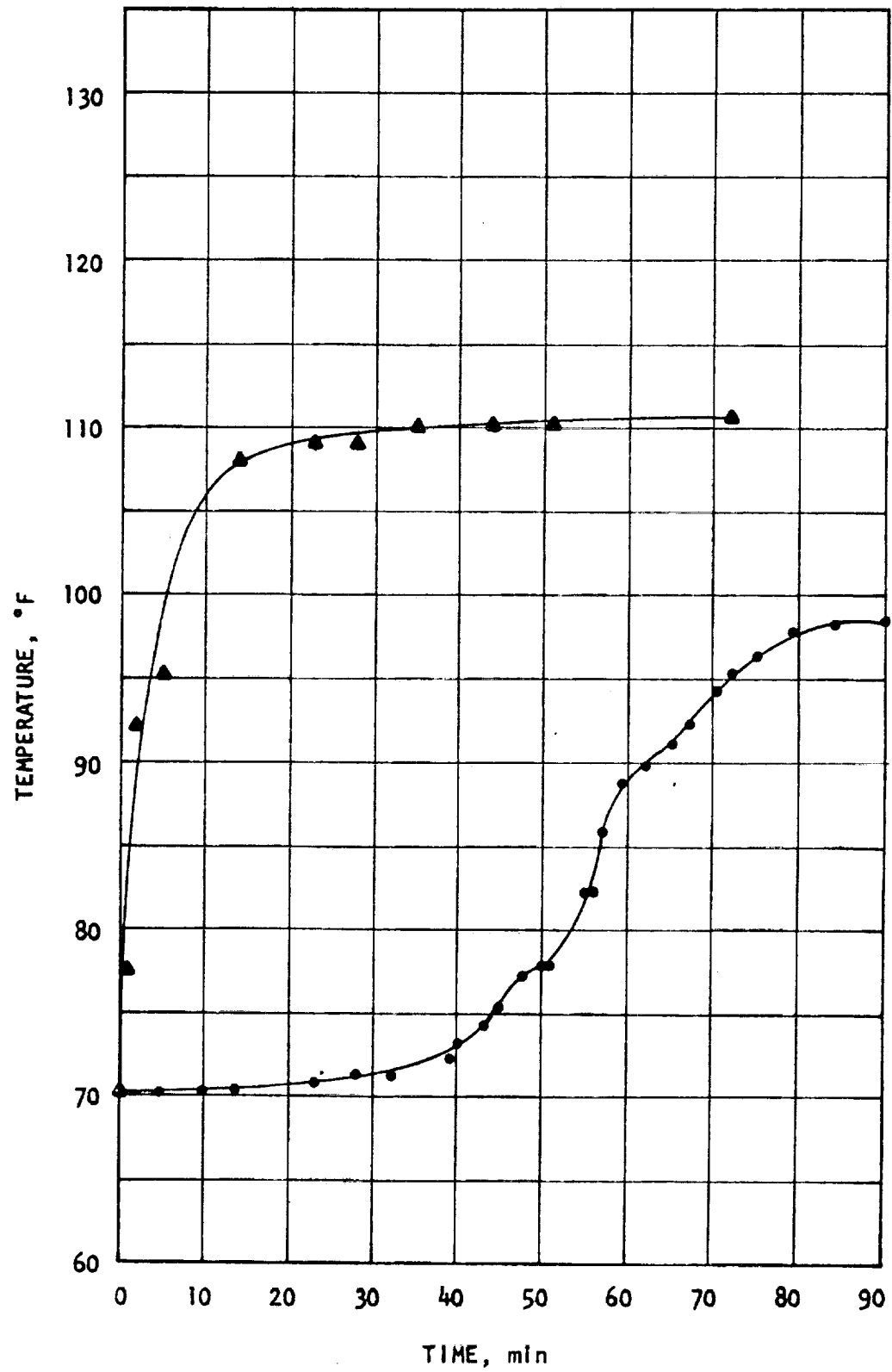
Figure 21.   Transient Temperature Data for Melting Using
115°F Bath and No Fins
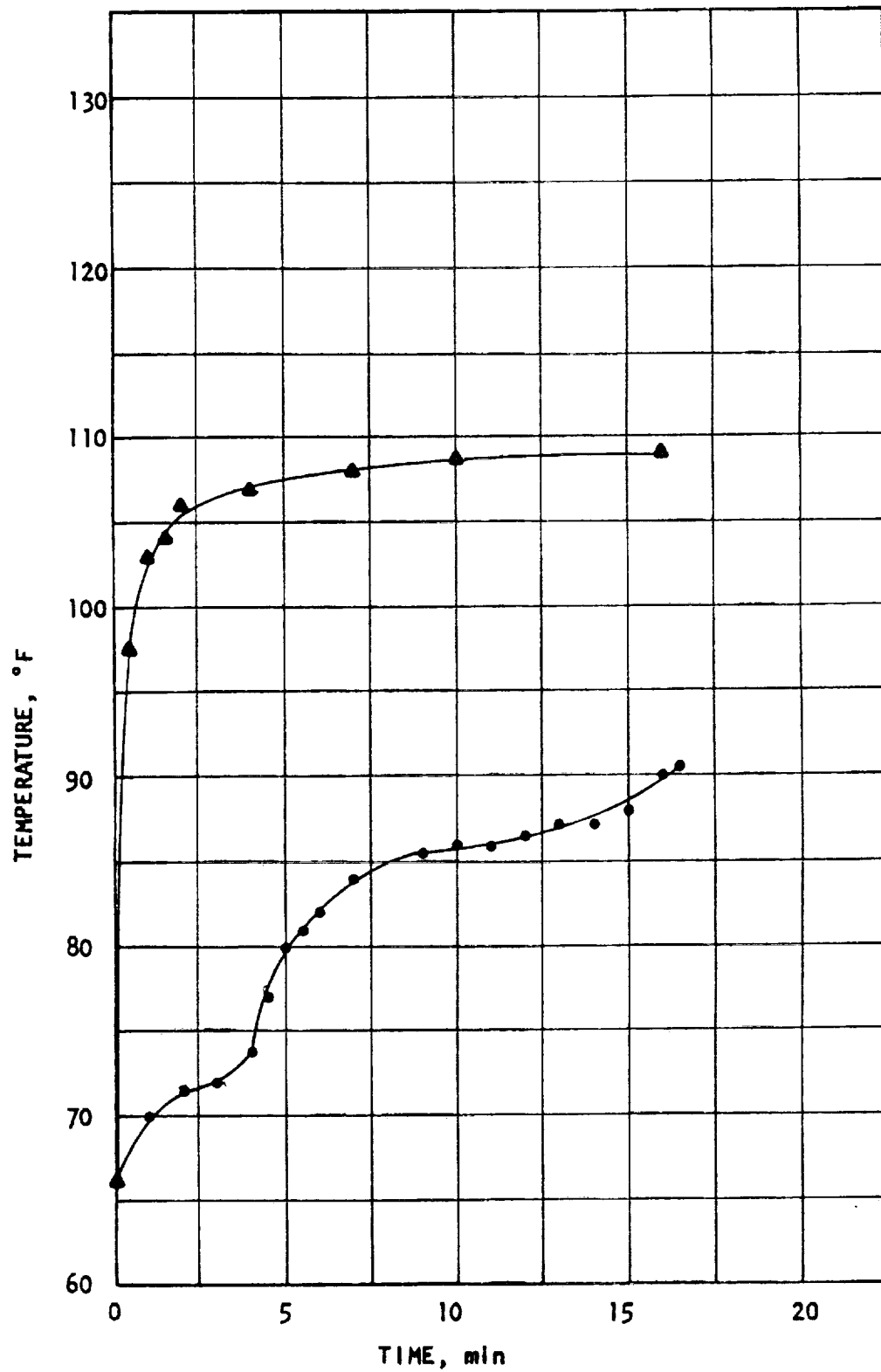
Figure 22.  Transient Temperature Data for Melting using
115°F Bath and 1/4 Inch Spaced Fins
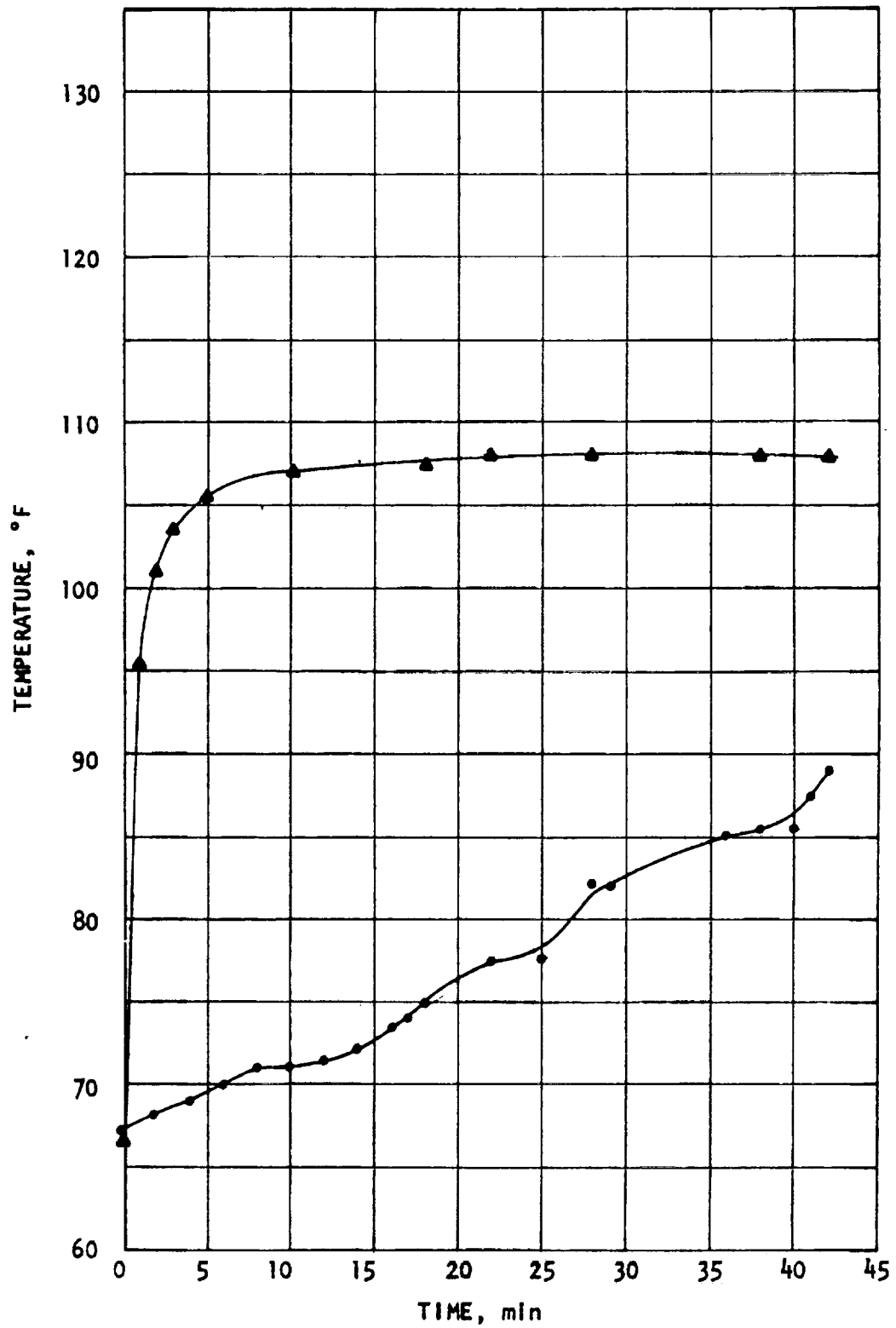
Figure 23.  Transient Temperature Data for Melting using
115°F Bath and 3/4 Inch Spaced Fins
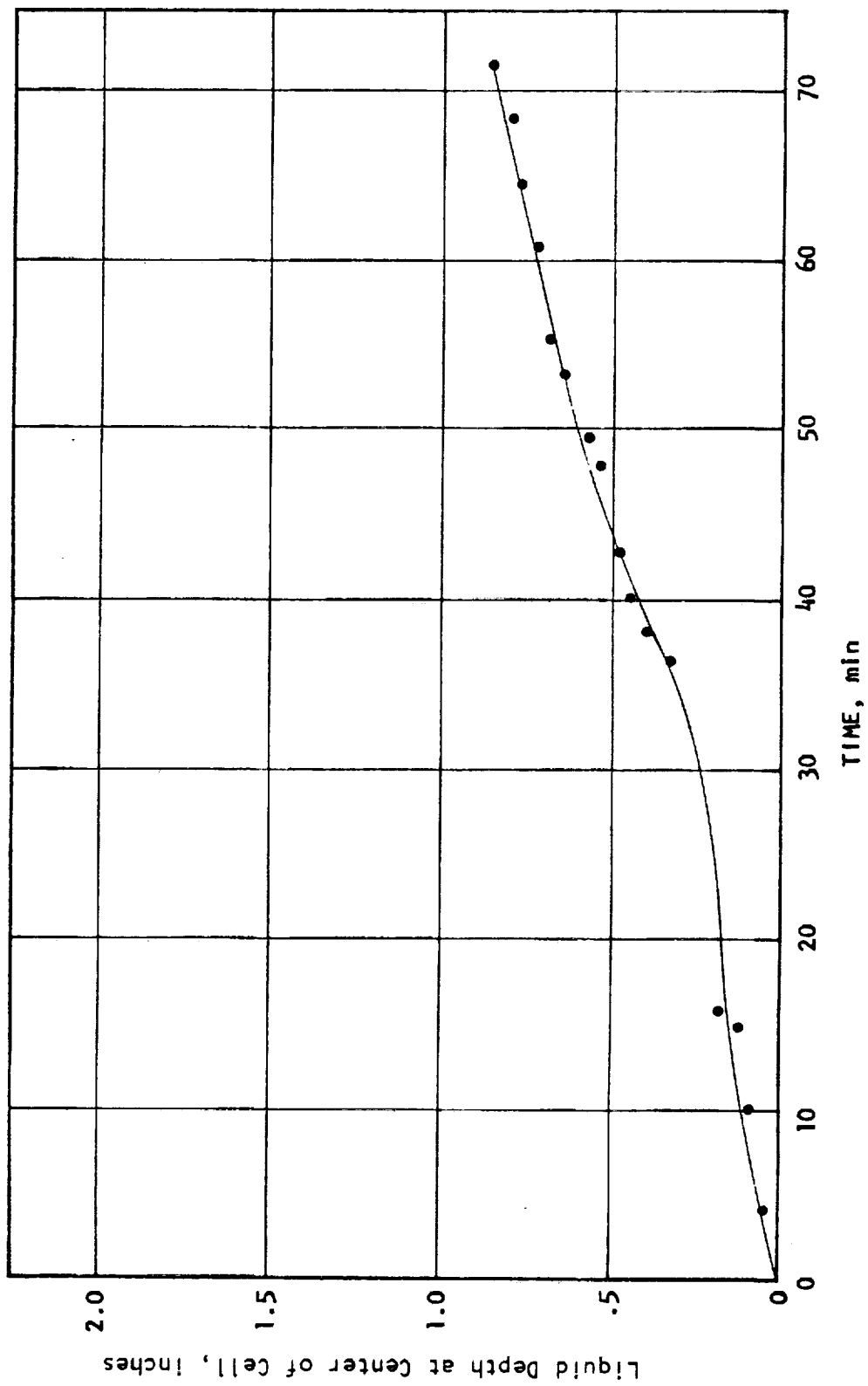
Figure 24. Interfacial Data for Melting using 115°F Bath and No Fins
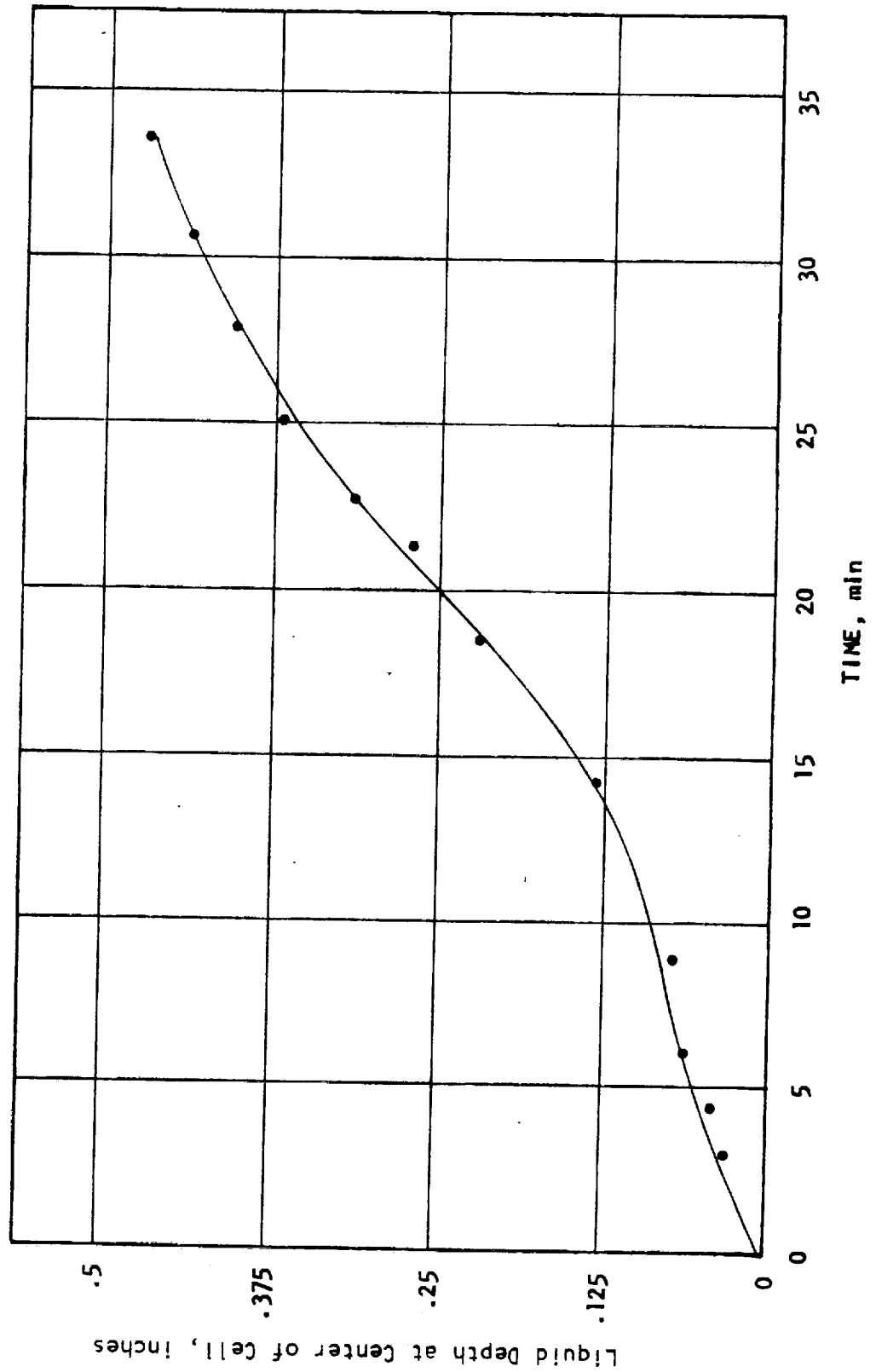
Figure 26.  Interfacial Data for Melting Using 115°F Bath and 3/4 Inch Spaced Fins
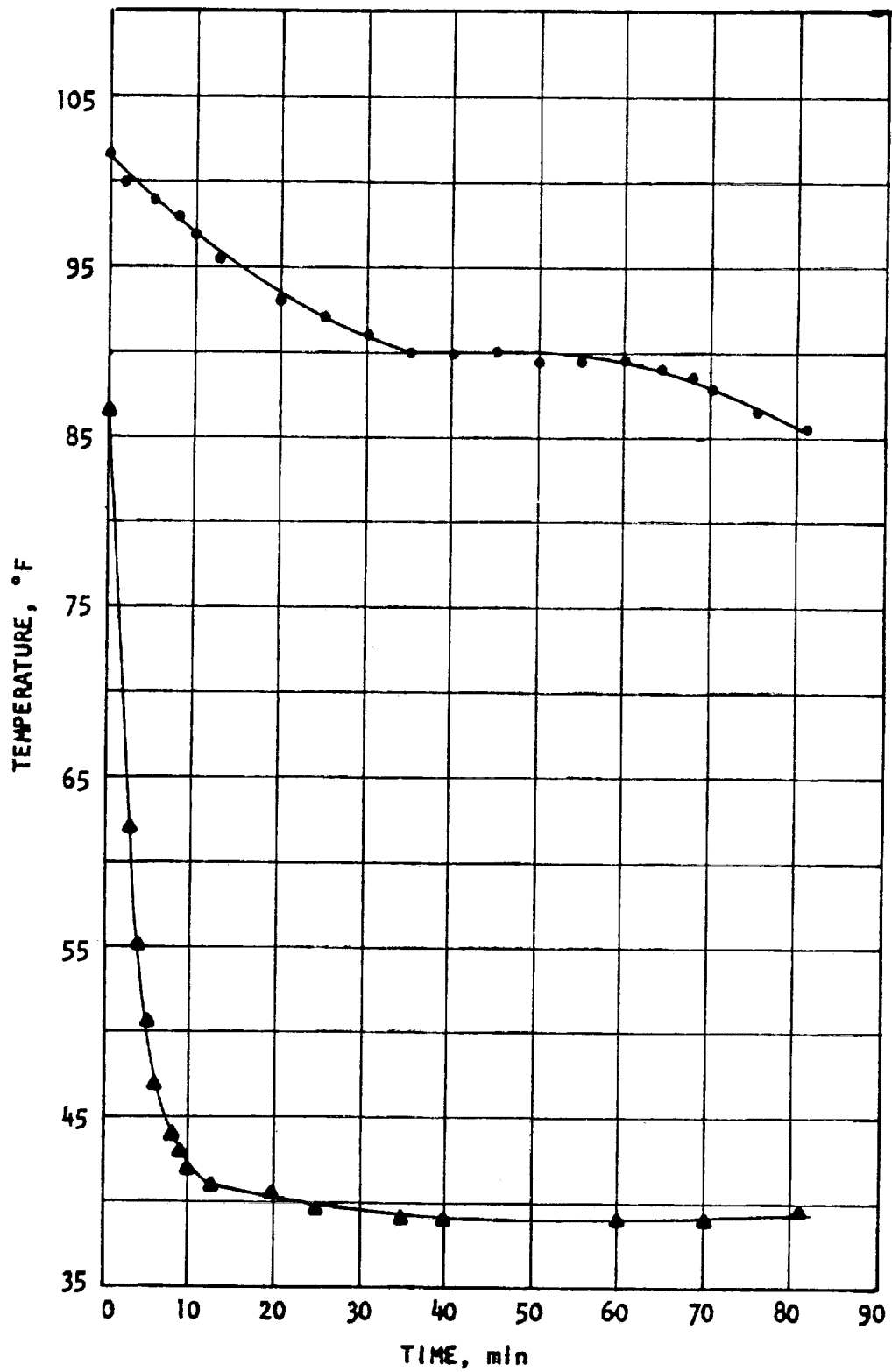
Figure 27.  Transient Temperature Data for Solidification
Using Ice Bath and No Fins
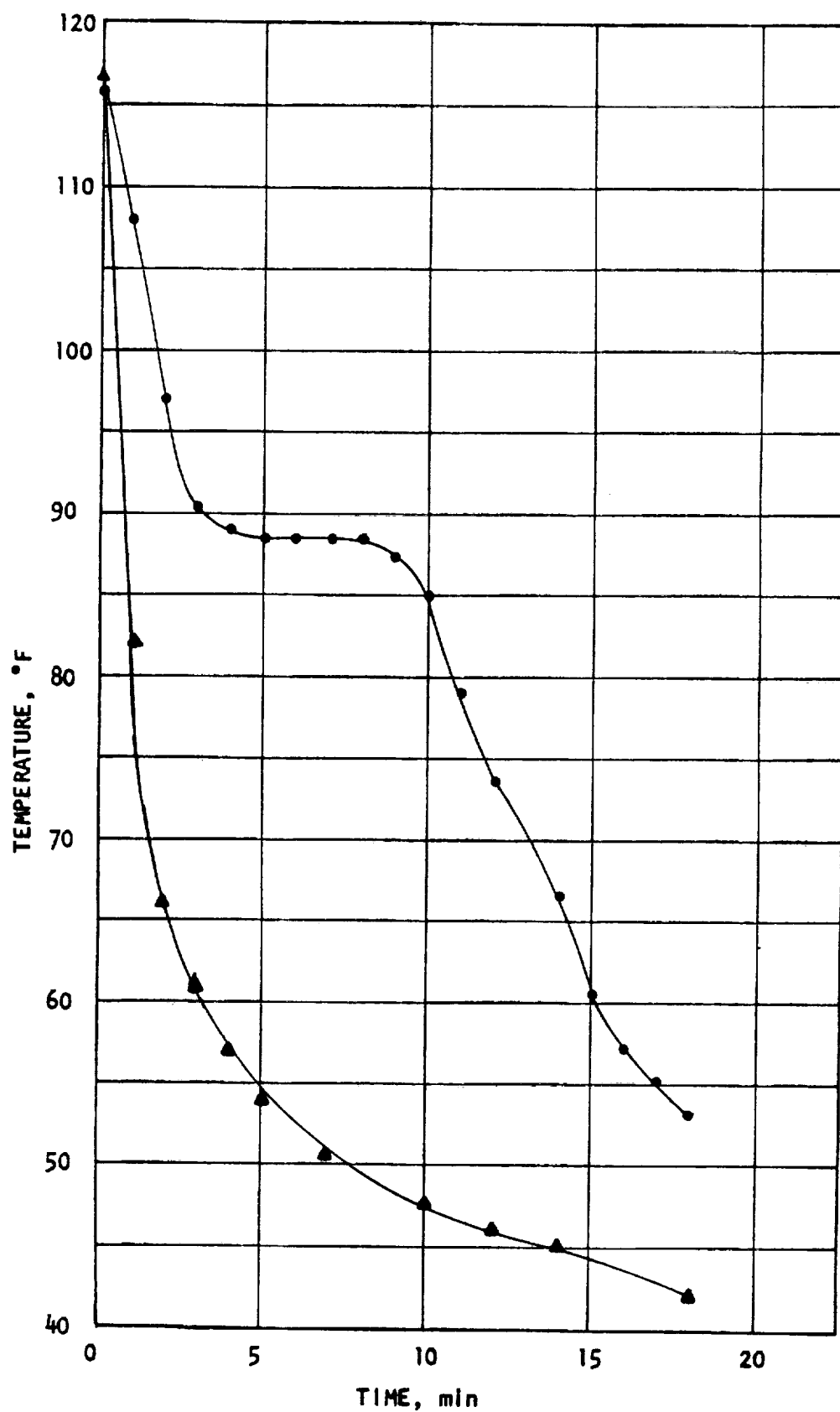
Figure 28.    Transient Temperature Data for Solidification
Using Ice Bath and 1/4 Inch Spaced Fins
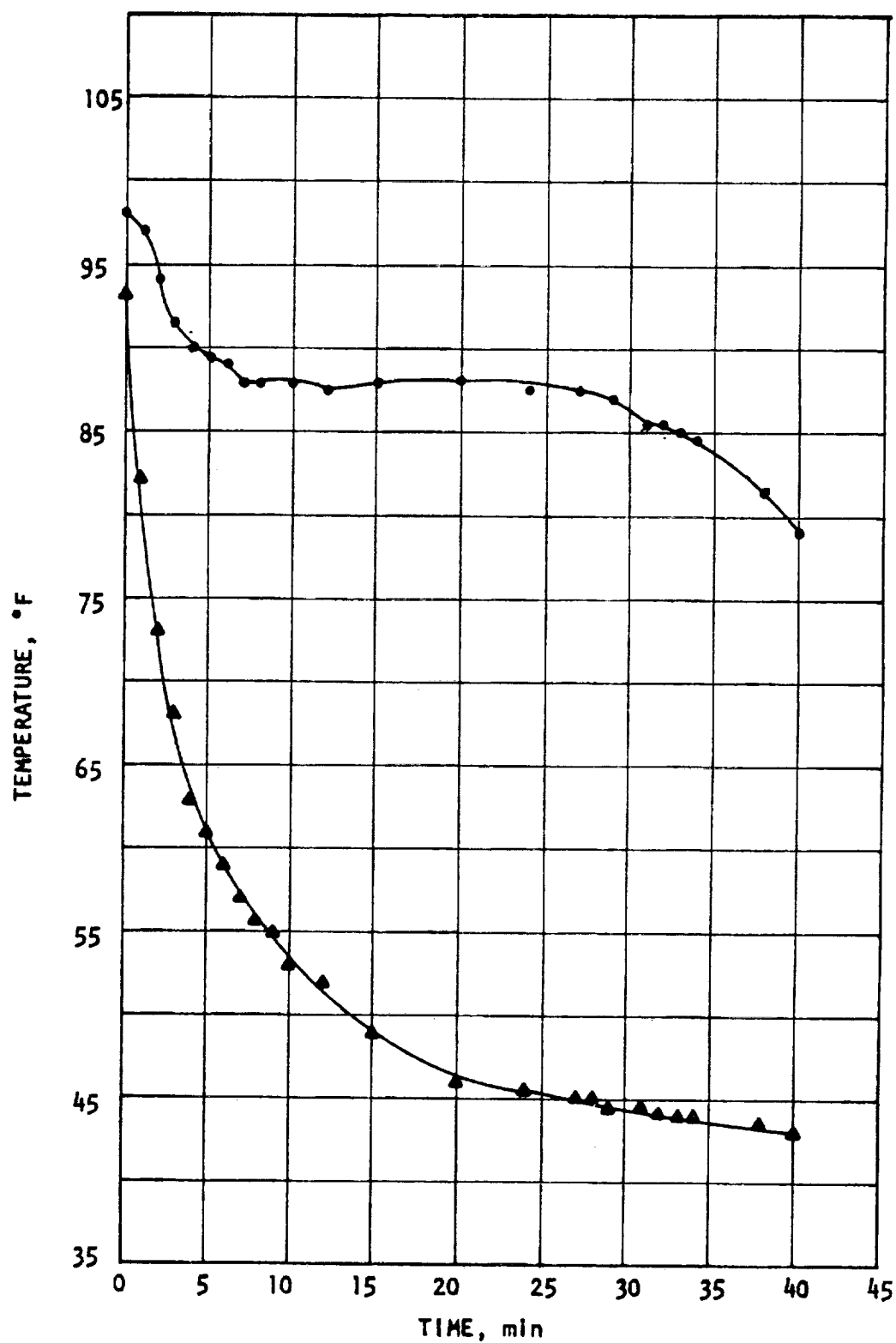
Figure 29.  Transient Temperature Data for Solidification
Using Ice Bath and 3/4 Inch Spaced Fins
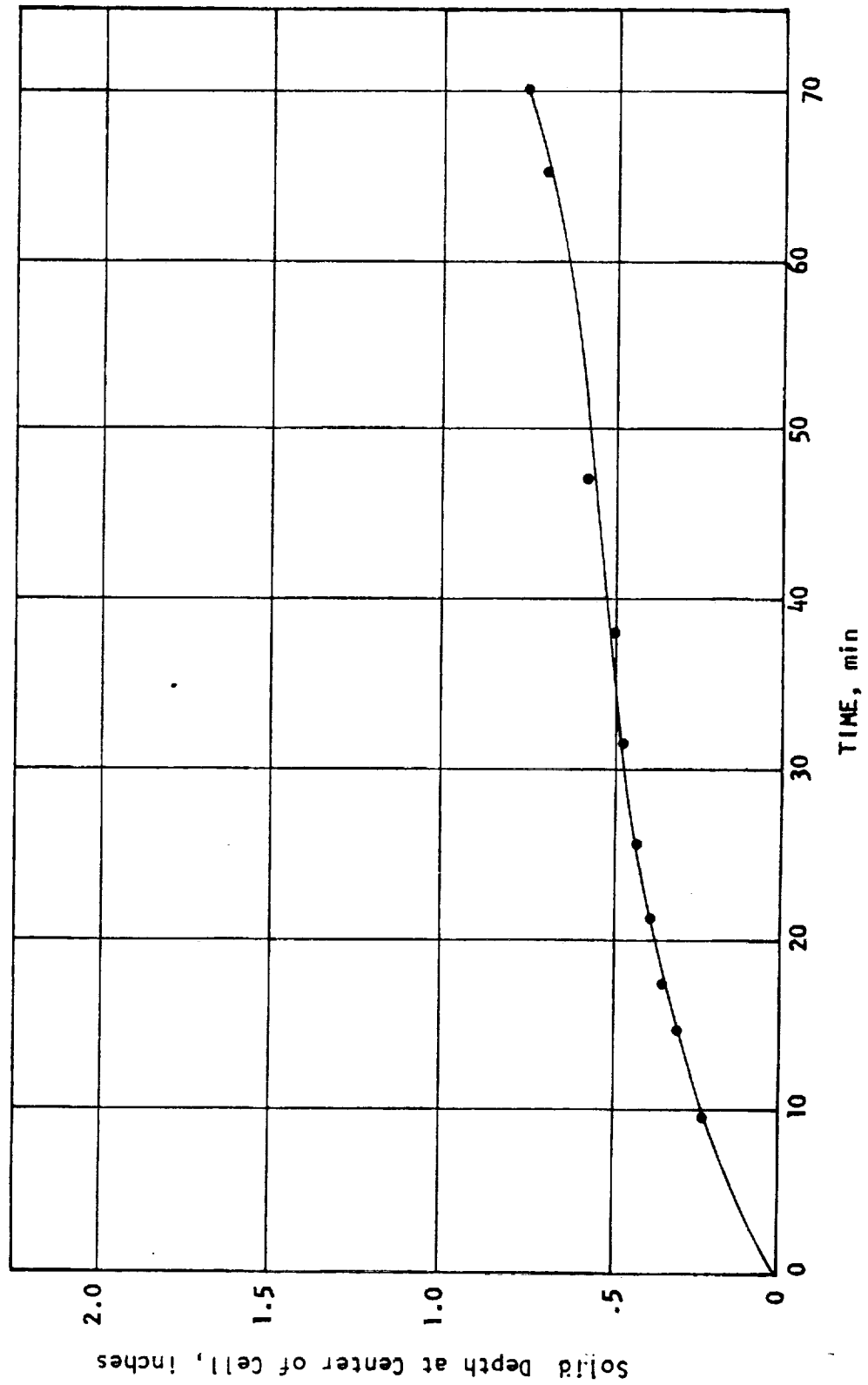
Figure 30.   Interfacial Data for Solidification Using Ice Bath and No Fins
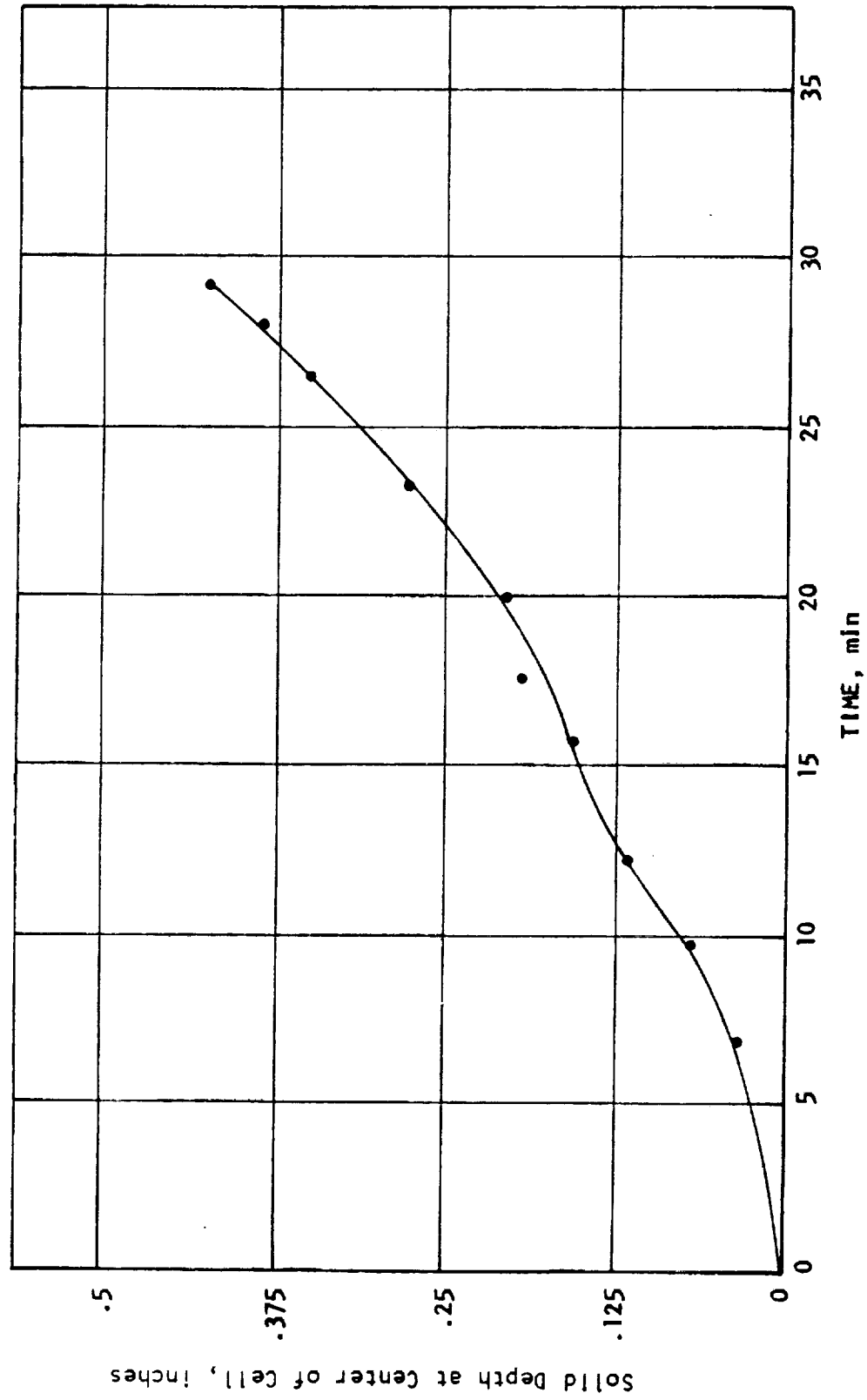
Figure 31. Interfacial Data for Solidification Using Ice Bath and 3/4 Inch Spaced Fins
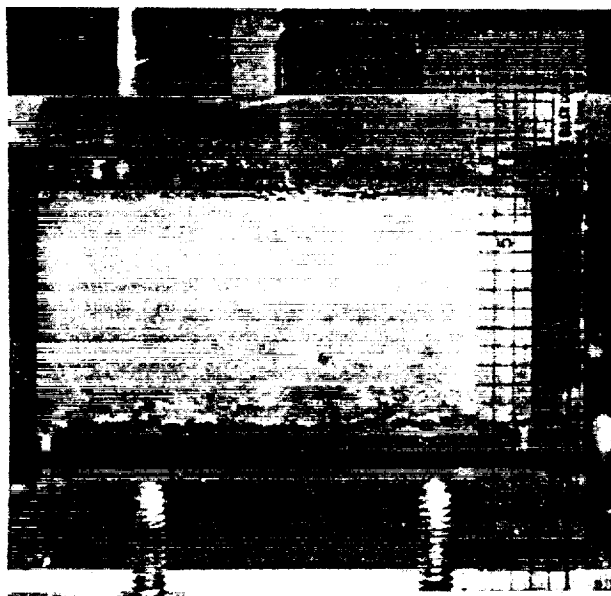
Figure 32. Photograph of Melting Without Fins
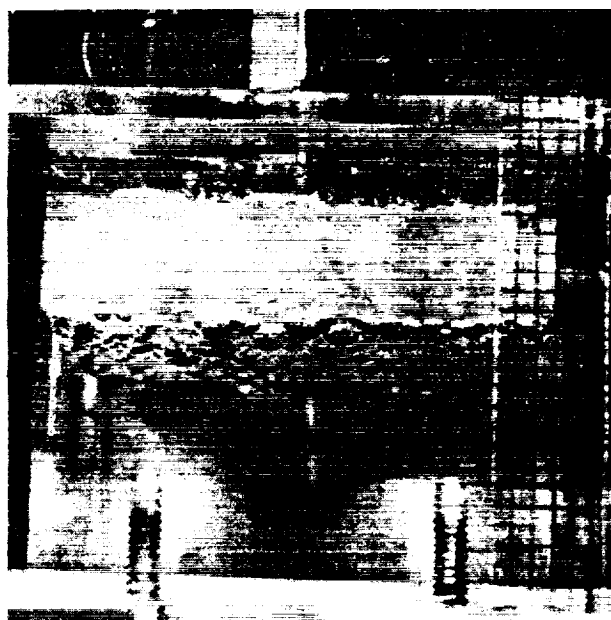


Figure 33. Photograph of Melting Without Fins
Illustrating Presence of Bubbles at
the Interface
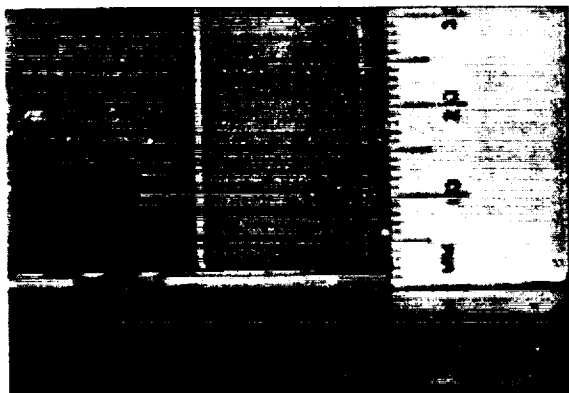
(a) 3 minutes after start
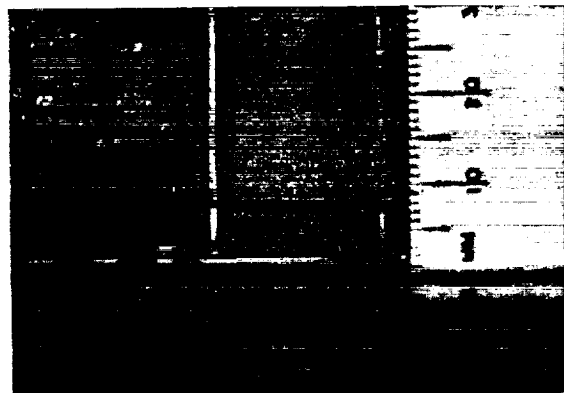
(b) 6 minutes after start
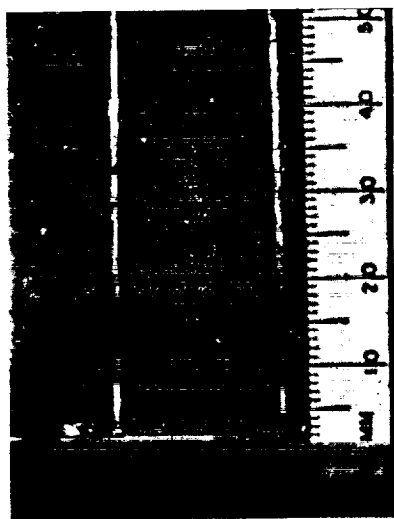
(c) 12 minutes after start
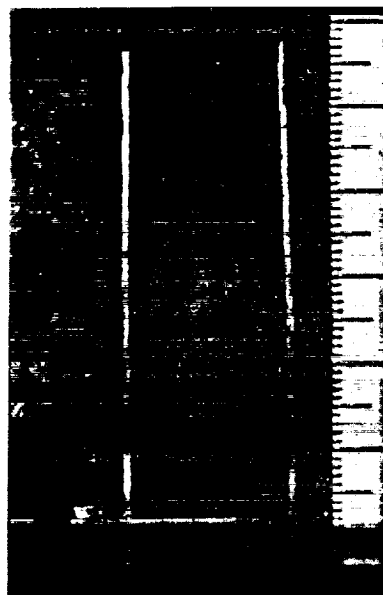
(d) 18 minutes after start

Figure 34.  Sequence of Photographs of Melting with 3/4 Inch
            Spaced Fins (Bath Temperature of 115°F)
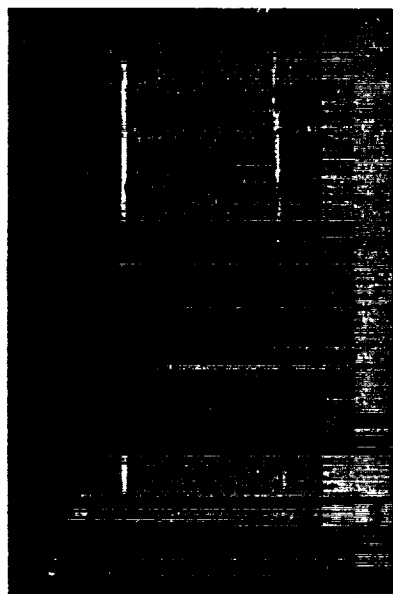
(a) 24 minutes after start

(b) 31 minutes after start

(c) 35 minutes after start
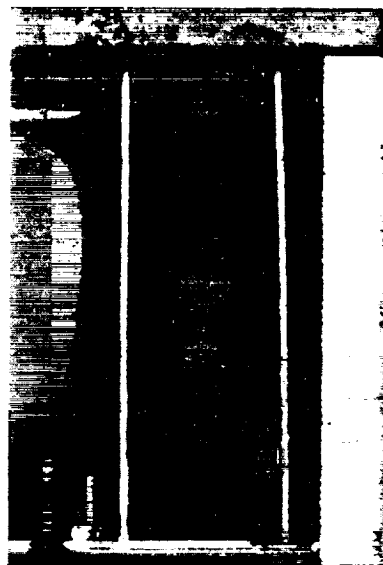
(d) 45 minutes after start

Figure 35. Continued Sequence of Photographs of Melting with 3/4 Inch Spaced Fins (Bath Temperature of 115°F)

a sequence of photographs of melting with 3/4 inch spaced fins. Figures
36(a) through 36(f) represent a sequence of photographs of freezing with
3/4 inch spaced fins while Figures 37(a) through 37(d) show freezing
with 1/4 inch spaced fins.

Bubbles were observed to agglomerate at the interface in the melting
tests. These appeared consisently even when a sample of paraffin had been
repeatedly melted and solidified. Figure 33 illustrates their presence
for the case where no fins were present.

Comparison of Figures 18 and 20 reveals that, for cases of approximately
the same base temperature, the rate at which the wax melted in the center
of the cell was faster for the case of no fins that it was for the case
of 3/4 inch spaced fins. Figures 34(a) through 34(d) and Figures 35(a)
through 35(d) aid in an explanation of this. The paraffin melted rapidly
adjacent to the fin along the entire height of the fins. Toward the
latter stages of melting, a slug of solid was left suspended in the liquid.
Adherence of this slug to the end plexiglass plates is apparently the
reason that the slug did not fall. The convective patterns in the liquid
for a situation such as that illustrated in Figure 35(c) are different
than those which occur when the liquid remains enclosed as is the case
when the heat transfer along the fins is insufficient to cause early
melting. This suggests that success in using the steady state correlation
of Reference 1 in predicting interfacial position at the center of the
cell is probably limited to cases where the interface progression is near
planar.

Figures 36(a) through 36(f) and Figures 37(a) through 37(d) illustrate
the strong influence of high conducting fins on the solidification process.
The presence of dendrites is also evident.

(a) 3.5 minutes after start

(b) 6 minutes after start

(c) 9 minutes after start

(d) 19 minutes after start

(e) 30 minutes after start

(f) 35 minutes after start
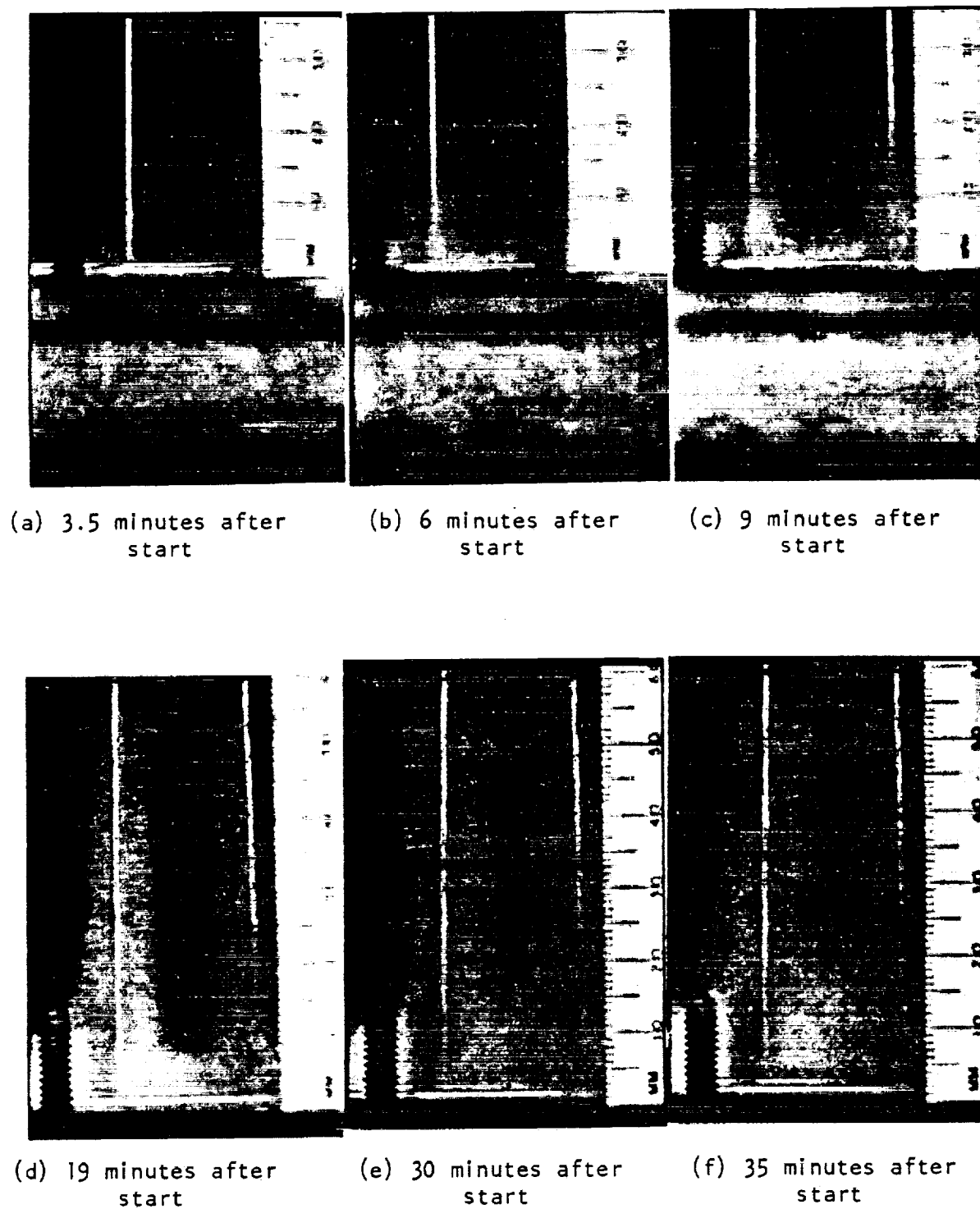
Figure 36.  Sequence of Photographs of Freezing with 3/4 Inch Spaced Fins
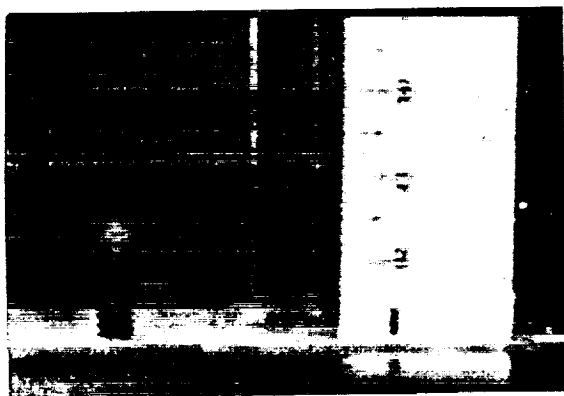
(a) 5.5 minutes after start
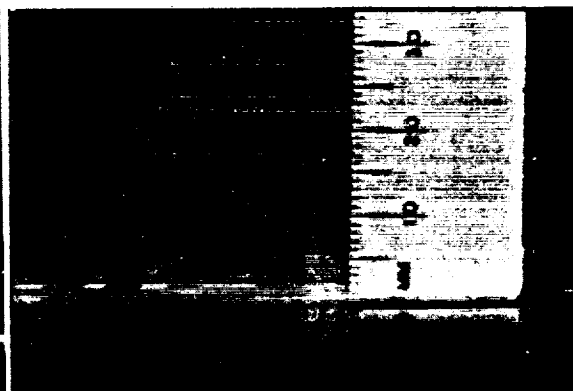
(b) 8.5 minutes after start
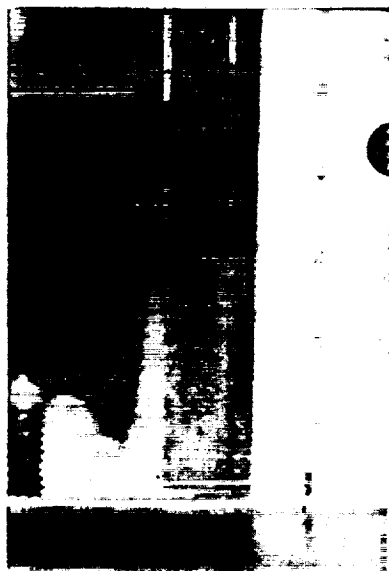
(c) 10.5 minutes after start

(d) 12.5 minutes after start

Figure 37. Sequence of Photographs of Freezing with 1/4 Inch Spaced Fins

## III.  EXPERIMENTAL INVESTIGATION OF UNIT WITH FILLERS

Apparatus and Procedure:

An experimental study was made of the heat transfer to a rectangular
enclosure filled with nonadecane.  Tests were performed without fins
included, with fins, and with aluminum honeycomb as a filler.  Each
experimental arrangement was heated from below using an electrical
resistance heater.  Total heat flux was measured by means of a flux
meter which is described later.  Electrical power measurements were not
used because of the uncertainty in the losses and the amount of energy
stored in the supporting structure for the heater.

A sketch of the experimental unit and unit housing are shown in
Figure 38.  The housing provided support and insulation for the
experimental unit.  The depth of the unit perpendicular to the plane
of Figure 38 was 5 inches.  The unit consisted of the following components.

The heater was a coiled wire having an electrical resistance of
4.3 ohms.  It was supported within a 1/2 inch thick ceramic block.  A
1/4 inch thick aluminum distribution plate was placed on top of the ceramic
block to reduce the nonuniformity of the heating.  Next, a heat flux
meter which consisted of a 1/4 inch piece of glass sandwiched between two
1/16 inch aluminum plates was located above the distribution plate.  The
paraffin was in contact with the top of the meter as shown so that the
upper surface of the heat flux meter served as the bottom (heated) surface
of the test unit.  The fins were either attached to the heated surface
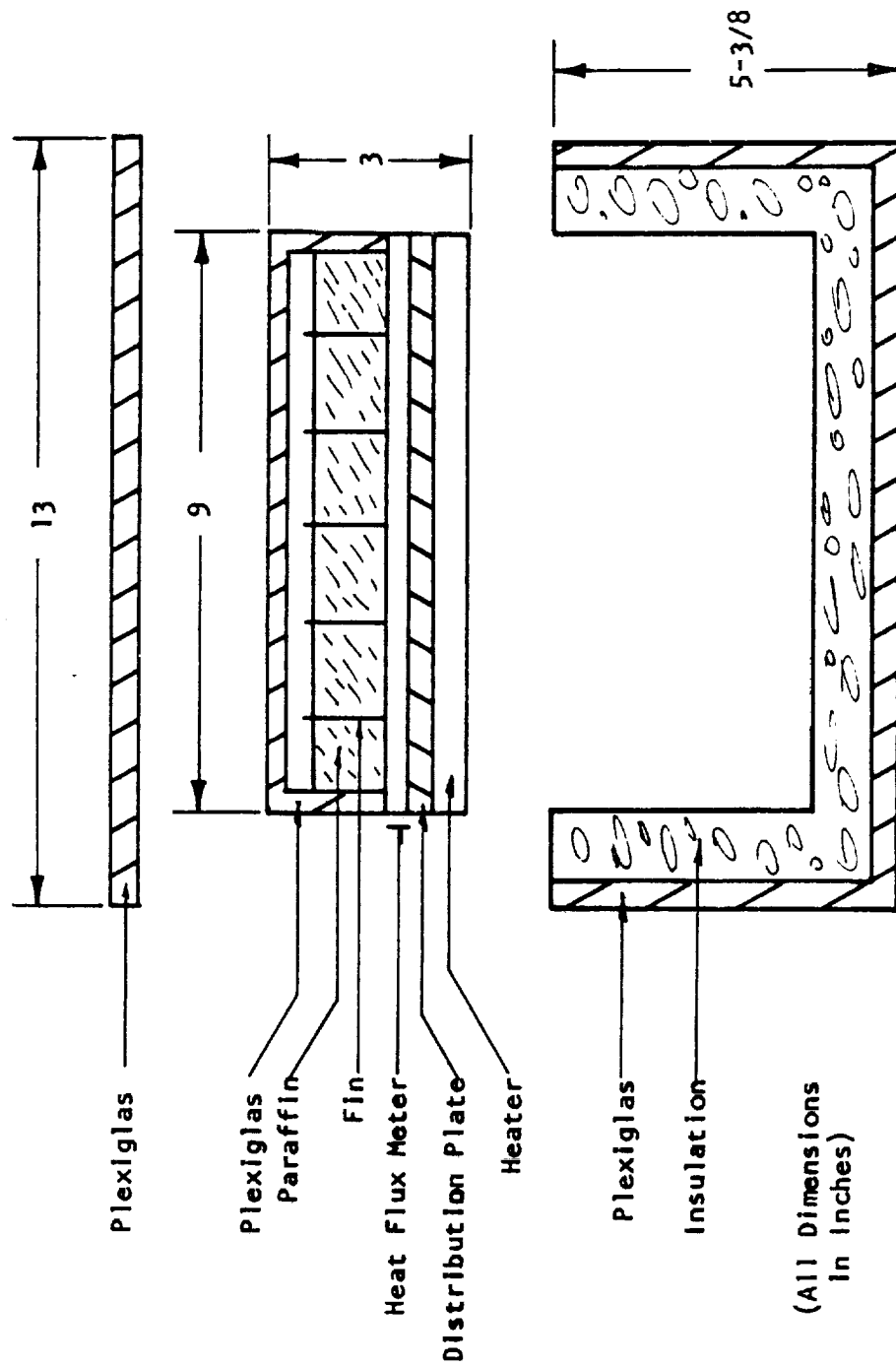
Figure 38. Experimental Unit and Unit Housing

with an aluminum base solder or, in the case of a honeycomb filler material, were forced against this surface with the aid of a weight. There was a small air space above the upper surface of the paraffin, and the enclosure was capped with a 1/4 inch thick plexiglass plate.

The fins were made of 1/16 inch aluminum plate positioned vertically in the unit. The honeycomb filler material which was used had a hexagonal cross section, 1/4 inch in minor diameter and 5/16 inch in major diameter. It was constructed of .003 inch thick aluminum sheet. Both the honeycomb and fins were 1-1/2 inches in height.

The heat flux meter was made of 1/4 inch window glass bonded between two 1/16 inch sheets of aluminum. The bonding material was a thin layer of aluminum base liquid solder. Eight thermocouples were attached to the meter, four in the upper aluminum plate and four in the lower plate. Each set of four was connected in parallel so that a single average temperature could be measured on either side. Both temperatures were monitored on a Honeywell Electronik 194 recording potentiometer. Thus, the $\Delta T$ across the glass plate was measured as a function of time. The assumption was made that each 1/16 inch aluminum plate was uniform in temperature because the thermocouples embedded in the plate were not exactly at the surface of the glass. To check the validity of this assumption, the Biot modulus Bi was estimated. The error introduced by the assumption that the aluminum plate is uniform in temperature is less than 5 percent if Bi < 0.1. Considering the upper aluminum plate, the significant length is 1/16 inch, $K_s$ is about 118 BTU/hr-ft°F, and h at the upper surface is about 45 BTU/hr-ft$^2$°F based on some preliminary experimental results. In this case, Bi = 0.00199 so the error introduced

here should be negligible.

To use the meter as a means of measuring heat flux, the assumption was made that the heat transfer per unit area is given by the temperature difference across the meter divided by the thermal resistance of the glass. This may be questionable since a certain amount of energy is retained in the meter. This stored energy is not considered in the simple steady state approximation. This problem was more severe during the first few minutes of an experiment when the temperatures were being brought to a desired level. It was observed from these experiments that the desired temperatures could be attained in about 15 minutes after melting begins; thereafter, a reasonably steady flux meter mean temperature could be maintained. Therefore, the following results are presented neglecting the first 15 minutes of each experiment.

A question still remains concerning the steadiness of this reasonably steady mean temperature after the initial fifteen minutes. For these experiments, the greatest rate of mean temperature change after the first 15 minutes was $4.3°F$ in a 35 minute period. Considering the heat flux meter as an energy absorbing mass, it absorbed $1.04$ BTU/ft$^2$ per $°F$ rise in temperature, or a total of $4.46$ BTU for each ft$^2$ of meter surface. Over the 35 minute period the rate of absorbed energy was $7.68$ BTU/hr-ft$^2$. The average total heat flux through the meter based on the $\Delta T$ across the meter was about $168$ BTU/hr-ft$^2$. This means that the magnitude of the absorbed energy is only about $4.6$ percent of the magnitude of the heat flux through the meter. This was, however, the maximum for all the experiments conducted, the percentages being less in most cases.

The general procedure for conducting experiments was to begin with

the entire system at room temperature (about 72°F). Voltage was then applied to the resistance heater. Initially, the voltage was set at 20 volts until the heated surface temperature $T_s$ was between 100°F and 105°F. At this time the input was reduced to about 10 volts so that the temperatures would quickly begin to approach a constant level. Then the voltage was adjusted manually to keep the mean temperature of the meter fairly constant. About fifteen minutes after $T_s$ had reached the melting temperature, the mean temperature had reached an approximately steady value. The surface temperature $T_s$ at this steady condition was about 105°F, but this varied a few degrees from experiment to experiment.

The time and temperatures on each side of the meter were all automatically recorded on the recording potentiometer. For those experiments where no fins were present, the interface location was measured. The experiments proceeded until the paraffin had melted or until the unmelted paraffin began to fall to the heated surface. This condition occurred during experiments with fins when about 90 percent of the solid had melted.

All experiments were repeated at least once although the surface temperatures were not exactly reproduced. Therefore, the heating rates for similar experiments were not exactly the same.

No data were taken of the interface location during the fin or honeycomb experiments. When fins were included, the interface had a parabolic shape as would be expected.

Four experimental arrangements were tested. Each experiment is described by a letter code. Experiments A, B, and C were conducted using no fins or filler material of any kind. Experiments D and E

utilized the honeycomb filler material described earlier. Experiments F and G used 1/16 inch aluminum fins placed 1-1/16 inch apart. Experiment H was conducted with the same fins placed 13/16 inch apart.

The heat flux through the meter is given by

$$\dot{q}/A = k_g (\Delta T)_g / \Delta x \tag{1}$$

where $k_g$ is the glass conductivity, $\Delta x$ is the thickness of the glass, and $(\Delta T)_g$ is the temperature difference across the glass. The convective heat transfer relation is

$$\dot{q}/A = h (\Delta T)_c \tag{2}$$

where $h$ is the convective heat transfer coefficient and $(\Delta T)_c$ is the appropriate temperature difference. In this case, this difference was taken to be $(T_s - T_f)$, the difference in the surface and fusion temperatures. A fundamental assumption of this approach was that all of the energy which crossed the meter entered the paraffin by being convected from the heated surface or conducted through the fins. There was some heat loss from the sides of the meter, but this loss was considered to be small because of insulation and the small area involved. Therefore, setting Equations (1) and (2) equal, it follows that

$$h = \frac{k_g}{\Delta x} \frac{(\Delta T)_g}{(\Delta T)_c} \tag{3}$$

Equation (2) incorporates the assumption that sensible heating of the solid phase is negligible.

The published thermal conductivity of glass is approximately 0.45 Btu/hr-ft°F. This varies according to the type of glass. There was also

a possibility of some contact resistance between the glass and the aluminum plates. Because of this uncertainty, $K_g$ was left as an unknown. The quantity $h/k_g$ was then determined from experimental measurements and the relation

$$\frac{h}{k_g} = \frac{1}{\Delta x} \frac{(\Delta T)_g}{(\Delta T)_c} \tag{4}$$

This quantity has the units of $ft^{-1}$.

Experimental Results:

Figure 39 is a summary of some experimental results of $h/k_g$ as a function of time from the start of melting. As discussed earlier, the first 15 minutes are omitted because of the initial transients. Only one experiment for the case of 1/16 inch fins spaced 13/16 inch apart is included. The solid paraffin fell early during the attempt to repeat this experiment.

The three experiments using no fins demonstrate generally good agreement. The heat transfer coefficient changed very little in time and was less than the values for experiments with fins or honeycomb.

The two tests with the honeycomb filler show some disagreement, but both show a similar decline of h with time. The difference in the average value of these two experiments is probably a result of different contact resistances between the honeycomb and the surface. This was a forced, rather than a bonded contact, and good contact was not positively attained.

The two experiments using 1/16 inch fins spaced 1-11/16 inches apart show high initial values of h which decrease rapidly and then approach
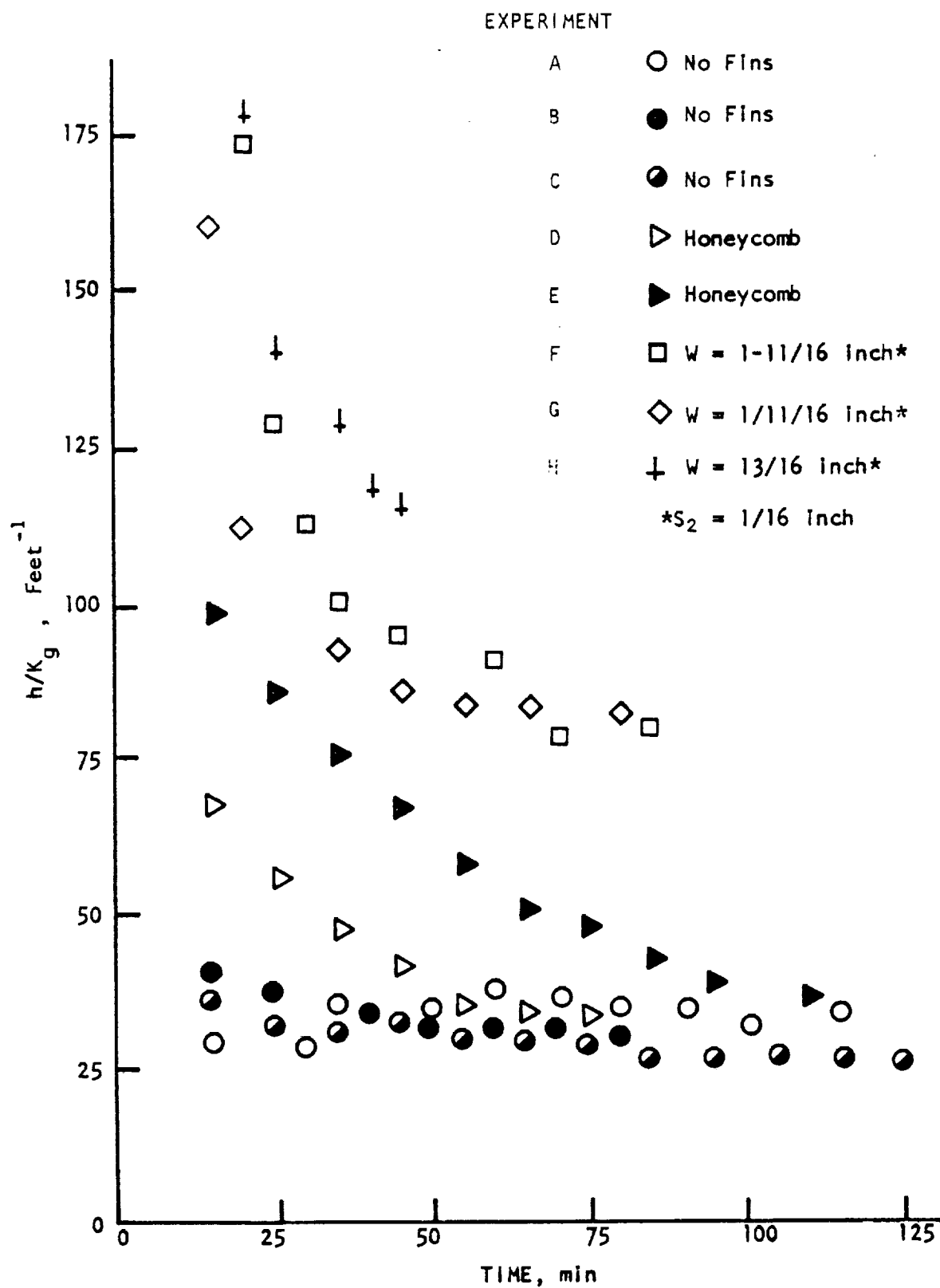
Figure 39. Relationship Between h/K$_g$ and Time

a constant value.

Experiment H shows a rapid initial decrease in h. The bulk of the paraffin melted so fast that an asymptotic value of h was not reached.

The work of O'Toole and Silveston (1) as discussed in Part V of this report makes it possible to compare the melting experiments containing no fins with previous steady experiments. Those authors reviewed a large quantity of data dealing with steady state convection between horizontal layers, and they presented the results as a plot of Nu versus Ra. They performed a regression analysis to obtain the best fit equations relating the Nusselt number to the Rayleigh number. In order to compare the steady state predictions to the melting data obtained without fins, the characteristic height used in the Rayleigh number was the location of the interface above the heated surface. The properties of nonadecane given in Appendix A were used and the value of the thermal conductivity of glass was assumed to be 0.45. Since the interface location was a function of time, comparisons were made at several time values during the duration of Experiment C. The comparisons of experimentally determined Nusselt numbers and those given by the correlation of O'Toole and Silveston are given in Table 1. The agreement is considered good when considered in light of the sources of uncertainties introduced. A possible significance of this agreement is that the steady state predictions may be used with some confidence for a transient phase change problem for the range of conditions experienced in this work.

Table 1.  Comparison of Predicted and Experimental Nu Values for
         Experiment C.

| Time (min) | L(inches) | Experiment C | | Predicted |
| | | Ra | Nu | Nu |
|---|---|---|---|---|
| 20 | .10 | 1,200 | -- | -- |
| 30 | .18 | 6,100 | 2.56 | 2.06 |
| 40 | .26 | 18,700 | 3.56 | 2.73 |
| 50 | .34 | 47,000 | 4.28 | 3.45 |
| 60 | .42 | 89,000 | 5.30 | 4.05 |
| 70 | .50 | 159,000 | 6.26 | 5.69 |
| 80 | .58 | 249,000 | 6.60 | 6.52 |
| 90 | .66 | 343,000 | 7.18 | 7.21 |
| 100 | .74 | 466,000 | 8.36 | 7.90 |
| 110 | .82 | 619,000 | 9.05 | 8.62 |
| 120 | .90 | 812,000 | 10.00 | 9.37 |

## IV. NUMERICAL STUDY

A portion of the overall study was devoted to a numerical analysis of a two-dimensional symmetrical section of a typical PCM capacitor cell formed by use of straight fins. A schematic of such an arrangement is shown in Figure 40.

When solving a heat conduction problem numerically, finite difference analogs for the appropriate terms in the conduction equation are formulated. These formulations may be made using an implicit approach or an explicit approach. These two approaches can be outlined for a two-dimensional nodal network with the aid of the notation shown in Figure 41.
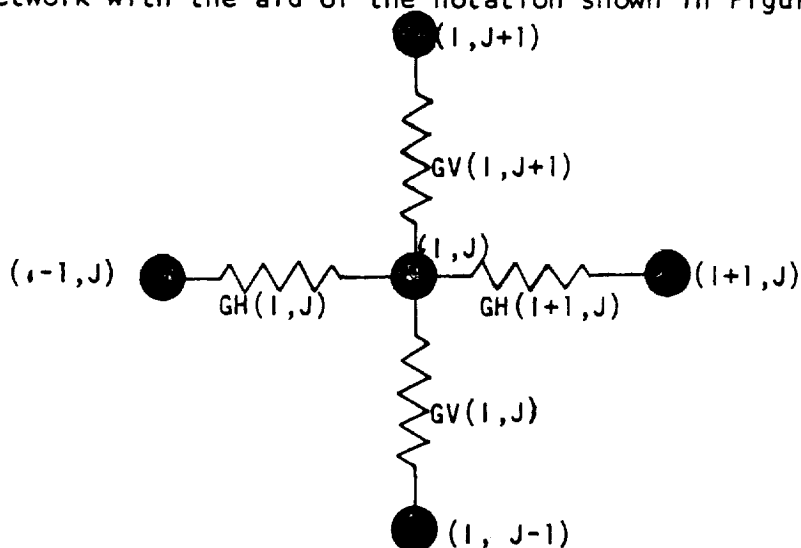


Figure 41.    General Nodal Designation and Interconnecting
              Thermal Conductance Notation

Figure 41 illustrates a general node (I, J), its four adjacent nodes, and the notational scheme for designation of the interconnecting thermal conductances. Physical arguments can be used to formulate the difference analogs. The summation of heat transfer to node (I, J) from all adjacent nodes should equal the product of the nodal capacitance and the difference in its old and new temperature. With reference to Figure
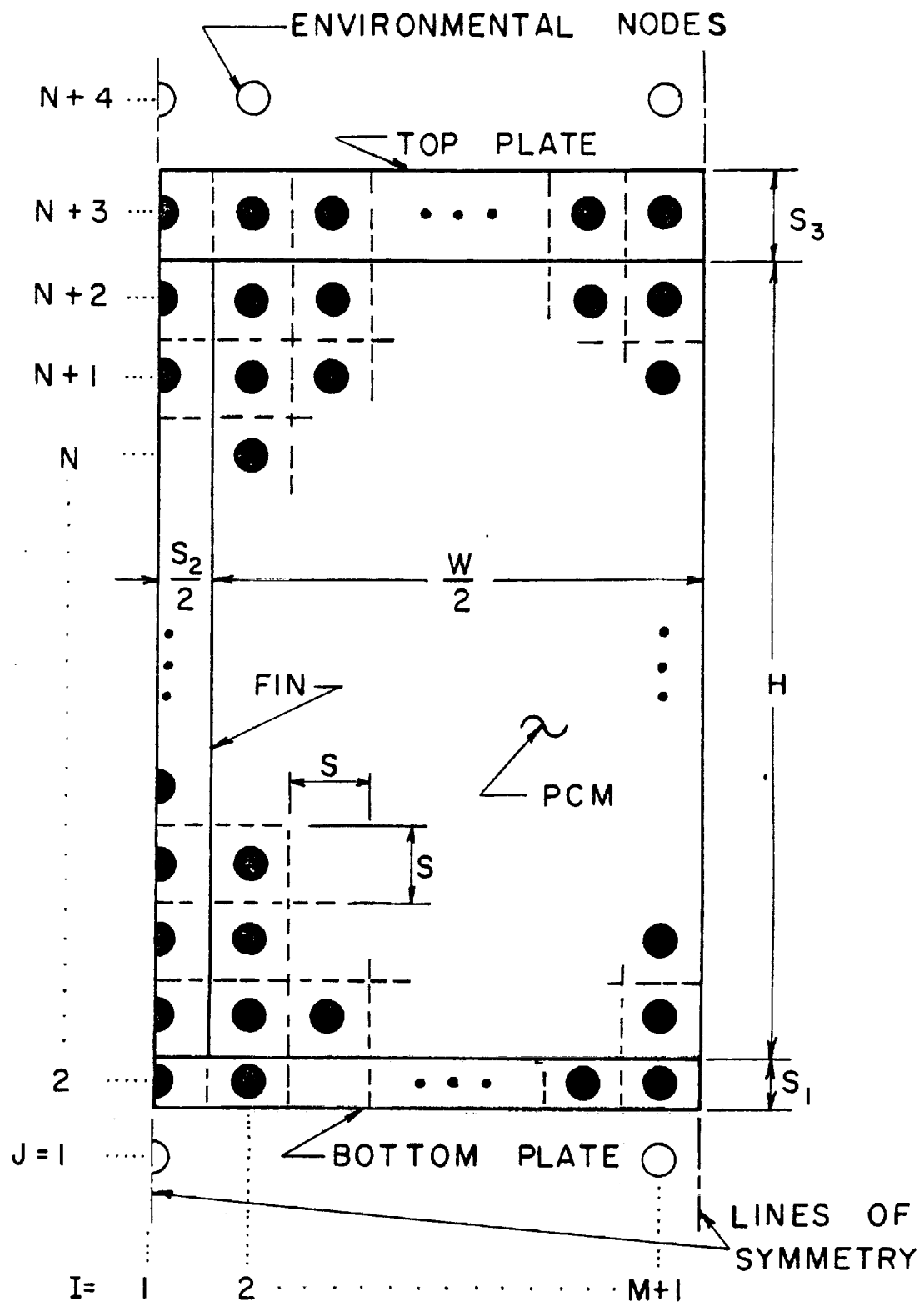
Figure 40. Symmetrical Section of Cell and Nodal Arrangement.

41, the explicit formulation based on this physical approach is

$$GH(I,J)[T(I-1,J) - T(I,J)] + GH(I+1,J)[T(I+1,J) - T(I,J)]$$

$$+ GV(I,J)[T(I,J-1) - T(I,J)] + GV(I,J+1)[T(I,J+1) - T(I,J)]$$

$$= \frac{C(I,J)[T'(I,J) - T(I,J)]}{\Delta t} \tag{5}$$

In this explicit formulation, all temperatures used in determining the heat transfer are evaluated at the old time level. The implicit formulation is

$$GH(I,J)[T'(I-1,J) - T'(I,J)] + GH(I+1,J)[T'(I+1,J) - T'(I,J)]$$

$$+ GV(I,J)[T'(I,J-1) - T'(I,J)] + GV(I,J+1)[T'(I,J+1) - T'(I,J)]$$

$$= \frac{C(I,J)[T'(I,J) - T(I,J)]}{\Delta t} \tag{6}$$

In the implicit formulation, all temperatures used in determining the heat transfer are evaluated at the new time level. In equations (5) and (6), primes denote temperatures evaluated at the new time level.

Numerical solution of the explicit formulation given by equation (5) is straightforward but subject to a restriction (see Reference 2) on the allowable time step given by

$$\Delta t \leq \frac{C(I,J)}{GH(I,J) + GH(I+1,J) + GV(I,J) + GV(I,J+1)} \tag{7}$$

For a nodal arrangement, the node whose characteristics yield the smallest time step as given by equation (7) governs the entire solution. For a typical finned PCM capacitor, inclusion of fin temperatures as unknowns introduces a severe time restriction. The thermal capacitance of a fin node is very low while the vertical conductances along the fin are large.

The implicit formulation is not restricted by a stability requirement, but the solution is not as simple. Solution of a system of nodes involves solving simultaneously a set of equations equal in number to the number of nodes. In general, this requires a general matrix inversion routine.

Reference 3 has outlined an alternate method known as the alternating-direction-implicit method (ADI). The method involves writing the analogs to the space derivatives explicitly in one direction and implicitly in the other. This set of equations are solved for one time step then the formulations are reversed. This second formulation is then solved for one time step and the resulting solution is taken to be correct. As an example pertinent to Figure 40 an implicit formulation in the horizontal direction (J = constant) and an explicit formulation in the vertical direction (I = constant) is

$$GH(I,J)[T'(I-1,J) - T'(I,J)] + GH(I+1,J)[T'(I+1,J) - T'(I,J)]$$
$$+ GV(I,J)[T(I,J-1) - T(I,J)] + GV(I,J+1)[T(I,J+1) - T(I,J)]$$

$$= \frac{C(I,J)[T'(I,J) - T(I,J)]}{\Delta t} \tag{8}$$

When equation (8) has been written for all nodes along a horizontal row (J = constant), the system of equations constitute a tridiagonal coefficient matrix and the solution can readily be obtained by means of the Thomas algorithm described in Reference 3. The formulation which is implicit in the vertical direction and explicit in the horizontal direction is

$$GH(I,J)[T(I-1,J)-T(I,J)] + GH(I+1,J)[T(I+1,J)-T(I,J)]$$
$$+ GV(I,J)[T'(I,J-1)-T'(I,J)] + GV(I,J+1)[T'(I,J+1)-T'(I,J)]$$

$$= \frac{C(I,J)[T'(I,J) - T(I,J)]}{\Delta t} \tag{9}$$

The ADI method consists of either solving equation (8) successively for each horizontal row and then reversing directions and successively solving equation (9) for each vertical row or vice-versa. For the first case, time is advanced by one time increment and equation (8) is successively solved for each horizontal row. The temperatures thusly predicted are not considered correct; they are, however, next used as old values in solving equation (9) successively for each vertical row. At this time, the resulting temperatures are considered correct. This alternating scheme is then continuously repeated to achieve the desired solution. It is stated in Reference 3 that this method has been shown to be stable for any ratio of time increment to space increment as long as the same time increment is used for the successive applications of equations (8) and (9).

Conceptually, the ADI method appeared attractive for the numerical problem considered in this work. Some effort during participation in the 1972 NASA/ASEE Summer Program was devoted to a study of its application. Pursuit along this line was exploratory since the discussion of the method in Reference 3 pertained to a homogeneous and isotropic medium. The method was formulated for a typical two-dimensional cell using the notation shown in Figure 41, and a Fortran computer program was written to facilitate computations.

For the preliminary exploration of the method, the problem was treated solely as a conduction problem without including any technique for handling the phase change. Since there appeared to be no stated preference as to which direction should be solved first in the alternating scheme, solutions were examined for both cases.

After several computer runs, it became evident that the ADI method applied to the fin-PCM problem was not independent of the time increment. When the procedure involved solving for unknowns along a horizontal row first, the solutions were unstable unless a sufficiently small time step was used. It was interesting that more reliable results were obtained when the procedure involved solving for unknowns along a vertical column first. The disappointing feature was that it seemed necessary to restrict the time step to that given by equation (7) in order for the solutions to be independent of the direction which was pursued first.

As a matter of interest, a modified formulation was considered where all temperatures along a horizontal row or along a vertical row were considered as new values when the values along that respective row were being sought. The horizontally implicit, vertically explicit formulation is

$$GH(I,J)[T'(I-1,J)-T'(I,J)] + GH(I+1,J)[T'(I+1,J)-T'(I,J)]$$
$$+ GV(I,J)[T(I,J-1)-T'(I,J)] + GV(I,J+1)[T(I,J+1)-T'(I,J)]$$
$$= \frac{C(I,J)[T'(I,J) - T(I,J)]}{\Delta t} \qquad (10)$$

The horizontally explicit, vertically implicit formulation is

$$GH(I,J)[T(I-1,J)-T'(I,J)] + GH(I+1,J)[T(I+1,J)-T'(I,J)]$$
$$+ GV(I,J)[T'(I,J-1)-T'(I,J)] + GV(I,J+1)[T'(I,J+1)-T'(I,J)]$$
$$= \frac{C(I,J)[T'(I,J) - T(I,J)]}{\Delta t} \qquad (11)$$

While there are no defendable physical arguments to support this modified approach as given by equations (10) and (11), their solution by the ADI technique yielded results which appeared relatively good. The predicted

PCM temperatures were slightly lower than the values given by the direct ADI method using the small time increment.

Numerical Solutions Using the Explicit Formulation:

The prime handicap in using the explicit approach is the restriction on the allowable time step. The approach was utilized in an effort to obtain prediction that could be compared with some MSFC in-house data. In this case, the time step restriction was circumvented since measured temperatures along the fins were used as boundary conditions thereby eliminating temperatures of the small capacitance fin nodes from the list of unknowns. This effort was originated in the summer of 1971 and pursued further under the objectives of this work.

In this numerical study attention was focused on a symmetrical section of a typical cell. The section was subdivided into a network of nodes and a Fortran computer program was written to facilitate numerical heat transfer predictions. The section and nodal arrangement are shown in Figure 40. There are MXN nodes in the PCM where M and N denote integers. While the computer program was written to apply in general to any cell compatible with the geometry shown in Figure 40, runs were made using specific data corresponding to the in-house experimental work. For these experiments fin locations provided PCM cell widths of 0.25, 0.50 and 0.75 inches. The fins were strips of 0.008 inch thick aluminum. The bottom plate was 0.032 - inch thick aluminum. The top plate was 0.25 - inch thick plexiglass. The cell height H was about 2.5 inches and its length was 5.0 inches. The utilized PCM was nonadecane. A large amount of data was obtained for both freezing and melting tests. The data consisted of transient temperature measurements at several locations inside the capacitor and film histories of the fusion front motion.

The computational procedure started with specification of initial temperatures for all nodes and calculation of all pertinent parameters. Measured temperatures for the bottom plate and certain nodes along the fin were input as transient boundary conditions. At time t the heat transfer rate to each node was determined. This amounted to evaluation of the left-hand side of equation (5). This rate was stored and subsequently used to determine the temperature of the node at time t + $\Delta$t by equation (5). Before proceeding in time, the computation was iterated by computing again the heat transfer rate to node (I,J) using the new temperatures found by equation (5). Then the average of the old and new rates was then used in equation (5) to predict more accurate values of the new temperatures. This procedure was repeated at each time step.

For each node in the PCM, an accumulative record was maintained of the stored energy. When the nodal temperature reached the fusion temperature, it was held constant until sufficient energy had been absorbed or rejected to account for the latent heat of fusion. For each time step during the phase change, a fraction of the node which had changed phase was calculated based on the accumulated energy. The fraction was then used in predicting the location of the fusion front.

Appropriate modifications of the predictive equations were made for nodes located on or near a boundary. The only unique deviation of the above procedure was in connection with determining the unspecified fin temperatures. Since the thermal capacitance of a node on the fin was several orders of magnitude lower than that of a node in the PCM, steady state relations were used to compute the instantaneous unspecified fin

temperatures.

In an attempt to include convection in the melting cases, the technique involved computation of a modified or effective thermal conductivity of the liquid. Correlations reported in Reference (1) were used to determine the effective conductivity. The procedure required keeping track of the liquid and computing a new thermal resistance in the liquid at each time step.

The program facilitated computation of temperatures, heat transfer rates, fusion front location and other related quantities. A copy of the program and a description of the steps are included in Appendix B. It was later discovered that the program would not run for the case of M = 1, and the necessary modifications were made to make it compatible with this case also.

Several runs were made for both freezing and solidification cases. Those made during the summer of 1971 are tabulated in Appendix B. Comparisons were made between the predicted fusion front location at the center of the cell and the corresponding measured value. In all cases where only conduction was considered, the predicted values fell significantly below the measured values.

For the melting cases, inclusion of a convective effect through use of an effective liquid conductivity yielded much improved agreement. The rate of melting agreed well, and the only difference appeared at the start which is apparently a consequence of using finite node sizes.

For solidification cases, convection should not contribute. The solidification process is characterized by dendritic formations. The presence of these formations introduces a much larger solid liquid interfacial area than the planar value employed in the difference

formulations. As a matter of interest, the predictions were altered by increasing the thermal conductances leading to node (I,J) as it was undergoing phase change by a multiplicative area factor to artifically allow for a larger contact area. The results for two cases are compared to the corresponding MSFC in-house data in Figures 42 and 43. As the area factor is increased, more computer time is required because of the stability criterion. This is the reason that the predictions for the larger factors were terminated early in Figures 42 and 43. It is interesting to note that this scheme tends to yield the correct trends in the early stages of solidification. For the two cases considered, area factors larger than 40 would be required to match the data. A copy of the solidification program with accommodations to facilitate the area factor is also included in Appendix B.

Solutions Based on Modified ADI Method:

While the modified ADI scheme as outlined by equations (8) and (9) has not been justified physically, it was explored as a basis for conducting some parametric studies. Several computer runs were made for melting cases, and the corresponding results are presented here. In these cases, no attempt was made to account for convection. The system was considered initially to be at 72°F and the base temperature was suddenly changed to 110°F and held constant.

There is a particular difficulty associated with an implicit method when treating phase change problems. In the explicit method, a nodal temperature can be adjusted to the fusion temperature as the node experiences phase change. Since the explicit method is a forward marching process, this adjustment can be achieved prior to calculations for
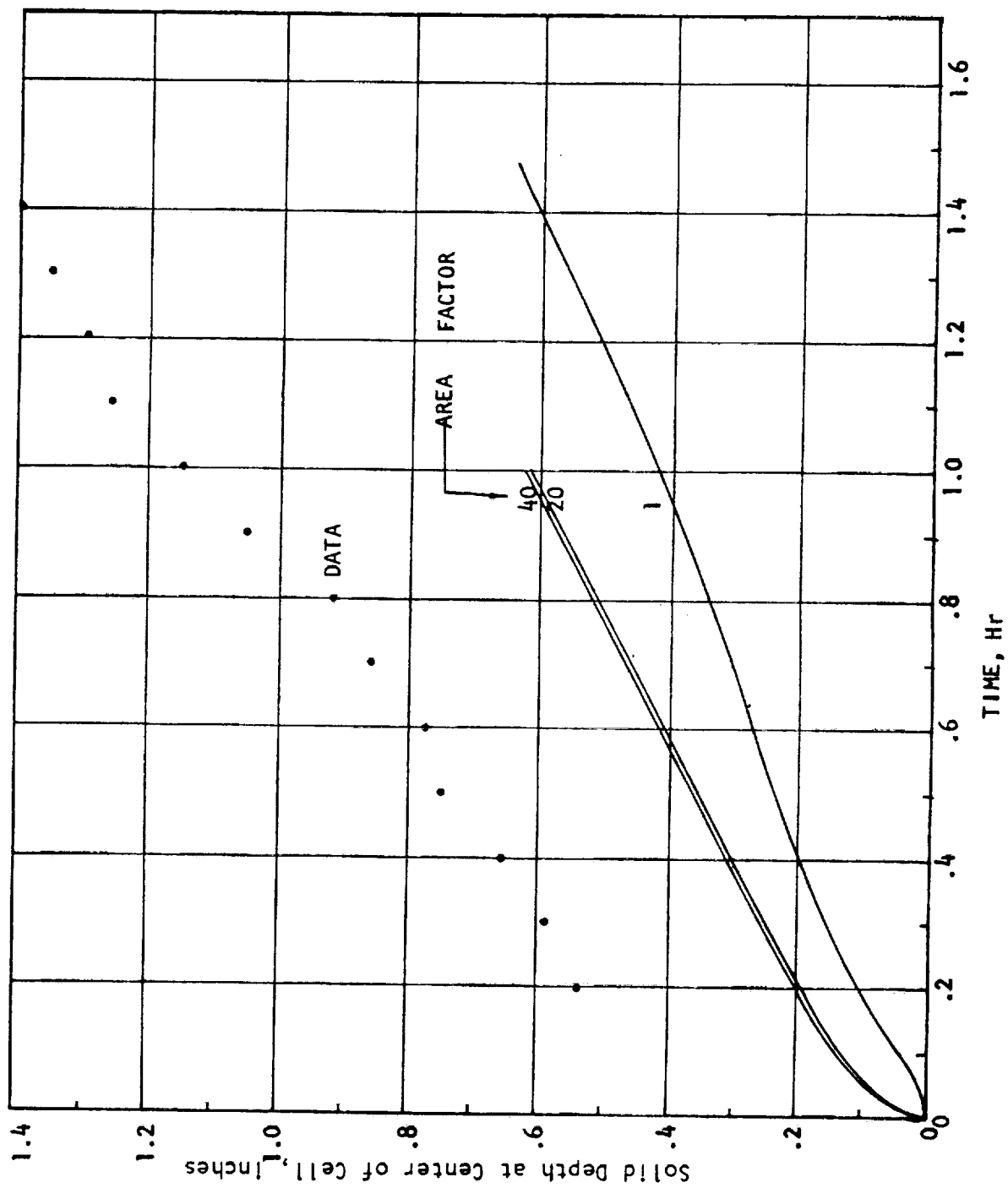
Figure 42. Comparison of Predicted Interfacial Positions at Center of Cell for MSFC In-House Solidification Run 230-15

neighboring nodes. However, since all nodal temperatures are predicted simultaneously in the implicit method, those nodes experiencing phase change are over predicted, and these values accordingly affect the accuracy of the predicted temperatures of neighboring nodes.

For the predictions presented here, when the temperature of a node exceeded its fusion value, the temperature was adjusted to the fusion value and the net heat transfer to the node from its neighboring nodes was calculated. The node was allowed to accumulate energy until the latent heat of fusion was matched. At this point, the node was considered to be melted, and its temperature was allowed to rise again.

The first set of numerical predictions is for constant cell height and width with fin thickness as a variable. The heat transfer from the heated surface to the paraffin plus that transferred through the fins was divided by the total area of the heated surface. This resultant heat transfer per unit area is plotted in Figure 44 as a function of time for several fin thicknesses. Each curve is terminated when the last solid paraffin node has completed its change of phase.

Figure 45 shows the total melt time as a function of fin thickness for two cell sizes. The melting time decreases with increasing fin thickness, but there appears to be little gain after a certain point.

For a particular cell height and fin thickness, the total melt time is plotted as a function of fin spacing in Figure 46.

The relative influence of the fins in transferring energy from the base to the paraffin is indicated in Figure 47 . This data indicates that the fins are the primary paths for energy transfer.

Page 69 missing
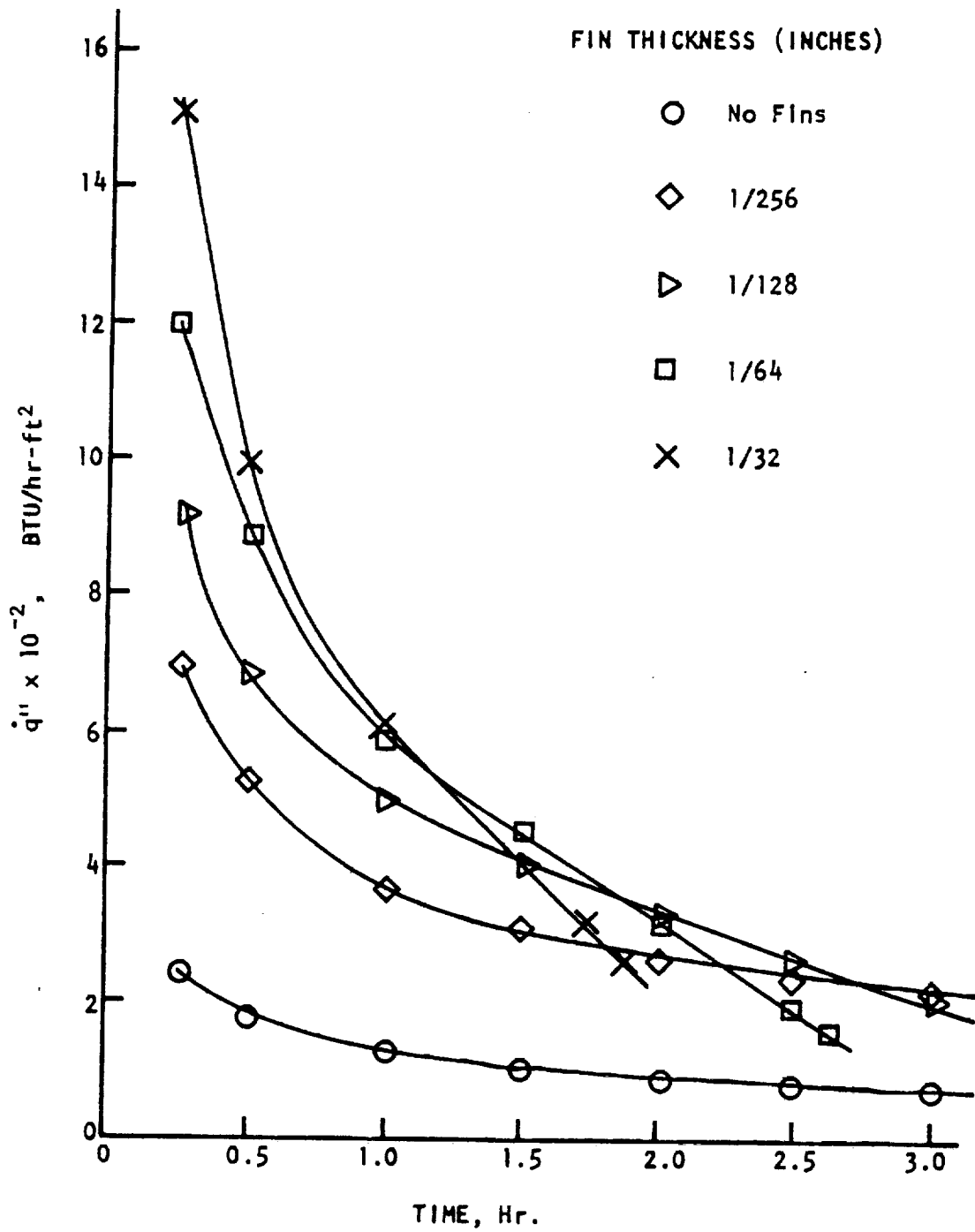
Figure 44. Heating Rate as a Function of Time for H = 0.156 Feet, W = 0.0625 Feet

FIN THICKNESS, Inches
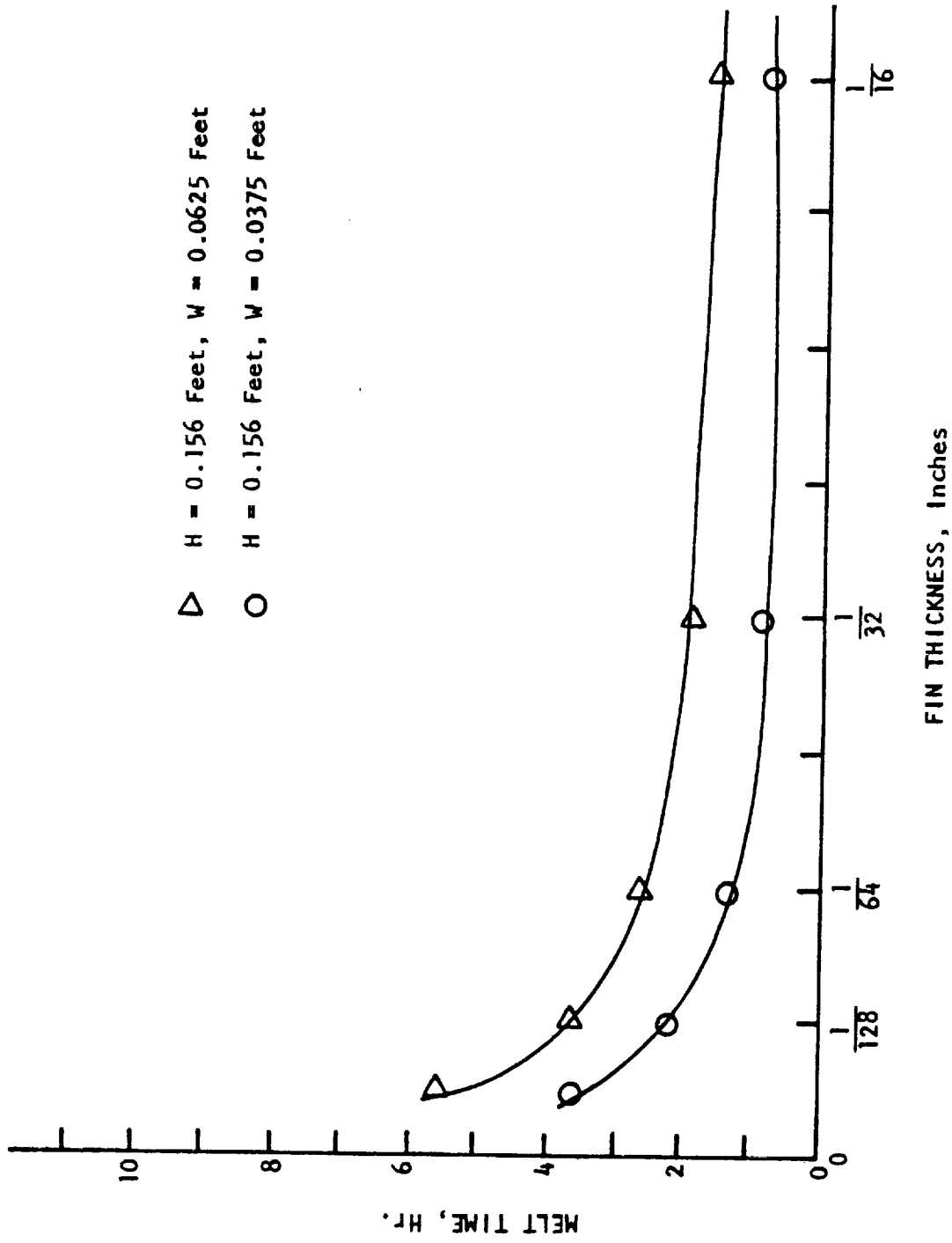
Figure 45. Melt Time as a Function of Fin Thickness

△  H = 0.156 Feet, W = 0.0625 Feet

○  H = 0.156 Feet, W = 0.0375 Feet

MELT TIME, Hr.

MELT TIME, Hr.

FIN SPACING, Feet

H = 0.156 Feet

$S_2$ = 1/32 Inches
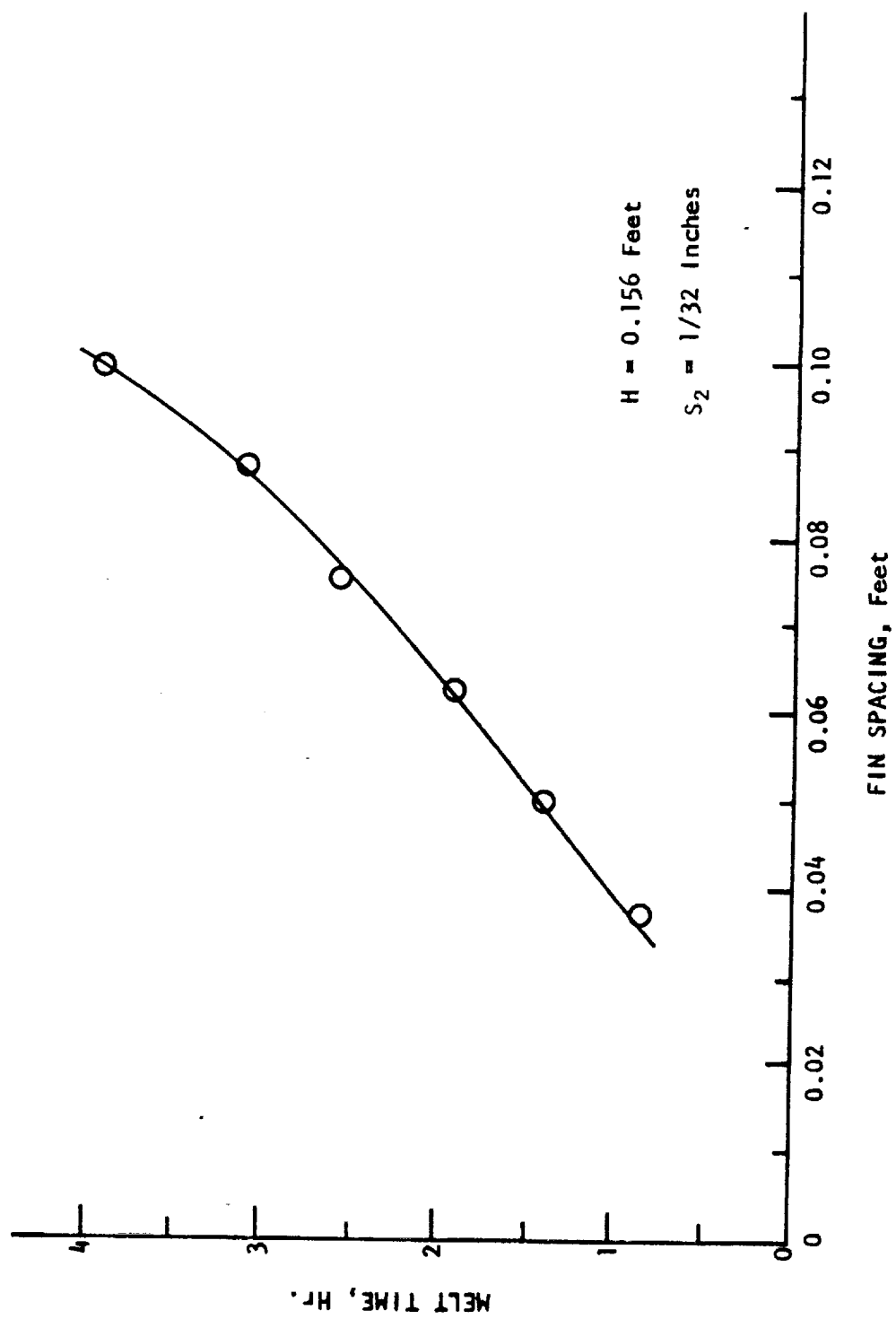
Figure 46. Melt Time as a Function of Fin Spacing
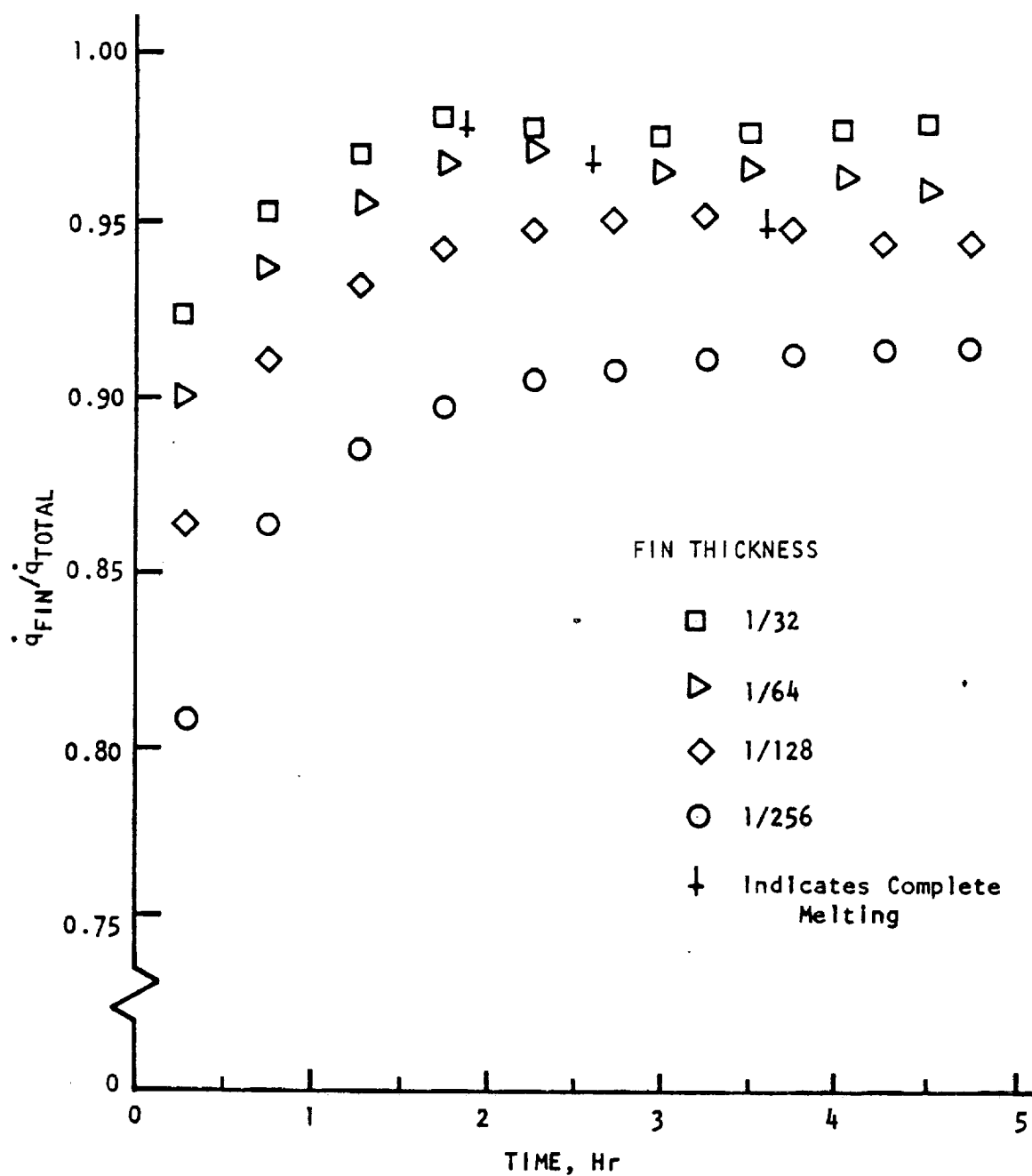
Figure 47. Ratio of Fin Heat Flux to Total Heat Flux as a Function of Time for H = 0.156 Feet and W = 0.0625 Feet

## V.  CONCLUSIONS AND RECOMMENDATIONS

General Observations:

With regard to the objectives of tasks 1, 2, 3, and 4, the results of the basic experiments which were described in part II of this report yield considerable insight.  These results not only support but strengthen the explanations of some previous thermal capacitor test data.  The temperature indicated by a thermocouple placed within a PCM as it is heated from below shows a slow, continuous transient rise until the interface has passed the thermocouple leaving it exposed in the liquid.  Once out in the liquid, the thermocouple indicates a pseudo temperature plateau.  The level of this plateau is a function of the base plate temperature as well as the material of the walls confining the PCM.  This plateau is not a well defined one since there is some variation in the average temperature.  The existence of this apparent plateau is explained by the presence of convective currents in the liquid which tend to mix the liquid layer thereby producing a near isothermal core region.  The duration of this plateau depends on the period of time that the thermocouple is exposed to this region.  The long time variation along with the superposed short time variation of the temperature reveals, however, the non-steady character of the currents.  The number of possible convective patterns and their dependence on cell geometry even for steady state conditions which have recently been reported by Prensner and Hsu (4) attest to the formidable task of predicting the transport mechanism in the liquid layer.  The convection does make a significant contribution to the heat transfer rate.  This is evident from the increased melting rate over that which would exist

with conduction alone.

For convective heat transfer between a heated lower surface and a cooled upper surface under steady state conditions, O'Toole and Silveston (1) have given correlations for the Nusselt number as a function of the Rayleigh as follows:

$$1700 \leq Ra \leq 3500 \qquad Nu = 0.00238\ Ra^{0.816} \qquad (12)$$

$$3500 < Ra < 10^5 \qquad Nu = 0.229\ Ra^{0.252} \qquad (13)$$

$$Ra > 10^5 \qquad Nu = 0.104\ Ra^{0.305}\ Pr^{0.084} \qquad (14)$$

Below a Rayleigh number of 1700, the mode of heat transfer is considered to be conduction only. While the nature of the cases considered in this report were not steady with heat transfer between two fixed surfaces, it was interesting to consider the utility of these correlations for a transient case. If the interfacial motion is relatively slow compared to the time scale of the convective currents, the steady state correlations may prove useful.

For the reported properties of nonadecane (Appendix A) at the fusion temperature, the Rayleigh number is given by

$$Ra = (1.68 \times 10^8)\ L^3\ \Delta T \qquad (15)$$

In this equation L denotes the distance between the two surfaces in units of feet and $\Delta T$ represents the corresponding temperature difference in °F. The following table shows the value of L corresponding to three selected values of $\Delta T$ at which the Rayleigh number equals $10^5$ as given by equation (15).

Table 2.   Height for Various $\Delta T$ when Ra [eqn. (15)] is $10^5$

| T | L |
|---|---|
| °F | inches |
| 20 | .372 |
| 40 | .295 |
| 60 | .258 |

With a temperature difference between the interface and bottom plate of 20°F, the Rayleigh number has exceeded $10^5$ when the liquid depth has exceeded 0.372 inches.  Since this value of depth is relatively low compared to the total range of liquid depths encountered in the experimental studies, attention is focused only on the correlation for large Rayleigh numbers [equation (14)].  An energy balance at the interface including neglection of sensible heating In the solid yields

$$h \ \Delta T = h_f \ \rho \ \frac{dL}{dt}$$

or

$$\frac{dL}{dt} = \frac{h \ \Delta T}{\rho \ h_f} \tag{16}$$

The heat transfer coefficient is related to the Nusselt number by

$$h = \frac{Nu \ k}{L} \tag{17}$$

Substitution of equation (14) into equation (17) results in

$$h = \frac{k}{L} \ (0.104) \ Ra^{0.305} \ Pr^{0.084} \tag{18}$$

For a constant property fluid with a constant temperature difference between the two surfaces, equation (18) can be written as

$$h = C \ L^{-0.085} \tag{19}$$

and equation (16) becomes

$$\frac{dL}{dt} = C_1 \, L^{-0.085} \tag{20}$$

where $C_1$ is a constant dependent on the fluid properties and temperature difference. Equation (20) shows that the interfacial velocity should be nearly constant with only a weak dependence on the liquid depth L. For example, a 500 percent increase in L results in only about a 14 percent decrease in the interfacial velocity.

Conclusions:

1. A number of basic experiments have provided additional data and have served to support some MSFC in-house data and conclusions pertinent to the phenomena occurring during melting and solidification of a paraffin.

2. The level, which changes with heating rates, of an apparent temperature plateau indicated by a thermocouple located within a PCM cell during melting tests is not indicative of a changing fusion temperature, but it is governed by the thermal characteristics of the particular cell and the particular test. Convective currents within the liquid phase contribute significantly to this behavior.

3. The plateau indicated by a thermocouple located within the PCM for the cell sizes investigated so far during solidification occurs at the fusion temperature. During the course of the basic experiments, this level was observed to drop by 1 to 2 F below the reported fusion value. This trait appeared, however, to be more dependent on the length of service of the PCM than on cooling rate.

4. The solidification process is characterized by pronounced dendritic formations thereby rendering interfacial definition very difficult. The interface during melting is more clearly defined.

5. For the range of temperature differences considered in this study (up to 65 F), the steady state convective correlations of Reference 1 yield predictions that agree well with experimental melting rates provided the geometry and thermal characteristics of the cell are such that a reasonably flat interface exists. Some experiments with high conducting (copper) fins showed some variation from this behavior. This occurred when the paraffin melted quickly all along the fins leaving a slug of solid suspended within the liquid and with convective circulation around the slug. In these cases early falling of the slug appeared to have been prevented by adherence of the slug to the end plexiglass surfaces.

6. Some preliminary experiments on a total unit have provided a few relative comparisons of the influence of filler material on the heat transfer characteristics. Pursual of these type of experiments with improved heat transfer control should be promising in achieving correlation of filler influence.

7. In support of task 6, the computer program which incorporates an explicit numerical scheme is described in Appendix B.

8. In the numerical work where only conduction was included, interfacial positions for melting and solidification were underpredicted as compared to experimental data. For the melting cases, this can be explained because of the presence of convective effects. For solidification cases, the presence

of dendrites, as mentioned above, prohibits good interfacial definition experimentally and physically provides a much larger contact area between the liquid and solid than that included in the numerical work where a smooth interface is assumed.

9.  Complementary to conclusion 5 listed above, use of steady state convective correlations (Reference 1) in the numerical work by introduction of an effective liquid conductivity served to yield interfacial predictions that matched the data well. An inherent weakness of this approach is that it fails to provide accurate temperature predictions in the liquid region. To do so would require a complex study of the convective equations within a celluar enclosure.

10. Interfacial position data for solidification can also be matched by introduction of an increased contact area at the interface. With the explicit numerical formulation, this can be done, however, only at the expense of increased computer time.

11. While the explicit numerical approach is simple and the phase change process can be handled in a straight forward fashion, the main setback is the required computer time because of the allow-able time step given by the stability criterion. This fact is magnified for the case of a finned PCM cell when fin temperatures are also to be included as unknowns as the fins are typically very thin. Inclusion of fin temperatures as unknowns would be necessary in a general parametric study.

12. The alternating direction implicit method as outlined in Reference 3 does not appear to bypass the time problem when applied to non-isotropic arrangement such as the fin-PCM cell. A modified approach utilizing the general idea of this ADI scheme was studied

and some numerical results were obtained. This latter technique needs further exploration to verify its accuracy.

Recommendations:

In light of the work which has been performed as well as design needs revealed by the MSFC monitor of this study, the logical direction for future efforts is that of pursuing a parametric study which, hopefully, would support design of a total capacitor unit. The computer model can be used to perform a parametric study for finned arrangements, and current efforts are being devoted to this task.

Some means for correlating the heat transfer characteristics of various types of filler geometries would also be of tremendous value in design work. At this stage, the most promising avenue for obtaining such correlations appears to be that of conducting a well defined experimental program. Such an effort could be pursued with the facilities available at Tennessee Tech, but allotment for the work required to conduct such a program has not been made under the current supported activity.

# VI. LIST OF REFERENCES

1. O'Toole, J. L. and Silveston, P. L., "Correlations of Convective Heat Transfer in Confined Horizontal Layers," Chemical Engineering Progress Symposium Series, Vol. 57, No. 32, pp. 81-90, 1959.

2. Chapman, Alan J., Heat Transfer. New York: The MacMillan Company, pp. 186-194, 1967.

3. Von Rosenberg, Dale U., Methods for the Numerical Solution of Partial Differential Equations. New York: American Elsevier Publishing Company, Inc., pp. 87-90, 1969.

4. Prensner, Douglas S. and Hsu, George R., "Thermal Convection in Laterally Bounded Air Spaces," Proceedings of the Eighth Southeastern Seminar on Thermal Sciences, pp. 339-368, 1972.

APPENDICES

# APPENDIX A

## Properties of Nonadecane Used in Numerical Studies

| Property | Value | Units |
|---|---|---|
| Freezing Point | 89.8 | ($°F$) |
| Density | 47.2 | ($lbm/ft^3$) |
| Heat Capacity | 0.50 | ($BTU/lbm°F$) |
| Heat of Fusion | 73.357 | ($BTU/lbm$) |
| Conductivity | 0.087 | ($BTU/hr-ft°F$) |
| Thermal Expansion Coefficient | 0.00045 | ($F^{-1}$) |
| Dynamic Viscosity | 14.3 | ($lbm/hr-ft$) |

APPENDIX B

The computer program used to facilitate the explicit numerical study is outlined and described in this appendix. A copy of the program for a melting run with inclusion of convective effects is given in Section B.1. The corresponding notation is described in Section B.2. The steps are discussed in Section B.3. Figure B.1 is a skeleton flow chart, and Table B.1 presents a list of computer runs conducted during the summer of 1971 with designations corresponding to some MSFC in-house data.

It was later discovered that the program described in Section B.1 would not run for the case of $M = 1$. The statements causing this incompatibility are indicated in Section B.1 by an arrow placed at the left of the appropriate statement. These were subsequently modified.

A copy of the computer program for a solidification case is given in Section B.4. Comparison of appropriate statements with those shown in Section B.3 generally illustrates the modification to accommodate $M = 1$.

The statements which were included in the solidification program to allow changing the effective interfacial area for nodes experiencing melting are underlined.

B.I. COMPUTER PROGRAM FOR MELTING

```
1          DIMENSION  RV(5,31) , RH(5,31) , C(5,31) , QS(5,31), T1(5,31)
2          DIMENSION T2(5,31) , F(5,31) , Q(5,31) , QRAT(5,31), T3(1,31)
3          DIMENSION TM1(9), TM2(9), TM3(9), TM4(9), TIM(9)
4          DIMENSION QRA2(5, 31)
5    COMPUTATIONAL PARAMETERS
6          N=27
7          M=4
8          AM=M
9          MM=M+1
10         NN=N+2
11         NJ=N+3
12         NI=N+4
13         ND=9
14         NDP=8
15         TAU=1.1
16         KCOUNT=1
17         MCOUNT=1
18         MFIN=500
19         EPS=1.E-06
20         KCHK=1000
21         JOE=1
22         DT=1.0E-04
23         TAU2=(10.*DT)+(DT/3.)
24   PHYSICAL PROPERTIES
25         TAMB=80.
26         TIN=73.5
27         HTOP=1.E-08
28         HBOT=5.0
29         G=(32.2*3600.*3600.)
30     WAX
31         DEN=47.2
32         TK=0.087
33         CP=0.5
34         TTR=73.04
35         HTR=22.108
36         TMELT=89.8
37         HMELT=73.357
38         TREF=50.0
39         BETA=0.00045
40         VIS=14.3
41         CL=CP
42         TKL=TK
43     BOTTOM PLATE DENOTED BY 1
44         DEN1=171.0
45         TK1=93.0
46         CP1=0.22
47     FIN DENOTED BY 2
48         DEN2=171.0
49         TK2=93.0
50         CP2=0.22
51     TOP PLATE DENOTED BY 3
52         DEN3=72.5
53         TK3=0.09
54         CP3=0.33
```

```
55      GEOMETRY PARAMETERS
56          W=0.75/12.0
57          H=2.625/12.0
58          B=5.0/12.0
59          S=W/(2.0*AM)
60          S1=0.032/12.0
61          S2=0.008/12.0
62          S3=0.25/12.0
63          F2JM=1.0/(32.0*S*12.0)
64       VERTICAL RESISTANCES
65          RV(1,2)=(S1/(TK1*S2*B))+(2./(HBOT*S2*B))
66          DO 10 I=2,MM
67       10 RV(I,2)=(S1/(2.*TK1*S*B))+(1./(HBOT*S*B))
68          RV(1,3)=(S/(TK2*S2*B))+(S1/(TK1*S2*B))
69          DO 20 I=2,MM
70       20 RV(I,3)=(1./(2.*TK*B))+(S1/(2.*TK1*S*B))
71          DO 30 J=4,NN
72       30 RV(1,J)=((2.*S)/(TK2*S2*B))
73          DO 40 J=4,NN
74          DO 40 I=2,MM
75       40 RV(I,J)=(1./(TK*B))
76          RV(1,N+3)=(S3/(TK3*S2*B))+(S/(TK2*S2*B))
77          DO 50 I=2,MM
78       50 RV(I,N+3)=(S3/(2.*TK3*S*B))+(1./(2.*TK*B))
79          RV(1,N+4)=(S3/(TK3*S2*B))+(2./(HTOP*S2*B))
80          RV(2,N+4)=(S3/(2.*TK3*B*(S+(S2/2.))))+(1./(HTOP*B*(S+(S2/2.))))
81 ─────▶ DO 60 I=3,MM
82       60 RV(I,N+4)=(S3/(2.*TK3*S*B))+(1./(HTOP*S*B))
83       HORIZONTAL RESISTANCES
84          RH(2,N+3)=((S2+S)/(2.*TK3*S3*B))
85 ─────▶ DO 70 I=3,MM
86       70 RH(I,N+3)=(S/(TK3*S3*B))
87          DO 80 J=3,NN
88       80 RH(2,J)=(S2/(2.*TK2*S*B))+(1./(2.*TK*B))
89          DO 90 J=3,NN
90 ─────▶ DO 90 I=3,MM
91       90 RH(I,J)=(1./(TK*B))
92          RH(2,2)=((S2+S)/(2.*TK1*S1*B))
93 ─────▶ DO 100 I=3,MM
94      100 RH(I,2)=(S/(TK1*S1*B))
95          RH(2,N+3)=RH(2,N+3)+RV(1,N+3)
96       NODAL CAPACITANCES
97          C(1,2)=((DEN1*S1*S2*B*CP1)/2.)
98          DO 110 I=2,MM
99      110 C(I,2)=(DEN1*S1*S*B*CP1)
100         DO 120 J=3,NN
101     120 C(1,J)=((DEN2*S2*S*B*CP2)/2.)
102         C(1,N+3)=((DEN3*S2*S3*B*CP3)/2.)
103         C(2,N+3)=(S3*B*(S+(S2/2.))*DEN3*CP3)
104 ────▶ DO 130 I=3,MM
105     130 C(I,N+3)=(DEN3*S3*S*B*CP3)
106         DO 140 J=3,NN
107         DO 140 I=2,MM
108     140 C(I,J)=(DEN*(S**2)*B*CP)
109 ────▶ Q1=(C(3,4)*(TTR-TREF))
110         Q2=Q1+((DEN*(S**2)*B*HTR))
```

```
111 ──►Q3=Q2+((C(3,4))*(TMELT-TTR))
112       Q4=Q3+((DEN*(S**2)*B*HMELT))
113  INITIALIZATION OF PERTINENT QUANTITIES
114       TIME=0.0
115       QWAX=0.0
116       QBW=0.0
117       QSW=0.0
118       QTW=0.0
119       QTOP=0.0
120       QFTR=0.0
121       QTTR=0.0
122       V1=0.0
123       V2=0.0
124       DMO=0.0
125       DO 150 J=2,NJ
126       DO 150 I=1,MM
127   150 T1(I,J)=TIN
128 ──► IF(TIN.LT.TTR)QSIN=(C(3,4)*(TIN-TREF))
129 ──► IF(TIN.GT.TTR.AND.TIN.LT.TMELT) QSIN=Q2+((C(3,4))*(TIN-TTR))
130 ──► IF(TIN.GT.TMELT)QSIN=Q4+((C(3,4))*(TIN-TMELT))
131       DO 160 I=1,MM
132   160 T1(I,N+4)=TAMB
133       DO 170 J=3,NN
134       DO 170 I=2,MM
135   170 QS(I,J)=QSIN
136       DO 180 I=1,MM
137       Q(I,2)=0.0
138   180 Q(I,N+3)=0.0
139       DO 190 J=3,NN
140   190 Q(1,J)=0.0
141       DO 199 J=2,NI
142       DO 199 I=1,MM
143       F(I,J)=0.0
144   199 QRAT(I,J)=0.0
145       READ(5,11) (TM1(I), I=1,ND)
146       READ(5,11) (TM2(I), I=1,ND)
147       READ(5,11) (TM3(I), I=1,ND)
148       READ(5,11) (TM4(I), I=1,ND)
149       READ(5,11) (TIM(I), I=1,ND)
150    11 FORMAT(8F10.0)
151       WRITE(6,22) TIME,W,H,N,M
152    22 FORMAT(1X,5HTIME=,E15.8,10X,2HW=,E15.8,10X,2HH=,E15.8,10X,2HN=,I2,
153       15X,2HM=,I2)
154       WRITE(6,33)Q1,Q2,Q3,Q4
155    33 FORMAT(1X,3HQ1=,E15.8,10X,3HQ2=,E15.8,10X,3HQ3=,E15.8,10X,3HQ4=,E1
156       5.8)
157       WRITE(6,44)
158    44 FORMAT(2X,4HI J,5X,19HVERTICAL RESISTANCE,6X,21HHORIZONTAL RESIST
159       ANCE,6X,17HNODAL CAPACITANCE,6X,11HTEMPERATURE,5X,7HQS(I,J))
160       DO 200 J=2,NI
161       DO 200 I=1,MM
162       IF(J.EQ.N+4) GO TO 1
163       GO TO 2
164     1 QS(1,J)=0.0
165       RH(I,J)=1.E08
166       C(I,J)=0.0
```

```
167    2 IF(I.EQ.1)RH(I,J)=1.E08
168      IF(J.EQ.2.OR.J.EQ.N+3)QS(I,J)=0.0
169      IF(I.EQ.1)QS(I,J)=0.0
170      WRITE(6,55)I,J,RV(I,J),RH(I,J),C(I,J),T1(I,J),QS(I,J)
171   55 FORMAT(1X,I2,1X,I2,5X,E15.8,10X,E15.8,10X,E15.8,6X,E16.8,4X,E15.8)
172  200 CONTINUE
173      DO 889 J=3,NN
174  889 T3(1,J)=T1(1,J)
175 COMPUTATION SECTION  COMPUTATION SECTION COMPUTATION SECTION
176    3 TIME=TIME+DT
177      DO 210 J=3,NJ
178      QRAT(1,J)=((T1(2,J)-T1(1,J))/RH(2,J))+((T1(1,J-1)-T1(1,J))/RV(1,J)
179     +((T1(1,J+1)-T1(1,J))/RV(1,J+1))
180      QRAT(MM,J)=((T1(M,J)-T1(MM,J))/RH(MM,J))+((T1(MM,J-1)-T1(MM,J))/RV
181      (MM,J))+((T1(MM,J+1)-T1(MM,J))/RV(MM,J+1))
182  210 CONTINUE
183      DO 211 J=3,NJ
184  →   DO 211 I=2,M
185      QRAT(I,J)=((T1(I-1,J)-T1(I,J))/RH(I,J))+((T1(I+1,J)-T1(I,J))/RH(I+
186      1,J))+((T1(I,J-1)-T1(I,J))/RV(I,J))+((T1(I,J+1)-T1(I,J))/RV(I,J+1)
187      )
188  211 CONTINUE
189  212 DO 220 J=3,NJ
190      DO 220 I=1,MM
191  220 QS(I,J)=QS(I,J)+(QRAT(I,J)*DT)
192      DO 240 I=2,MM
193  240 T2(I,N+3)=T1(I,N+3)+((QRAT(I,N+3)*DT)/C(I,N+3))
194      T2(1,N+3)=T2(2,N+3)
195      DO 250 J=3,NN
196      DO 250 I=2,MM
197      IF(QS(I,J).LT.Q1)T2(I,J)=TREF+(QS(I,J)/C(I,J))
198      IF(QS(I,J).GE.Q1.AND.QS(I,J).LE.Q2) T2(I,J)=TTR
199      IF(QS(I,J).GT.Q2.AND.QS(I,J).LT.Q3) T2(I,J)=TTR+((QS(I,J)-Q2)/C(I,
         J))
200      IF(QS(I,J).GE.Q3.AND.QS(I,J).LE.Q4) T2(I,J)=TMELT
201    WHEN GOING FROM MELT TO FREEZE OR VICE-VERSA CHANGE THE FOLLOWING CARD
202      IF(QS(I,J).GT.Q3.AND.QS(I,J).LT.Q4) F(I,J)=(QS(I,J)-Q3)/(DEN*(S**2
203      )*B*HMELT)
204      IF(QS(I,J)GT.Q4)   T2(I,J)=TMELT+((QS(I,J)-Q4)/C(I,J))
205    WHEN GOING FROM MELT TO FREEZE OR VICE-VERSA CHANGE THE FOLLOWING CARD
206      IF(QS(I,J).GE.Q4)F(I,J)=1.0
207      IF(QS(I,J).LE.Q3) F(I,J)=0.0
208  250 CONTINUE
209 SPECIFICATION AND/OR DETERMINATION OF FIN TEMPERATURES
210          THE FOLLOWING DO LOOP ASSUMES FIN TEMPERATURES FOR ITERATION
211      DO 255 J=3,NN
212  255 T2(1,J)=T3(1,J)
213      DO 260 L=1,NDP
214      IF(TIME.GE.TIM(L).AND.TIME.LE.TIM(L+1)) GO TO 4
215  260 CONTINUE
216    4 FAC=(TIME-TIM(L))/(TIM(L+1)-TIM(L))
217      T2(1,2)=TM1(L)+((TM1(L+1)-TM1(L))*FAC)
218      T2(1,8)=TM2(L)+((TM2(L+1)-TM2(L))*FAC)
219      T2(1,15)=TM3(L)+((TM3(L+1)-TM3(L))*FAC)
220      T2(1,21)=TM4(L)+((TM4(L+1)-TM4(L))*FAC)
221      DO 270 I=1,MM
```

```
222    270 T2(I,2)=T2(1,2)
223    UNSPECIFIED FIN TEMPERATURES DETERMINED BY STEADY STATE EQUATIONS
224    256 MCOUNT=MCOUNT+1
225        DO 280 J=3,NN
226        T3(1,J)=T2(1,J)
227        IF(J.EQ.8.OR.J.EQ.15) GO TO 5
228        IF(J.EQ.21) GO TO 5
229        T2(1,J)=((T2(1,J-1)/RV(1,J))+(T2(2,J)/RH(2,J))+(T2(1,J+1)/RV(1,J+1
230        )))/((1./RV(1,J))+(1./RH(2,J))+(1./RV(1,J+1)))
231      5 CONTINUE
232    280 CONTINUE
233        IF(MCOUNT.GT.MFIN) GO TO 8
234        DO 281 J=3,NN
235        DIF=T2(1,J)-T3(1,J)
236        IF(ABS(DIF).GT.EPS) GO TO 256
237    281 CONTINUE
238        IF(JOE.EQ.2) GO TO 285
239        JOE=JOE+1
240        DO 888 J=3,NJ
241        DO 888 I=1,MM
242    888 QS(I,J)=QS(I,J)-(QRAT(I,J)*DT)
243        DO 282 J=3,NJ
244        QRA2(1,J)=((T2(2,J)-T2(1,J))/RH(2,J))+((T2(1,J-1)-T2(1,J))/RV(1,J)
245        )+((T2(1,J+1)-T2(1,J))/RV(1,J+1))
246        QRA2(MM,J)=((T2(M,J)-T2(MM,J))/RH(MM,J))+((T2(MM,J-1)-T2(MM,J))/RV
247        (MM,J))+((T2(MM,J+1)-T2(MM,J))/RV(MM,J+1))
248    282 CONTINUE
249        DO 283 J=3,NJ
250 ----> DO 283 I=2,M
251        QRA2(I,J)=((T2(I-1,J)-T2(I,J))/RH(I,J))+((T2(I+1,J)-T2(I,J))/RH(I+
252        1,J))+((T2(I,J-1)-T2(I,J))/RV(I,J))+((T2(I,J+1)-T2(I,J))/RV(I,J+1)
253        )
254    283 CONTINUE
255        DO 284 J=3,NJ
256        DO 284 I=1,MM
257    284 QRAT(I,J)=(QRAT(I,J)+QRA2(I,J))/2.0
258        GO TO 212
259    285 MCOUNT=1
260        DO 286 I=1,MM
261    286 QRAT(I,2)=((T2(I,2)-T1(I,2))*C(I,2)/DT)
262        DO 287 I=1,MM
263    287 QS(I,2)=QS(I,2)+(C(I,2)*(T2(I,2)-T1(I,2)))
264        DO 290 I=2,MM
265        QBW=(T2(I,2)-T2(I,3))/RV(I,3)+QBW
266    290 QTW=(T2(I,N+3)-T2(I,N+2))/RV(I,N+3)+QTW
267        QBT=QBW+((T2(1,2)-T2(1,3))/RV(1,3))
268        DO 300 J=3,NN
269    300 QSW=QSW+((T2(1,J)-T2(2,J))/RH(2,J))
270        DO 310 I=1,MM
271    310 QTOP=((T2(I,N+3)-TAMB)/RV(I,N+4))+QTOP
272        DO 311 J=3,NN
273    311 QFTR=QFTR+QRAT(1,J)
274        DO 312 I=1,MM
275    312 QTTR=QTTR+QRAT(1,NJ)
276        QWAX=(QBW+QTW+QSW)*DT+(QWAX)
277        RATIO=QSW/QBW
```

```
278          ERROR=((QBT-(QBW+QSW+QTW+QTOP+QFTR+QTTR))*100.0)/QBT
279          DO 930 J=3,NN
280          DO 930 I=2,MM
281          V2=V2+(F(I,J)*(S**2)*B)
282      930 CONTINUE
283          DAVG=((2.0*V2)/(W*B))*12.0
284          QMELT=((V2-V1)*DEN*HMELT)/DT
285          V1=V2
286          V2=0.0
287          DELT=ABS(T2(1,2)-TMELT)
288          PR=(VIS*CL)/TKL
289          RA=((DEN**2)*G*CL*BETA*DELT*(DAVG**3))/(VIS*TKL*1728.0)
290          IF(T2(1,2).LE.TMELT) RA=0.0
291          IF(RA.GT.1.E05)TK=(TKL*0.104*(RA**0.305)*(PR**0.084))
292          IF(RA.GE.3500.0.AND.RA.LE.1.E05) TK=(TKL*0.229*(RA**0.252))
293          IF(RA.GE.1700.0.AND.RA.LT.3500.0) TK=(TKL*0.00238*(RA**0.816)
294          TKR=TK/TKL
295          DO 945 I=2,MM
296          IF(F(I,3).LT.0.25) GO TO 945
297          RV(I,3)=(1./(2.*TK*B))+(S1/(2.*TK1*S*B))
298      945 CONTINUE
299          DO 946 J=4,NN
300          DO 946 I=2,MM
301          IF(F(I,J).LT.EPS) GO TO 946
302          RV(I,J)=(1./(TK*B))
303      946 CONTINUE
304          DO 947 I=2,MM
305          IF(F(I,NN).LT.0.75) GO TO 947
306          RV(I,N+3)=(S3/(2.*TK3*S*B))+(1./(2.*TK*B))
307      947 CONTINUE
308          DO 950 J=3,NN
309          IF(F(2,J).LT.0.25) GO TO 949
310          RH(2,J)=(S2/(2.*TK2*S*B))+(1./(2.*TK*B))
311      949 CONTINUE
312   ----> DO 950 I=3,MM
313          IF(F(I,J).LT.EPS) GO TO 950
314          RH(I,J)=(1./(TK*B))
315      950 CONTINUE
316          IF(KCOUNT.EQ.KCHK) GO TO 6
317          KCOUNT=KCOUNT+1
318          GO TO 7
319        6 WRITE(6,66) TIME, QWAX, ERROR
320       66 FORMAT(1X,5HTIME=,E15.8,10X,5HQWAX=,E15.8,10X,6HERROR=,E15.8)
321          DO 313 J=3,NN
322          AJ=J-3
323          BJ=J-2
324          IF(F(2,J).GT.F2JM) DFLO=(BJ*S*12.0)
325          DFIN=(AJ*S*12.0)
326          IF(F(2,J).LT.EPS) GO TO 314
327      313 CONTINUE
328      314 DO 315 J=3,NN
329          AJ=J-3
330          IF(F(MM,J).LT.1.0) DMID=((AJ*S)+(F(MM,J)*S))*12.0
331          IF(F(MM,J).LT.1.0) GO TO 316
332      315 CONTINUE
333      316 WRITE(6,67) DFIN, DFLO, DAVG, DMID
```

```
334    67 FORMAT(1X,5HDFIN=,E15.8,10X,5HDFLO=,E15.8,10X,5HDAVG=,E15.8,10X,5H
335       DMID=,E15.8)
336       DDOT=(DMID-DMO)/DT
337       DMO=DMID
338       WRITE(6,68) RA, TKR, QMELT, DDOT
339    68 FORMAT(1X,3HRA=,E15.8,10X,4HTKR=,E15.8,10X,6HQMELT=,E15.8,10X,5HDD
340       OT=,E15.8)
341       WRITE(6,77) QBW, QSW, QTW, QBT, RATIO
342    77 FORMAT(1X,4HQBW=,E15.8,3X,4HQSW=,E15.8,3X,4HQTW=,E15.8,3X,4HQBT=,E
343       15.8,3X,6HRATIO=,E15.8)
344       WRITE(6,88)
345    88 FORMAT(2X,1HI,2X,1HJ,10X,11HTEMPERATURE,10X,15HFRACTION MELTED,10X
346       ,11HENERGY RATE,10X,13HENERGY STORED)
347       DO 320 J=2,NJ
348       DO 320 I=1,MM
349       WRITE(6,99)I,J,T2(I,J),F(I,J),QRAT(I,J),QS(I,J)
350    99 FORMAT(1X,I2,1X,I2,8X,E15.8,8X,E15.8,8X,E15.8,8X,E15.8)
351   320 CONTINUE
352       KCOUNT=1
353     7 QBW=0.0
354       QSW=0.0
355       QTW=0.0
356       QTOP=0.0
357       QTTR=0.0
358       QFTR=0.0
359       DO 330 J=2,NJ
360       DO 330 I=1,MM
361   330 T1(I,J)=T2(I,J)
362       JOE=1
363       IF(TIME.LT.TAU) GO TO 3
364     8 WRITE(6,111) MCOUNT
365   111 FORMAT(1X,I3)
366       STOP
367       END
```

## B.2. DESCRIPTION OF PROGRAM NOTATION

AJ            J-3, used in computing interface location

AM            value of integer M converted to floating point

B             length of section, ft.

BETA          volume expansivity of wax, $R^{-1}$

BJ            J-2, used in computing interface location

C(I,J)        thermal capacitance of node (I,J), Btu/F

CL            constant pressure specific heat of wax, Btu/lbmF

CP            constant pressure specific heat of wax, Btu/lbmF

CP1           constant pressure specific heat of bottom plate, Btu/lbmF

CP2           constant pressure specific heat of fin, Btu/lbmF

CP3           constant pressure specific heat of top plate, Btu/lbmF

DAVG          average height of liquid based on amount melted, in.

DDOT          interfacial velocity for nodes adjacent to centerline (I=MM), in/hr.

DELT          absolute value of temperature difference between bottom plate
              and interface, F.

DEN           wax density, $lbm/ft^3$

DEN1          bottom plate density, lbm/ft

DEN2          fin density, $lbm/ft^3$

DEN3          top plate density, $lbm/ft^3$

DFLO[1]       approximate interfacial location for nodes adjacent to fin (I=2)
              based on amount melted being equal to F2JM, in.

DFIN          interfacial position for nodes adjacent to fin (I=2) based on any
              amount being melted, in.

DIF           temperature difference used in comparing new and old temperatures
              during iteration when solving steady state equations for unspecified
              fin temperatures, °F.

DMID          interfacial position for node adjacent to centerline, in.

DMO       DMID evaluated at previous time, in.

DT       time increment, hr.

EPS       arbitrarily set small number used as a comparator

ERROR       percent error in computed energy balance based on transfer rates, percent.

F(I,J)       mass fraction of node (I,J) which has undergone phase change since start of process

FAC       time ratio used in linearly interpolating specified fin temperatures at a particular time in terms of bracketed data values.

F2JM       fraction of S which corresponds to 1/32 inch (arbitrary)

G       acceleration of gravity, $ft/hr^2$

H       PCM section height (See Figure 40), ft.

$HBOT^2$       heat transfer coefficient between external fluid and bottom plate, $Btu/hr-ft^2-F$

HMELT       heat of fusion, Btu/lbm

$HTOP^3$       heat transfer coefficient between external fluid and top plate, $Btu/hr-ft^2-F$

HTR       heat of transition, Btu/lbm.

I       integer designation of vertical column in which a mode is located (See Figure 40)

J       integer designation of horizontal row in which a mode is located (See Figure 40)

JOE       counter used in refining the heat transfer computation before progressing in time

KCHK       integer used to control printing of results at desired times (See definition of KCOUNT)

KCOUNT       integer counter used to print our results at times when KCOUNT = KCHK

M       number of wax nodes in a horizontal row

MCOUNT       counter used in determining unspecified fin temperatures

MFIN       maximum value of MCOUNT which when exceeded causes program to stop

MM       M+1 (See Figure 40)

| | |
|---|---|
| N | number of wax nodes in a vertical column |
| ND | number of data points for measured fin temperatures |
| NDP | ND-1 |
| NI | N+4 |
| NJ | N+3 |
| NN | N+2 |
| PR | Prandtl number |
| Q(I,J) | unnecessary variable - replaced where needed by QS(I,J) |
| QBT | instantaneous heat transfer rate through bottom, Btu/hr |
| QBW | instantaneous heat transfer rate through bottom to wax only, Btu/hr |
| QFTR | instantaneous rate of heat transfer to fin, Btu/hr. |
| QMELT | energy which acounts for amount of wax melted at any time, Btu. |
| QRAT(I,J) | the instantaneous net rate of heat transfer to node I,J, Btu/hr. |
| QS(I,J) | the energy stored by node I,J above TREF for wax and above 0 for metal nodes, Btu |
| QSIN | the energy stored by node I,J above TREF corresponding to initial temperature throughout network, Btu. |
| QSW | instantaneous heat transfer rate from fin to wax, Btu/hr. |
| QTOP | instantaneous heat transfer rate out of top of section, Btu/hr. |
| QTTR | instantaneous rate of heat transfer to top plate, Btu/hr. |
| QTW | instantaneous heat transfer rate from top plate to wax, Btu/hr |
| QWAX | net energy transfer to wax since start, Btu. |
| Q1 | energy stored by wax node above TREF corresponding to start of phase transition, Btu. |
| Q2 | energy stored by wax node above TREF corresponding to end of phase transition, Btu. |
| Q3 | energy stored by wax node above TREF corresponding to start of melting, Btu. |
| Q4 | energy stored by wax node above TREF corresponding to end of melting, Btu. |

| | |
|---|---|
| QRA2(I,J) | instantaneous rate of heat transfer to node I,J based on temperatures obtained from QRAT(I,J) and then used to correct temperature predictions, Btu/hr |
| RA | Rayleigh number for liquid wax |
| RATIO | ratio of instantaneous heat transfer rate from fin to wax to that from bottom plate to wax |
| RH(I,J) | horizontal thermal resistance between node I-1,J and node I,J, hr-F/Btu |
| RV(I,J) | vertical thermal resistance between node I,J and I,J-1, Hr-F/Btu |
| S | wax node width, ft. |
| S1 | bottom plate thickness, ft. |
| S2 | fin thickness, ft. |
| S3 | top plate thickness, ft. |
| TAMB | temperature of environment external to top plate, °F |
| TAU | limiting time value to stop program, Hr. |
| TIME | instantaneous value of time, Hr. |
| TIN | initial temperature of all nodes, °F |
| TK | wax thermal conductivity (artificially allowed to vary in liquid to account for convection), Btu/hr-ft-F |
| TKL | thermal conductivity of liquid, Btu/hr-ft-F |
| TKR | ratio of effective thermal conductivity to thermal conductivity |
| TMELT | fusion temperature of wax, °F |
| TREF | arbitrary reference temperature (should be less than TIN), °F |
| TTR | transition temperature, °F |
| T1(I,J) | temperature of node I,J at time t, °F |
| T2(I,J) | temperature of node I,J at time t+Δt, °F |
| T3(1,J) | temperature of node 1,J in fin at beginning of each iteratine step used in finding steady state solution, °F |
| TAU2 | arbitrarily defined time value used in print-out control, Hr. |

| | |
|---|---|
| TK1 | thermal conductivity of bottom plate, Btu/hr-ft-F |
| TK2 | thermal conductivity of fin, Btu/hr-ft-F |
| TK3 | thermal conductivity of top plate, Btu/hr-ft-F |
| TIM(L) | time value corresponding to input data of measured fin temperatures, hr. |
| TM1(L) | measured bottom plate temperature (input data), °F |
| TM2(L) | first measured fin temperature (input data), °F |
| TM3(L) | second measured fin temperature (input data), °F |
| TM4(L) | third measured fin temperature (input data), °F |
| VIS | viscosity of liquid, lbm/hr-ft |
| V1 | volume of wax melted at time t, ft$^3$ |
| V2 | volume of wax melted at time t+$\Delta$t, ft$^3$ |
| W | width of wax cell, ft |

---

[1] This assumes that some finite thickness must have melted before it would be detectable on the film. The number DFIN is the height corresponding to a node with any amount melted.

[2] This was included to be general but has not been used to date as bottom plate temperatures were specified as input data.

[3] This has been included but set at a small value to essentially correspond to the top being insulated.

B.3. DISCUSSION OF COMPUTER PROGRAM FOR MELTING

In the following discussion, references are made to line numbers corresponding to those designated on the copy of the program.

| LINES | DISCUSSION |
|---|---|
| 1 - 4 | required dimension statements for subscripted variables; values should be (MM, NI) for all double subscripted variables except T3 for which they should be (1, NJ); values should be ND for single subscripted variables; NOTE: Q(MM,NI) is superfluous and can be omitted with lines 136 - 140. |
| 5 - 23 | specification of computational parameters |
| 24 - 54 | specification of physical properties |
| 55 - 63 | specification of geometry parameters |
| 64 - 82 | computation of all vertical thermal resistance values RV (I,J) |
| 83 - 95 | computation of all horizontal thermal resistance values RH(I,J); note that line 95 is a special definition which amounts to bypassing node (1,N+3) which was done to overcome stability criterion required by this small corner node |
| 96 - 108 | computation of all nodal capacitance values C(I,J) |
| 109 - 112 | computation of energy stored by a wax node relative to TREF for the start and end of phase transition and the start and end of fusion, respectively |
| 113 - 144 | initialization of pertinent quantities; the initial value of the stored energy depends on the relationship of the initial temperature to the reference temperature TREF; note that lines 136 - 140 are superfluous and can be omitted; some initialization of certain parameters is done in the DO loop between lines 160 and 172 which are set primarily to avoid random print-out and are not essential to the computation done in the heart of the program |
| 145 - 150 | input data values for measured fin and bottom plate temperatures and corresponding time values |

| 151 - 172 | print out of initial values for checking purposes and print out of certain computed quantities for informational purposes |
|---|---|
| 173 - 174 | initially defines T3(1,J) for all fin nodes and sets these equal to the initial temperatures T1(1,J) |
| 175 | beginning of main computation scheme |
| 176 | time is stepped forward by $\Delta t$ |
| 177 - 188 | loops which compute and store the net rate of heat transfer to nodes (I,J) based on old temperatures T1(I,J); the rate of heat transfer to node (I,J) is given by |

$$\dot{q}(I,J) = \frac{T(I-1,J)-T(I,J)}{RH(I,J)} + \frac{T(I+1,J)-T(I,J)}{RH(I,J)}$$

$$+ \frac{T(I,J-1)-T(I,J)}{RV(I,J)} + \frac{T(I,J+1)-T(I,J)}{RV(I,J+1)}$$

this expression must be modified accordingly for nodes near a boundary which are not surrounded by four neighbors .

| 189 - 191 | computation of total energy stored by node (I,J) since the start which is given by |

$$Q_{stored} = \sum_{time} \dot{q}\Delta t$$

| 192 - 193 | computation of new top plate temperatures T2(I,N+3) from the expression |

$$T2(I,J) = T1(I,J) + \frac{\dot{q}(I,J)\Delta t}{C(I,J)}$$

| 194 | sets the corner top plate node (1,N+3) temperature equal to that of the second node (2,N+3); omission of the corner node in the computation scheme was done to avoid stability problems due to its small size |
| 195 - 208 | computation of new wax node temperatures from the energy stored by the nodes and their capacity and/or phase change enthalpy values; when the stored energy lies between Q1 and Q2 the new temperature is forced to be the transition temperature and when it lies between Q3 and Q4 the new temperature; is forced to be the fusion temperature; also the fraction of the node which has undergone |

phase change is calculated from the relationship of the stored energy to Q3 and Q4; note that certain designated cards need to be changed when running the program for freezing as contrasted to melting

209 - 210        beginning of determination of fin temperatures

211 - 212        all new fin temperatures are set to T3(1,J) which simply represents an assumed value always corresponding to the previously computed value except at the very beginning at which time it is set as the initial temperature

213 - 220        interpolation scheme which assigns new temperatures to the three nodes on the fin and one on the bottom plate corresponding to positions where temperature measurements were made; the new temperatures are linearly interpolated from the input data

221 - 222        assigns all nodes along the bottom plate the same value of new temperature

223        beginning of iteration process to determine unspecified fin temperatures from steady state equation; fin nodes were not treated as transient cases due to their extremely small capacitances that would impose a severe stability criterion

224 - 237        iteration process used to determine unspecified fin temperatures; in each iteration, T2(1,J) is computed from steady state equations and then compared with T3(1,J) which corresponds to the calculated temperatures during the previous iterative step; the iteration is continued until the differences between computed fin temperatures and their corresponding values for the previous iterative step are all acceptably small; should the iteration exceed MFIN counts the program is directed to stop

238        when counter JOE equals 2, the new temperatures at all nodes are considered to be the solution at the particular time and the program advances to line 259

239        increase of counter JOE to 2

240 - 242        the energy stored at each node (I,J) is reset back to its original value; this is to allow for an improved computation of the net heat transfer rate to each node to be made and then a recomputation of the stored energy and the corresponding new temperatures

243 - 254        computation of net heat transfer rate to each node using new temperatures T2

| | |
|---|---|
| 255 - 257 | calculation of net heat transfer rate to each node as the average of that based on old temperatures T1 and new temperatures T2 |
| 258 | return to line 189 which consists of redirecting the computation through that of computing improved new temperatures, energy storage values, and fractional melted values by using the improved (averaged) heat transfer rate (Lines 255 - 257); this corrective technique is only employed once |
| 259 - 278 | computation of various heat transfer quantities from the new temperatures obtained at time t+$\Delta$t |
| 279 - 282 | computation of volume of melted wax |
| 283 | computation of average liquid depth from the volume melted |
| 284 | computation of energy required to melt the wax which has melted |
| 285 - 286 | resetting of V1 and V2 for next time step |
| 287 | determination of absolute value of temperature difference between bottom plate and the fusion temperature |
| 288 | computation of the Prandtl number |
| 289 - 290 | computation of the Rayleigh number |
| 291 - 293 | determination of effective liquid conductivity due to convection by using correlations of O'Toole and Silveston |
| 294 | computation of ratio of effective liquid conductivity to actual value |
| 295 - 315 | recomputation of thermal resistances in the liquid by using the effective thermal conductivity rather than the actual value |
| 316 | counter check which controls printing out of desired results as well as computation of interfacial position |
| 317 | counter advance |
| 318 | by-pass of printing results except when line 316 is executed |

| | |
|---|---|
| 319 - 320 | write statement for printing results |
| 321 - 332 | computation of interface position for columns next to fin and next to centerline |
| 333 - 335 | write statement for printing results |
| 336 - 337 | calculation of interfacial velocity and renaming interfacial position to provide for determining its change at the next time step |
| 338 - 351 | write statements and corresponding formats for printing results |
| 352 - 358 | reinitialization of pertinent quantities for next time step. |
| 359 - 361 | setting new temperatures for current time step to be old temperatures for the next time step |
| 362 | reinitialization of counter |
| 363 | comparison of time to upper limit value which when exceeded results in stopping the program |
| 364 - 365 | printing out of value of counter used in fin temperature iteration |
| 366 | STOP |
| 367 | END |
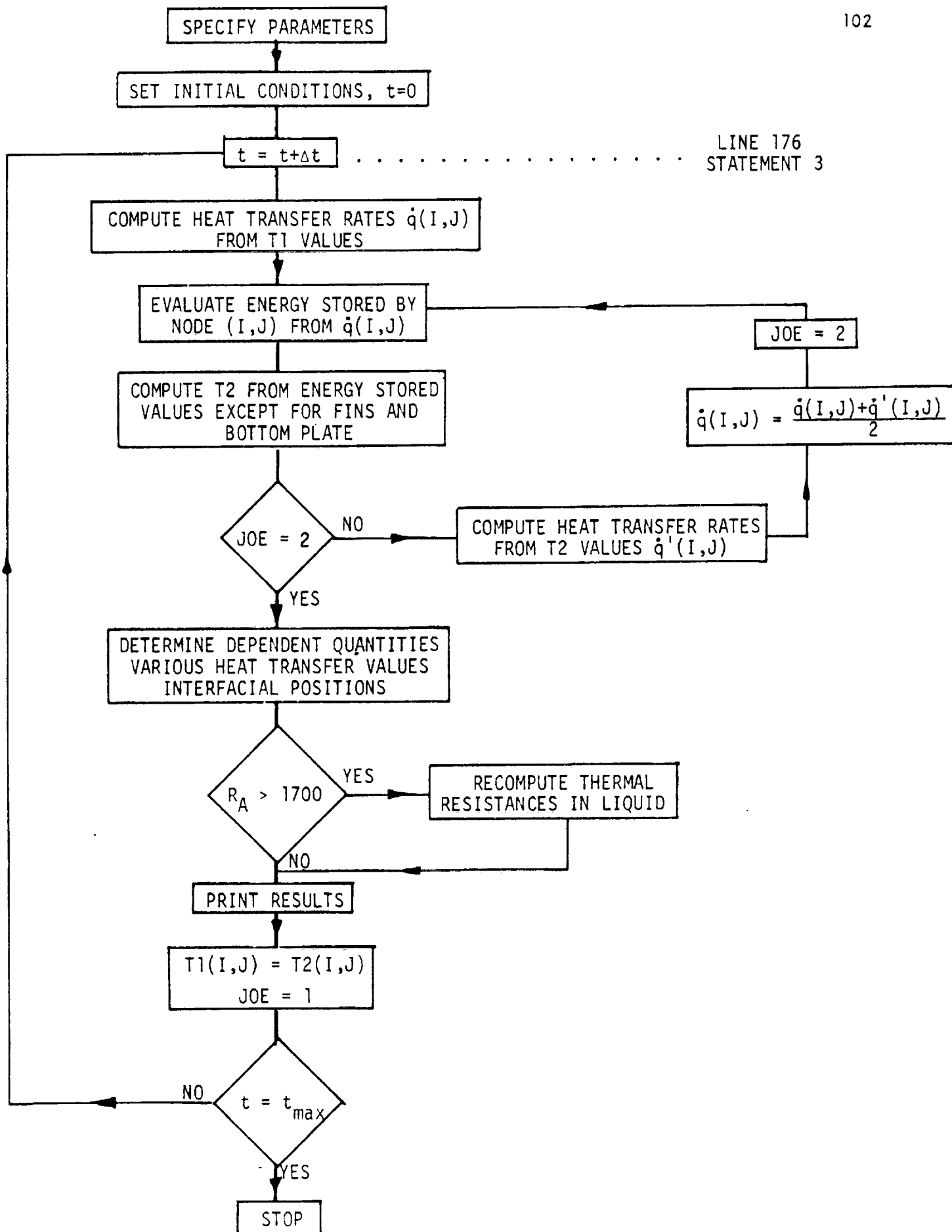
Figure B.1.   Skelton Flow Chart.

Table B.1. Tabulation of Computer Runs During Summer 1971.

| | | | | | | | MELT RUNS |
|---|---|---|---|---|---|---|---|

**230-5**

| Date 1971 | $T_{melt}$ °F | K Btu/hr-ft-F | $C_p$ Btu/lbmF | $\Delta t$ hr | $t_{max}$ hr | MxN | Remarks |
|---|---|---|---|---|---|---|---|
| 7-23 | 90.0 | 0.08 | 0.5 | 0.01 | 0.5 | 2x14 | |
| 7-26 | 90.0 | 0.08 | 0.5 | 0.01 | 1.1 | 2x14 | |
| 7-26 | 90.0 | 0.08 | 0.4 | 0.01 | 1.1 | 2x14 | |
| 7-26 | 90.0 | 0.08 | 0.5 | 0.005 | 1.1 | 2x14 | |
| 7-27 | 89.8 | 0.08 | 0.4 | 0.01 | 1.1 | 2x14 | |
| 7-27 | 89.8 | 0.08 | 0.4 | 0.01 | 1.1 | 2x14 | Fin temperatures unspecified |
| 7-29 | 89.8 | 0.08 | 0.4 | 0.01 | 1.1 | 2x14 | DFIN & DMID - Questionable |
| 7-29 | 89.8 | 0.087 | 0.4 | 0.01 | 1.1 | 2x14 | |
| 7-29 | 89.8 | 0.4 | 0.4 | 0.005 | 1.1 | 2x14 | Artificial K |
| 7-29 | 89.8 | 0.08 | 0.4 | 0.001 | 0.01 | 4x27 | |
| 8-3 | 89.8 | 0.08 | 0.4 | 0.001 | 1.1 | 4x27 | |
| 8-6 | 89.8 | 0.087 | 0.4 | 0.0005 | 1.1 | 2x14 | With Convection |
| 8-12 | 89.8 | 0.087 | 0.5 | 0.0001 | 0.5 | 4x27 | With Convection |

**230-8**

| Date 1971 | $T_{melt}$ °F | K Btu/hr-ft-F | $C_p$ Btu/lbmF | $\Delta t$ hr | $t_{max}$ hr | MxN | Remarks |
|---|---|---|---|---|---|---|---|
| 7-29 | 89.8 | 0.087 | 0.4 | 0.01 | 4.6 | 2x14 | |

**230-42**

| Date 1971 | $T_{melt}$ °F | K Btu/hr-ft-F | $C_p$ Btu/lbmF | $\Delta t$ hr | $t_{max}$ hr | MxN | Remarks |
|---|---|---|---|---|---|---|---|
| 8-13 | 89.8 | 0.087 | 0.5 | 0.0001 | 1.9 | 4x27 | With Convection |

| | | | | | | | FREEZE RUNS |
|---|---|---|---|---|---|---|---|

**230-15**

| Date 1971 | $T_{melt}$ °F | K Btu/hr-ft-F | $C_p$ Btu/lbmF | $\Delta t$ hr | $t_{max}$ hr | MxN | Remarks |
|---|---|---|---|---|---|---|---|
| 8-3 | 89.8 | 0.087 | 0.4 | 0.005 | 1.9 | 2x14 | |
| 8-4 | 89.8 | 0.08 | 0.4 | 0.001 | 0.3 | 4x27 | Error in DMID |
| 8-5 | 89.8 | 0.087 | 0.4 | 0.005 | 1.9 | 2x14 | Modified DFIN & DMID |
| 8-5 | 89.8 | 0.08 | 0.4 | 0.001 | 0.3 | 4x27 | |
| 8-10 | 89.8 | 0.08 | 0.4 | 0.001 | 1.9 | 4x27 | DFIN Questionable at large t |
| 8-16 | 89.8 | 0.087 | 0.5 | 0.01 | 1.9 | 2x14 | |

**230-7**

| Date 1971 | $T_{melt}$ °F | K Btu/hr-ft-F | $C_p$ Btu/lbmF | $\Delta t$ hr | $t_{max}$ hr | MxN | Remarks |
|---|---|---|---|---|---|---|---|
| 8-11 | 89.8 | 0.08 | 0.4 | 0.001 | 1.6 | 4x27 | DFIN Questionable at large t |

## B.4. COMPUTER PROGRAM FOR SOLIDIFICATION

```
C       TEST 230-15 FREEZE TEST 3/4 INCH CELL
        DIMENSION RV(5,31), RH(5,31), C(5,31), QS(5,31), T1(5
       1,31)
        DIMENSION T2(5,31), F(5,31), QRAT(5,31), T3(1,31),QRA2
       1(5,31)
        DIMENSION TM1(25), TM2(25), TM3(25), TM4(25), TIM(25)
        DIMENSION VR(5,31), HR(5,31)
C COMPUTATIONAL PARAMETERS
        N=27
        M=4
        AM=4
        MM=4+1
        NN=N+2
        NJ=N+3
        NI=N+4
        NO=23
        NOP=22
        TAU=1.5
        KCOUNT=1
        MCOUNT=1
        MFIN=500
        EPS=1.E-06
        KCHK=1000
        JOE=1
        DT=0.00005
        TAU2=(10.*DT)+(DT/3.)
        AF=40.
        UN=1.0-EPS
C PHYSICAL PROPERTIES
        TAMB=80.
        TIN=100.
        HTOP=1.E-08
        HBOT=5.
        G=(32.174*3600.*3600.)
C       WAX
        DEN=47.2
        TK=0.087
        CP=0.5
        TTR=73.04
        HTR=22.108
        TMELT=89.8
        HMELT=73.357
        TREF=50.
        BETA=0.00045
        VIS=14.3
        CL=CP
        TKL=TK
C       BOTTOM PLATE DENOTED BY 1
        DEN1=171.
        TK1=93.
        CP1=0.22
```

```
C    FIN DENOTED BY 2
     DEN2=171.
     TK2=93.
     CP2=0.22
C    TOP PLATE DENOTED BY 3
     DEN3=72.5
     TK3=0.09
     CP3=0.33
C GEOMETRY PARAMETERS
     W=0.75/12.0
     H=2.625/12.0
     B=5.0/12.0
     S=W/(2.*AM)
     S1=0.032/12.0
     S2=0.008/12.0
     S3=0.25/12.0
     F2JM=1.0/(32.0*S*12.0)
C    VERTICAL RESISTANCES
     RV(1,2)=(S1/(TK1*S2*B))+(2./(HBOT*S2*B))
     DO 10 I=2,MM
  10 RV(I,2)=(S1/(2.*TK1*S*B))+(1./(HBOT*S*B))
     RV(1,3)=(S/(TK2*S2*B))+(S1/(TK1*S2*B))
     DO 20 I=2,MM
  20 RV(I,3)=(1./(2.*TK*B))+(S1/(2.*TK1*S*B))
     DO 30 J=4,NN
  30 RV(1,J)=((2.*S)/(TK2*S2*B))
     DO 40 J=4,NN
     DO 40 I=2,MM
  40 RV(I,J)=(1./(TK*B))
     RV(1,N+3)=(S3/(TK3*S2*B))+(S/(TK2*S2*B))
     DO 50 I=2,MM
     RV(I,N+4) = (S3/(2.*TK3*S*B)) + (1./(HTOP*S*B))
  50 RV(I,N+3)=(S3/(2.*TK3*S*B))+(1./(2.*TK*B))
     RV(1,N+4)=(S3/(TK3*S2*B))+(2./(HTOP*S2*B))
     RV(2,N+4)=(S3/(2.*TK3*B*(S+(S2/2.))))+(1./(HTOP*B*(S+
    1(S2/2.))))
C    HORIZONTAL RESISTANCES
     DO 70 I=2,MM
     RH(I,2) = (S/(TK1*S1*B))
  70 RH(I,N+3)=(S/(TK3*S3*B))
     DO 80 J=3,NN
     DO 80 I=2,MM
  80 RH(I,J) = (1./(TK*B))
     DO 90 J=3,NN
  90 RH(2,J)= (S2/(2.*TK2*S*B)) + (1./(2.*TK*B))
     RH(2,2)=((S2+S)/(2.*TK1*S1*B))
     RH(2,N+3)=((S2+S)/(2.*TK3*S3*B))
     RH(2,N+3)=RH(2,N+3)+RV(1,N+3)
C NODAL CAPACITANCES
     C(1,2)=((DEN1*S1*S2*B*CP1)/2.)
     DO 110 I=2,MM
```

```
110 C(I,2)=(DEN1*S1*S*B*CP1)
    DO 120 J=3,NN
120 C(1,J)=((DEN2*S2*S*B*CP2)/2.)
    C(1,N+3)=((DEN3*S2*S3*B*CP3)/2.)
    DO 130 I=2,MM
130 C(I,N+3)=(DEN3*S3*S*B*CP3)
    C(2,N+3)=(S3*B*(S+(S2/2.))*DEN3*CP3)
    DO 140 J=3,NN
    DO 140 I=2,MM
140 C(I,J)=(DEN*(S**2)*B*CP)
    Q1 = (C(2,3)*(TTR-TREF))
    Q2=Q1+((DEN*(S**2)*B*HTR))
    Q3 = Q2 + ((C(2,3))*(TMELT-TTR))
    Q4=Q3+((DEN*(S**2)*B*HMELT))
C INITIALIZATION OF PERTINENT QUANTITIES
    TIME=0.0
    QWAX=0.0
    QBW=0.0
    QSW=0.0
    QTW=0.0
    QTOP=0.0
    QFTR=0.0
    QTTR=0.0
    V1=0.0
    V2=0.0
    DMO=0.0
    DO 150 J=2,NJ
    DO 150 I=1,MM
150 T1(I,J)=TIN
    IF(TIN.LT.TTR)QSIN=(C(2,3)*(TIN-TREF))
    IF(TIN.GT.TTR.AND.TIN.LT.TMELT) QSIN=Q2+(C(2,3)*(TIN
   1-TTR))
    IF(TIN.GT.TMELT)QSIN=Q4+((C(2,3))*(TIN-TMELT))
    DO 160 I=1,MM
160 T1(I,N+4)=TAMB
    DO 170 J=3,NN
    DO 170 I=2,MM
170 QS(I,J)=QSIN
    DO 199 J=2,NI
    DO 199 I=1,MM
    F(I,J)=0.0
199 QRAT(I,J)=0.0
    READ(5,11) (TM1(I), I=1,ND)
    READ(5,11) (TM2(I), I=1,ND)
    READ(5,11) (TM3(I), I=1,ND)
    READ(5,11) (TM4(I), I=1,ND)
    READ(5,11) (TIM(I), I=1,ND)
 11 FORMAT(8F10.0)
    DO 910 KTC=1, ND
910 TIM(KTC)=TIM(KTC)/3600.
    WRITE(6,22) TIME,W,H,N,M
```

```
   22 FORMAT(1X,5HTIME=,E15.8,10X,2HW=,E15.8,10X,2HH=,E15.8
     1,10X,2HN=,I2,15X,2HM=,I2)
      WRITE(6,33)G1,G2,G3,G4
   33 FORMAT(1X,3HQ1=,E15.8,10X,3HQ2=,E15.8,10X,3HQ3=,E15.8
     1,10X,3HQ4=,E15.8)
      WRITE(6,44)
   44 FORMAT(2X,4HI   J,5X,19HVERTICAL RESISTANCE,6X
     1,21HHORIZONTAL RESISTANCE,6X,17HNODAL CAPACITANCE,6X
     2,11HTEMPERATURE,5X,7HQS(I,J))
      DO 200 J=2,NI
      DO 200 I=1,MM
      IF(J.EQ.N+4) GO TO 1
      GO TO 2
    1 QS(I,J)=0.0
      RH(I,J)=1.E08
      C(I,J)=0.0
    2 IF(I.EQ.1) RH(I,J)=1.E08
      IF(J.EQ.2.OR.J.EQ.N+3) QS(I,J)=0.0
      IF(I.EQ.1) QS(I,J)=0.0
      WRITE(6,55)I,J,RV(I,J),RH(I,J),C(I,J),T1(I,J),QS(I,J)
   55 FORMAT(1X,I2,1X,I2,5X,E15.8,10X,E15.8,10X,E15.8,6X
     1,E15.8,4X,E15.8)
  200 CONTINUE
      DO 400 J=3,NJ
      DO 400 I=2,MM
      VR(I,J)=RV(I,J)
  400 HR(I,J)=RH(I,J)
      DO 889 J=3,NN
  889 T3(1,J)=T1(1,J)
C COMPUTATION SECTION    COMPUTATION SECTION COMPUTATION
C      SECTION
    3 TIME=TIME+DT
      DO 210 J=3,NJ
      QRAT(1,J)=((T1(2,J)-T1(1,J))/RH(2,J))+((T1(1,J-1)-T1(1
     1,J))/RV(1,J))+((T1(1,J+1)-T1(1,J))/RV(1,J+1))
      QRAT(MM,J)=((T1(M,J)-T1(MM,J))/RH(MM,J))+((T1(MM,J-1)
     1-T1(MM,J))/RV(MM,J))+((T1(MM,J+1)-T1(MM,J))/RV(MM,J
     2+1))
  210 CONTINUE
      IF(M.EQ.1)GO TO 212
      DO 211 J=3,NJ
      DO 211 I=2,M
      QRAT(I,J)=((T1(I-1,J)-T1(I,J))/RH(I,J))+((T1(I+1,J)-T1
     1(I,J))/RH(I+1,J))+((T1(I,J-1)-T1(I,J))/RV(I,J))+((T1(I
     2,J+1)-T1(I,J))/RV(I,J+1))
  211 CONTINUE
  212 DO 220 J=3,NJ
      DO 220 I=1,MM
  220 QS(I,J)=QS(I,J)+(QRAT(I,J)*DT)
      DO 240 I=2,MM
  240 T2(I,N+3)=T1(I,N+3)+((QRAT(I,N+3)*DT)/C(I,N+3))
```

```
      T2(1,N+3)=T2(2,N+3)
      DO 250 J=3,NN
      DO 250 I=2,MM
      IF(QS(I,J).LT.Q1) T2(I,J)=TREF+(QS(I,J)/C(I,J))
      IF(QS(I,J).GE.Q1.AND.QS(I,J).LE.Q2) T2(I,J)=TTR
      IF(QS(I,J).GT.Q2.AND.QS(I,J).LT.Q3) T2(I,J)=TTR+((QS(I
     1,J)-Q2)/C(I,J))
      IF(QS(I,J).GE.Q3.AND.QS(I,J).LE.Q4) T2(I,J)=TMELT
C     WHEN GOING FROM MELT TO FREEZE OR VICE-VERSA CHANGE THE
C          FOLLOWING CA
      IF(QS(I,J).GT.Q3.AND.QS(I,J).LT.Q4) F(I,J)=(Q4-QS(I
     1,J))/(DEN*(S**2)*3*HMELT)
      IF(QS(I,J).GE.Q4) F(I,J)=0.0
      IF(QS(I,J).GT.Q4) T2(I,J)=TMELT+((QS(I,J)-Q4)/C(I,J))
C     WHEN GOING FROM MELT TO FREEZE OR VICE-VERSA CHANGE THE
C          FOLLOWING CA
      IF(QS(I,J).LE.Q3) F(I,J)=1.0
  250 CONTINUE
C SPECIFICATION AND/OR DETERMINATION OF FIN TEMPERATURES
C          THE FOLLOWING DO LOOP ASSUMES FIN TEMPERATURES
C        FOR ITERATION
      DO 255 J=3,NN
  255 T2(1,J)=T3(1,J)
      DO 260 L=1,NDP
      IF(TIME.GE.TIM(L).AND.TIME.LE.TIM(L+1)) GO TO 4
  260 CONTINUE
    4 FAC=(TIME-TIM(L))/(TIM(L+1)-TIM(L))
      T2(1,2)=TM1(L)+((TM1(L+1)-TM1(L))*FAC)
      T2(1,8)=TM2(L)+((TM2(L+1)-TM2(L))*FAC)
      T2(1,15)=TM3(L)+((TM3(L+1)-TM3(L))*FAC)
      T2(1,21)=TM4(L)+((TM4(L+1)-TM4(L))*FAC)
      DO 270 I=1,MM
  270 T2(I,2)=T2(1,2)
C UNSPECIFIED FIN TEMPERATURES DETERMINED BY STEADY STATE
C        EQUATIONS
  256 MCOUNT=MCOUNT+1
      DO 280 J=3,NN
      T3(1,J)=T2(1,J)
      IF(J.EQ.8.OR.J.EQ.15) GO TO 5
      IF(J.EQ.21) GO TO 5
      T2(1,J)=((T2(1,J-1)/RV(1,J))+(T2(2,J)/RH(2,J))+(T2(1,J
     1+1)/RV(1,J+1)))/((1./RV(1,J))+(1./RH(2,J))+(1./RV(1,J
     2+1)))
    5 CONTINUE
  280 CONTINUE
      IF(MCOUNT.GT.MFIN) GO TO 8
      DO 281 J=3,NN
      DIF=T2(1,J)-T3(1,J)
      IF(ABS(DIF).GT.EPS) GO TO 256
  281 CONTINUE
      IF(JOE.EQ.2) GO TO 285
```

```
      JOE=JOE+1
      DO 888 J=3,NJ
      DO 888 I=1,MM
  888 QS(I,J)=QS(I,J)-(QRAT(I,J)*DT)
      DO 282 J=3,NJ
      QRA2(1,J)=((T2(2,J)-T2(1,J))/RH(2,J))+((T2(1,J-1)-T2(1
     1,J))/RV(1,J))+((T2(1,J+1)-T2(1,J))/RV(1,J+1))
      QRA2(MM,J)=((T2(M,J)-T2(MM,J))/RH(MM,J))+((T2(MM,J-1)
     1-T2(MM,J))/RV(MM,J))+((T2(MM,J+1)-T2(MM,J))/RV(MM,J
     2+1))
  282 CONTINUE
      IF(M.EQ.1)GO TO 283
      DO 283 J=3,NJ
      DO 283 I=2,M
      QRA2(I,J)=((T2(I-1,J)-T2(I,J))/RH(I,J))+((T2(I+1,J)-T2
     1(I,J))/RH(I+1,J))+((T2(I,J-1)-T2(I,J))/RV(I,J))+((T2(I
     2,J+1)-T2(I,J))/RV(I,J+1))
  283 CONTINUE
      DO 284 J=3,NJ
      DO 284 I=1,MM
  284 QRAT(I,J)=(QRAT(I,J)+QRA2(I,J))/2.0
      GO TO 212
  285 MCOUNT=1
      DO 401 J=3,NJ
      DO 401 I=2,MM
      IF(F(I,J).GT.EPS.AND.F(I,J).LT.UN) GO TO 402
      IF(F(I,J).GT.UN) GO TO 403
      GO TO 401
  403 RV(I,J)=VR(I,J)
      RH(I,J)=HR(I,J)
      GO TO 401
  402 RV(I,J)=VR(I,J)/AF
      RH(I,J)=HR(I,J)/AF
      RV(I,J+1)=VR(I,J+1)/AF
      RH(I+1,J)=HR(I+1,J)/AF
  401 CONTINUE
      DO 286 I=1,MM
  286 QRAT(I,2)=((T2(I,2)-T1(I,2))*C(I,2)/DT)
      DO 287 I=1,MM
  287 QS(I,2)=QS(I,2)+(C(I,2)*(T2(I,2)-T1(I,2)))
      DO 290 I=2,MM
      QBW=(T2(I,2)-T2(I,3))/RV(I,3)+QBW
  290 QTW=(T2(I,N+3)-T2(I,N+2))/RV(I,N+3)+QTW
      QBT=QBW+((T2(1,2)-T2(1,3))/RV(1,3))
      DO 300 J=3,NN
  300 QSW=QSW+((T2(1,J)-T2(2,J))/RH(2,J))
      DO 310 I=1,MM
  310 QTOP=((T2(I,N+3)-TAMB)/RV(I,N+4))+QTOP
      DO 311 J=3,NN
  311 QFTR=QFTR+QRAT(1,J)
      DO 312 I=1,MM
```

```
312 QTTR=QTTR+QRAT(I,NJ)
    QWAX=(QBW+QTW+QSW)*DT+(QWAX)
    RATIO=QSW/QBW
    ERROR=((QBT-(QBW+QSW+QTW+QTOP+QFTR+QTTR))*100.0)/QBT
    DO 930 J=3,NN
    DO 930 I=2,MM
    V2=V2+(F(I,J)*(S**2)*B)
930 CONTINUE
    DAVG=((2.0*V2)/(W*B))*12.0
    QMELT=((V2-V1)*DEN*HMELT)/DT
    QFREZ=QMELT
    V1=V2
    V2=0.0
    IF(KCOUNT.EQ.KCHK) GO TO 6
    KCOUNT=KCOUNT+1
    GO TO 7
  6 WRITE(6,66) TIME, QWAX, ERROR
 66 FORMAT(1X,5HTIME=,E15.8,10X,5HQWAX=,E15.8,10X,6HERROR=
   1,E15.8)
    DO 313 J=3,NN
    AJ=J-3
    BJ=J-2
    IF(F(2,J).GT.F2JM) DFLO=(BJ*S*12.0)
    DFIN=(AJ*S*12.0)
    IF(F(2,J).LT.EPS) GO TO 314
313 CONTINUE
314 DO 315 J=3,NN
    AJ=J-3
    IF(F(MM,J).LT.1.0) DMID=((AJ*S)+(F(MM,J)*S))*12.0
    IF(F(MM,J).LT.1.0) GO TO 316
315 CONTINUE
316 WRITE(6,67) DFIN, DFLO, DAVG, DMID
 67 FORMAT(1X,5HDFIN=,E15.8,10X,5HDFLO=,E15.8,10X,5HDAVG=
   1,E15.8,10X,5HDMID=,E15.8)
    DDOT=(DMID-DMO)/DT
    DMO=DMID
    WRITE(6,69) QFREZ, DDOT
 69 FORMAT(1X,6HQFREZ=,E15.8,10X,5HDDOT=,E15.8)
    WRITE(6,77) QBW, QSW, QTW, QBT, RATIO
 77 FORMAT(1X,4HQBW=,E15.8,3X,4HQSW=,E15.8,3X,4HQTW=,E15.8
   1,3X,4HQBT=,E15.8,3X,6HRATIO=,E15.8)
    WRITE(6,88)
 88 FORMAT(2X,1HI,2X,1HJ,10X,11HTEMPERATURE,10X,15HFRACTIO
   1N MELTED,10X,11HENERGY RATE,10X,13HENERGY STORED)
    DO 320 J=2,NJ
    DO 320 I=1,MM
    WRITE(6,99)I,J,T2(I,J),F(I,J),QRAT(I,J),QS(I,J)
 99 FORMAT(1X,I2,1X,I2,8X,E15.8,8X,E15.8,8X,E15.8,8X
   1,E15.8)
320 CONTINUE
    KCOUNT=1
```

```
  7 QBW=0.0
    QSW=0.0
    QTW=0.0
    QTOP=0.0
    QTTR=0.0
    QFTR=0.0
    DO 330 J=2,NJ
    DO 330 I=1,MM
330 T1(I,J)=T2(I,J)
    JOE=1
    IF(TIME.LT.TAU) GO TO 3
  8 WRITE(6,111) MCOUNT
111 FORMAT(1X,I3)
    STOP
    END
```

## APPENDIX C

## NOMENCLATURE

A      Area

ADI      Alternating direction implicit numerical method

Bi      Biot modulus $= \dfrac{hx}{k}$

C(I,J)      Thermal capacitance of node (I,J)

$C_p$      Heat capacity

GH      Horizontal Thermal Conductance

GV      Vertical Thermal Conductance

g      Acceleration of gravity

H      Height of PCM in Cell (Figure 40)

h      Convective heat transfer coefficient

$h_f$      Latent heat of fusion

I      Designation of nodal location (See Figure 40)

J      Designation of nodal location (See Figure 40)

k      Thermal conductivity

L      Distance between bottom surface of cell and liquid-solid interface at center of cell

M      Number of horizontal nodes In PCM (Figure 40)

N      Number of vertical nodes in PCM (Figure 40)

Nu      Nusselt number $= \dfrac{hx}{k_f}$

PCM      Phase change material

$\dot{q}$      Heat transfer rate

$\dot{q}''$      Heat transfer rate per unit area

Ra      Rayleigh number $= \dfrac{g\beta x^3 \Delta T}{\nu \alpha}$

| | |
|---|---|
| RH | Horizontal thermal resistance |
| RV | Vertical thermal resistance |
| S | Nodal spacing PCM |
| $S_1$ | Thickness of bottom plate |
| $S_2$ | Thickness of fin |
| $S_3$ | Thickness of top plate |
| T | Temperature |
| t | time |
| W | Width of PCM in Cell |
| x | Significant length |

GREEK SYMBOLS

| | |
|---|---|
| $\alpha$ | Thermal diffusivity $= \dfrac{k}{\rho c_p}$ |
| $\Delta$ | Denotes a finite increment |
| $\mu$ | Dynamic viscosity |
| $\nu$ | Kinematic viscosity |
| $\rho$ | Density |

SUBSCRIPTS

| | |
|---|---|
| f | fusion value |
| g | Glass |
| s | Surface |

SUPERSCRIPT

| | |
|---|---|
| ' | Denotes calculated value at time $t + \Delta t$ |

AN UNSOLICITED PROPOSAL FOR RESEARCH

on

A STUDY OF THE HEAT TRANSFER

CHARACTERISTICS OF A PCM THERMAL CAPACITOR

by
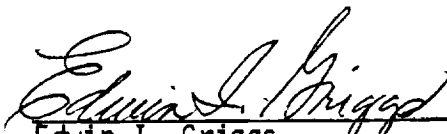
Edwin I. Griggs
Department of Mechanical Engineering
Tennessee Technological University
Cookeville, Tennessee 38501

Submitted to
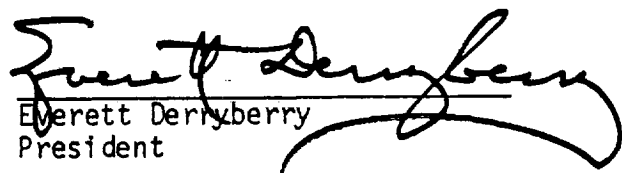
September 1971

ENDORSEMENTS:

Edwin I. Griggs
Principal Investigator

Leighton E. Sissom
Chairman, Department of
Mechanical Engineering

James Seay Brown
Dean, College of Engineering

Everett Derryberry
President

PROPOSED RESEARCH:

A Study of the Heat Transfer Characteristics of a
PCM Thermal Capacitor

INSTITUTION:

Tennessee Technological University
Cookeville, Tennessee 38501

INSTITUTIONAL REPRESENTATIVE:

Dr. Nofflet Williams
Director of Institutional Research
(615) 528-3281

PRINCIPAL INVESTIGATOR:

Dr. Edwin I. Griggs
Department of Mechanical Engineering
(615) 528-3357

TOTAL REQUESTED FUNDING:

$5,000

PROPOSED STARTING DATE:

As Soon As Possible

DURATION OF PROPOSED RESEARCH:

Four Academic Quarters

## ABSTRACT

There is an increasing use in the space program of phase-change materials for energy storage and thermal control. In the design and testing of thermal capacitors employing a phase-change material (PCM), there exists a need to understand the influence of the different modes of heat transfer on the overall capacitor performance.

In this unsolicited proposal, support in the amount of $5,000 is requested for an extension of the study initiated by the proposer during his participation in the 1971 NASA/ASEE Summer Faculty Fellowship Research Program at MSFC. The work is to be performed at the home institution of the proposer in coordination with an appropriate MSFC monitor.

The objective of the proposed research is to study the thermal characteristics of a PCM capacitor with particular emphasis on seeking practical design correlations. A selected member(s) of the n-paraffin family will serve as the PCM for the investigation which will encompass both analytical and experimental efforts. A concern of the study will be the influence of natural convection on the performance of a finned PCM capacitor.

The investigation is a useful step towards understanding the role of gravity on PCM performance and should contribute to interpretation of ground test data for flight applications. This should be helpful in the Skylab program where flight capacitors will be used to augment the space radiators in the primary cluster coolant loop of the airlock module and in the habitability support system coolant loop on the orbiting workshop. In addition the results should also be beneficial in the extension of the PCM concept to other applications.

## INTRODUCTION

When unit mass of a substance undergoes a change of phase, an amount of energy equal to its latent beat is absorbed or rejected at constant temperature. During this phase change, the effective thermal capacitance is infinite. Utilization of this principle for thermal control is attractive in situations involving any of the following requirements:

- Conservation of energy for later use.
- Increased thermal capacitance.
- Constant temperature control.
- Dampening of temperature oscillations.
- Time delay for a particular temperature excursion of intermittently or one-time operated components.

Each of the above requirements occurs in various aspects of space flight, and, since improved reliability is associated with the passive nature of PCM thermal control, the technique has become increasingly attractive.

Fusible materials have received considerable attention for use in PCM thermal control. While the heat of vaporization is larger than the heat of fusion, the large disparity in density between a liquid and its vapor presents containment and/or venting problems. Consequently, the solid-liquid transition appears to be preferable in many cases. Members of the n-paraffin family are presently being used and are considered to be the leading choices as a PCM for spacecraft oriented thermal control.

Typical PCM thermal capacitor designs consist of a container filled with the PCM. However, as the size of the PCM occupied region increases,

1

the less the entire unit will respond isothermally. Consequently, in the design of such units, it has been the practice to employ some type of metallic filler to improve the effective thermal diffusivity. A schematic of a possible capacitor cross-section is given in Figure 1. A more complex arrangement exists when orderly fins are replaced by a honeycomb type material. This scheme offers a challenging problem in optimization since it is desired to design a package which effectively exploits the advantages of using a PCM. A basic need is to understand the mechanisms of heat transfer in such arrangements.

The purpose of this proposed investigation is to conduct research on the heat transfer performance of a PCM capacitor employing a finned arrangement such as that shown in Figure 1 and which will seek correlations useful in capacitor design. The study is related to space flight applications of thermal capacitors which include uses on the Lunar Roving Vehicle and on Skylab in both the airlock module and the orbiting workshop. A tabulation of some of these applications is given in Appendix B.
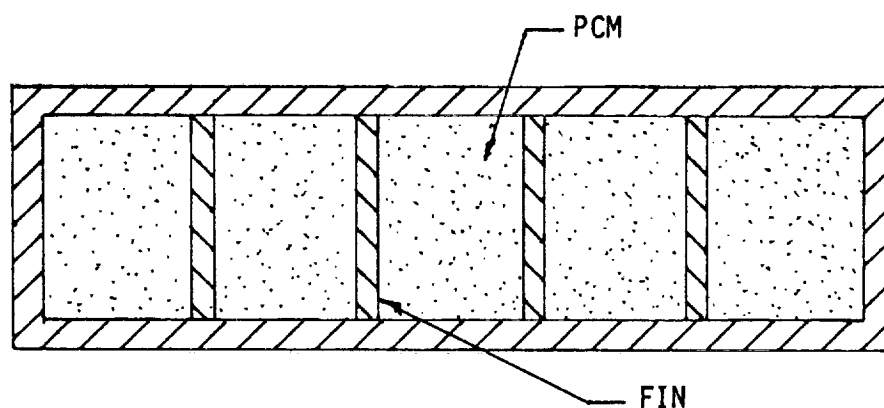
Figure 1. Thermal Capacitor Schematic

BACKGROUND FOR PROPOSED STUDY

During the summer of 1971, the proposer participated in the NASA/ASEE Faculty Fellowship Program. This provided him the opportunity to become acquainted with various applications of PCM thermal capacitors in space flight and some of the problems related to their design. A brief description of the results of his study in the area during this period is included in the Appendix.

The proposer hopes to return to MSFC during the summer of 1972 as a second-year NASA/ASEE Faculty Fellow and continue in the area. It is also his desire to pursue an active involvement in the study at his home institution throughout the academic year. The intent of this proposal is to seek support which would help make such participation possible.

PROPOSED STUDY

The proposed study will be a continuation of the study initiated by the proposer during the summer of 1971. The intent is to further investigate the heat transfer characteristics associated with the design and use of PCM thermal capacitors. The investigation will consist of three basic parts which are as follows:

(1) Literature Review - A continuing search of current periodicals and journals will be made for material related to heat transfer mechanisms and other characteristics associated with the solid-liquid phase change.

(2) Analytical Studies - Analytical (numerical) efforts will be devoted to the prediction of heat transfer in typical capacitor cells in an attempt to gain insight into useful design correlations.

(3) Experimental - Some basic experimental measurements of temperatures and interfacial motion during the phase change process will be conducted to provide additional data as well as first-hand insight into the traits.

More specific details of the above efforts will be coordinated with the MSFC monitor to provide pursuit along avenues of maximum mutual interest and benefit. In support of the study, MSFC will be expected to provide access to certain existing experimental data, certain PCM samples, and an existing test capacitor where such access is convenient and in the best interest of the work as agreed upon by the proposer and MSFC monitor.

It is felt that a significant effort can be devoted to this proposed work by the proposer with the facilities available at his home institution for the proposed funding of $5,000. The involvement would extend through at least four academic quarters.

## FACILITIES FOR RESEARCH

The Mechanical and Electrical Engineering Departments share a three year old, air-conditioned building with 55,000 square feet of floor space. Adequate floor space is available in the laboratories for conducting research in the proposed area. The laboratories are supplied with compressed air, natural gas and water lines. Trenches are provided in the floor for routing special power lines or instrumentation cables. In addition to class rooms and offices, general shop facilities are available. A machine shop and an electronics shop are assigned to Mechanical Engineering and these are staffed by full time technicians who are experienced in the fabrication of experimental research apparatus. (Additional details on available facilities are given in Appendix A.)

TENTATIVE BUDGET

| | | | NASA | TTU |
|---|---|---|---|---|
| 1. | SALARIES AND WAGES | | | |
| | a. | Principal Investigator and Research Assistant(s) | $ 3200 | |
| | b. | Other Personnel (Technician, Secretary, Draftsman, etc.) | 400 | $ 200 |
| | c. | Estimated Employee Benefits | 180 | 20 |
| | | Total Salaries and Wages | $ 3780 | $ 220 |
| 2. | PERMANENT EQUIPMENT | | 0 | 2500 * |
| 3. | EXPENDABLE EQUIPMENT AND SUPPLIES | | 0 | 200 |
| 4. | COMPUTER COSTS (5 hours @ 140/hr) | | 0 | 700 |
| 5. | TRAVEL | | 110 | 0 |
| 6. | PUBLICATION COSTS | | 0 | 150 |
| 7. | ESTIMATED INDIRECT COSTS | | 1110 | 0 |
| | TOTAL ESTIMATED COSTS | | $ 5000 | $ 3770 |

TOTAL FUNDS REQUESTED $5000

*Existing

APPENDICES

A. SUPPORTING FACILITIES

# SUPPORTING FACILITIES

Machine Shop. A well-equipped machine shop staffed by two full-time machinists is located in the building. This shop serves the research laboratory needs of the department. It is capable of handling all but the largest workpieces normally encountered in university research. With suitable arrangements the facilities of the Engineering Science and Chemical Engineering machine shops can provide additional capabilities. The shop services and facilities of the University Physical Plant and the Department of Industrial Technology are also available.

Electronics Shop. An electronics shop staffed by a full-time electronics technician is located in the department. Extensive service instrumentation provides instrument check-out, repair and calibration capabilities for all but the most severely damaged instruments and those requiring very specialized service. Backup capabilities are available from the Electrical Engineering electronics shop which is also staffed by a full-time electronics technician.

Library. The University library maintains a very good collection of textbooks and current journal publications in areas related to the proposed research. Excellent interlibrary loan service supplements back issue holdings of many reference publications. Fast service is primarily the result of the strategic geographical location of excellent sources such as the Oak Ridge Associated Universities Library, the University of Tennessee and the Georgia Institute of Technology.

Faculty. The Mechanical Engineering faculty posses depth in the area of thermal science. Five faculty members in addition to the proposer are actively engaged in thermal science research and education.

Computer Center. The D. W. Mattson Computer Center provides computational services for the entire University. Operation of the center is directed towards serving the needs of students and faculty in their pursuit of education and research and meeting the administrative requirements of the University. Currently installed is an IBM System/360 Model 40 with 131,676 bytes of immediate-access memory; three 2311 disk drive modules, each with seven million bytes of random access memory; one 1403 printer, with maximum print speed of 600 lines per minute; one 2540 card read-punch, with a read speed of 1000 cards per minute and a punch speed of 300 cards per minute. The System/360 computer is equipped with the standard, decimal, and floating-point instruction sets. Operating system (OS) release 14 is now in use, with the following languages being supported: Fortran IV, Cobol, Assembler, and PL/I (limited to the 48 character set).

Other equipment includes: 548 Alphabetic interpreter, 514 Repro-ducing punch, 082 Sorter, 059 Verifier, and seven 029 Keypunches. A Unit Record Room houses most of the keypunches, as well as reference manuals, library program files, control cards, and informative displays, for use by students and faculty.

An XDS Sigma 7 computer is scheduled to replace the IBM 360 Model 40 in September, 1971. In all respects, the Sigma 7 will improve the computational capabilities available.

B.  BRIEF SUMMARY OF BACKGROUND WORK

DURING SUMMER OF 1971

## NOTATION FOR APPENDIX B

| SYMBOL | DEFINITION | UNITS |
|--------|-----------|-------|
| C | Thermal Capacitance | Btu/°F |
| H | Height of PCM in Cell | in |
| I | Nodal Designation Integer (See Fig. B-1) | |
| J | Nodal Designation Integer (See.Fig. B-1) | |
| M | Number of Horizontal Nodes in PCM | |
| N | Number of Vertical Nodes in PCM | |
| q | Heat Transfer Rate | Btu/Hr |
| RH | Horizontal Thermal Resistance | Hr-°F/Btu |
| RV | Vertical Thermal Resistance | Hr-°F/Btu |
| S | Nodal Spacing in PCM | in |
| $S_1$ | Thickness of Bottom Plate | in |
| $S_2$ | Thickness of Fin | in |
| $S_3$ | Thickness of Top Plate | in |
| T | Temperature | °F |
| t | Time | Hr |
| W | Width of PCM in Cell | in |
| ' | Denotes Calculated Value at $t + \Delta t$ | |
| $\Delta$ | Denotes Finite Increment | |

## SPACE FLIGHT APPLICATIONS

To increase system reliability often lessened by the presence of moving parts in active systems, it is desirable to utilize passive systems in spacecraft where possible. Since thermal control with a PCM is passive, it has become a most attractive method for space flight applications.

Many of the thermal problems encountered by spacecraft are well suited to utilization of the PCM concept. The cyclic passing of a satellite from sunlight to darkness is an example where a PCM can be used to absorb excess energy during the heating phase and reject it during the cooling period. Since the phase transition occurs at constand temperature, the PCM-protected component temperature can thereby be maintained more nearly uniform. By exploiting the same principle in conjunction with radiators, a more efficiently designed radiator can be used since it is not necessary to design for peak loads. System components which function only during launch or during short-term missions such as those of the recent Lunar Roving Vehicle are representative of either short-term or one-time operated components which can be thermally protected by using a PCM to delay temperature excursions.

Some specific space flight applications in which a thermal capacitor has been or is planned to be used are listed in Table B-1.

TABLE B-1

Some Specific Space Flight Applications

| Application | Thermal Capacitor | Function |
|---|---|---|
| Pegasus III | Contamination Experiment | To provide a constant temperature reference for a thermocouple. |
| Apollo 15 Lunar Roving Vehicle | 1) DCE | To provide added thermal protection for the drive control electronics (DCE) package. |
| | 2) SPU | To increase thermal capacitance interacting with the signal processing unit (SPU). |
| | 3) LCRU | To increase thermal capacitance interacting with the lunar communications relay (LCRU). |
| Skylab | 1) Airlock | To augment the airlock module space radiator in the primary cluster coolant loop and to reduce temperature fluctuations at the radiator exit. |
| | 2) HHS | To augment the space radiator in the habitability support system coolant loop on the workshop and to dampen coolant temperature fluctuations. |
| | 3) Urine Freeze | To provide low temperature control of urine specimen in order to preserve its biological state for purpose of testing when it is returned to earth. |

LITERATURE REVIEW

Emergence of the concept of using a PCM for thermal energy storage and thermal control is not entirely new. Telkes (1)* has discussed the use of fusible materials in connection with solar house heating. Altman, Ross and Chang (2) have studied application of the heat of fusion for thermal energy storage in solar powered electrical generators. In a feasibility study related to thermal control of spacecraft, Fixler (3) analytically and experimentally investigated the use of a PCM. He reported that the PCM scheme has a definite weight advantage over louvered or force-circulation systems. Veselov, Kalisheva and Telepin (4) reported a study on using phase transition to improve thermostatic control of instruments (gravity meters). Shlosinger and Bentilla (5) and Bentilla, Sterrett and Karre (6) have presented an extensive survey on the characteristics and use of fusible materials for thermal control of spacecraft. Also a very comprehensive investigation into thermal control and energy storage by melting and freezing has been conducted by Grodzka (7), Grodzka and Fan (8) and Grodzka and Hoover (9). These latter references (5-9) contain numerous references pertinent to the field.

A major difficulty in analyzing the heat transfer mechanisms during phase-change processes is prediction of convective effects. Tien and Yen (10) have presented an approximate solution of a melting problem including natural convection. Their study, however, was restricted to a one-dimensional, semi-infinite region for a water-ice system. Boger and Westwater (11) have also studied the influence of buoyancy on the

---

* Underlined numbers in parentheses designate references listed at the end of this appendix.

melting and freezing process of a one-dimensional water-ice system. Golden and Stermole (12) summarized the findings of several phases of a research program in phase-change thermal control technology. One aspect of their study was an analytical and experimental investigation of the role of natural convection in phase-change thermal control devices. In their summary, it was reported that numerical difficulties had prevented any predictions of the convective effects.

Some recent reports have been devoted to the design and study of specific thermal capacitors. Humphries (13) proposed a study to determine a performance estimating technique for thermal capacitors. An investigation including performance predictions and test data correlations of the Skylab airlock module thermal capacitor has recently been presented by Stafford and Grote (14).

## NUMERICAL STUDY

For the study during the summer, extensive experimental data was available from tests on a test capacitor. The test capacitor had a geometry similar to that shown in Figure 1. Fin locations provided PCM cellwidths of 0.25, 0.50 and 0.75 inches. The fins were strips of 0.008 - inch thick aluminum. The bottom plate was 0.032 - inch thick aluminum. The top plate was 0.25 - inch thick plexiglas. The cell height H was about 2.5 inches and its length was 5.0 inches. The utilized PCM was nonadecane. A large amount of data was obtained for both freezing and melting tests. The data consisted of transient temperature measurements at several locations inside the capacitor and film histories of the fusion front motion.

In this numerical study attention was focused on a symmetrical section of a typical cell. The section was subdivided into a network of nodes and a Fortran computer program was written to facilitate numerical heat transfer predictions. The section and nodal arrangement are shown in Figure B-1. There are MXN nodes in the PCM where M and N denote integers. While the computer program was written to apply in general to any cell compatible with the geometry shown in Figure B-1, runs were made using specific data corresponding to the experimental work as described above.

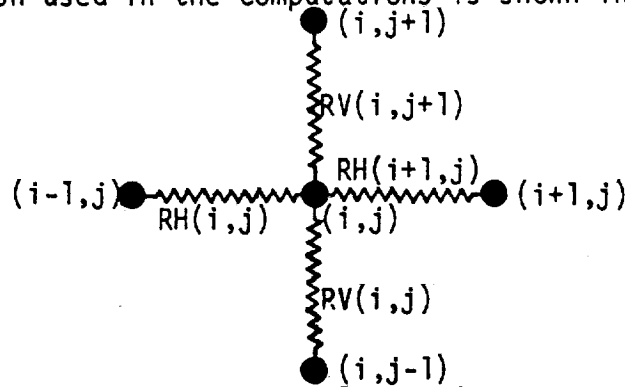The notation used in the computations is shown in Figure B-2



Figure B-2. Nodal Notation

The computational procedure started with specification of initial temperatures for all nodes and calculation of all pertinent parameters. Measured temperatures for the bottom plate and certain nodes along the fin were input as transient boundary conditions. At time t the heat transfer rate to each node was determined by

$$q(i,j) = \frac{T(i-1,j) - T(i,j)}{RH(i,j)} + \frac{T(i+1,j) - T(i,j)}{RH(i+1,j)}$$

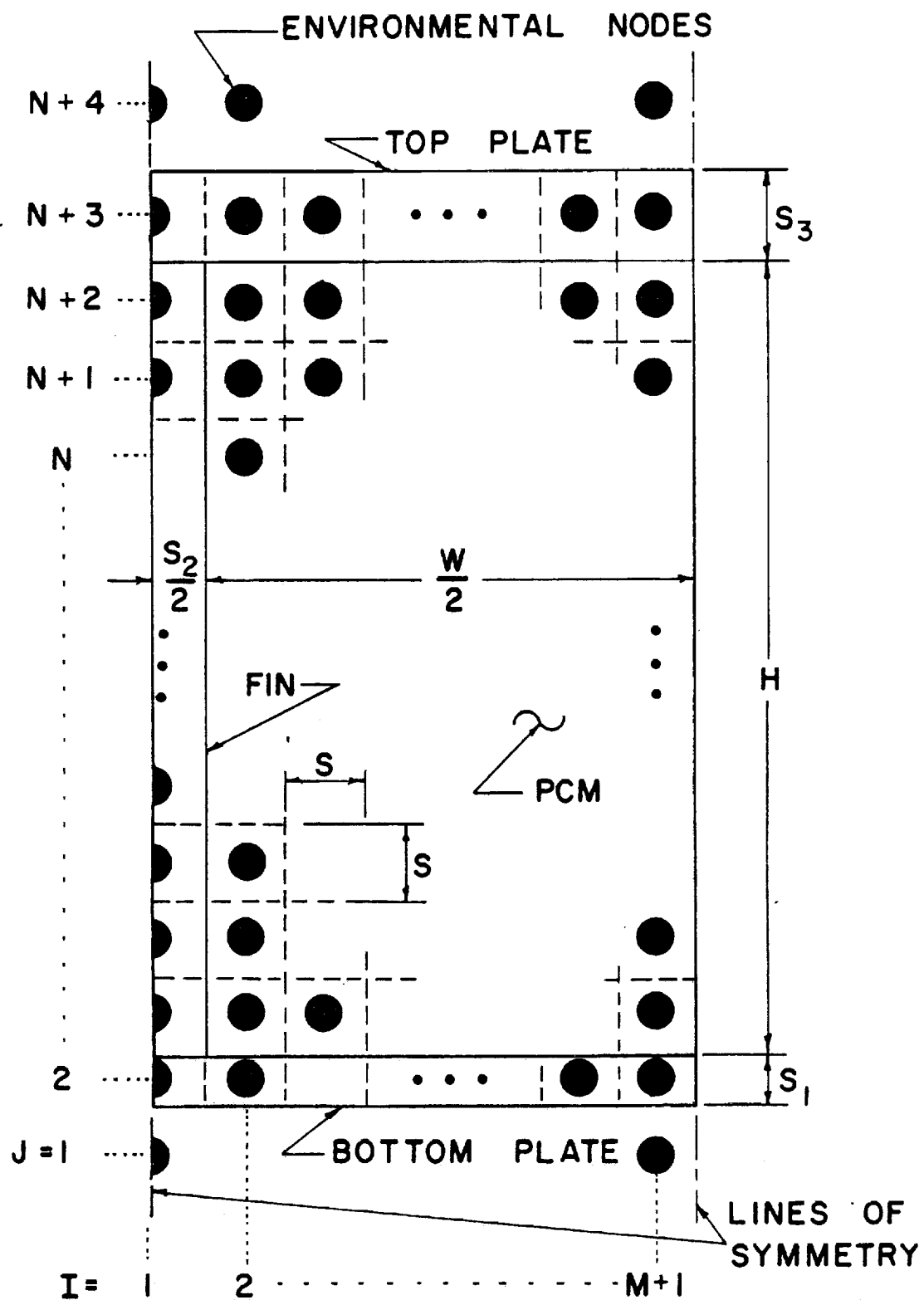$$+ \frac{T(i,j-1) - T(i,j)}{RV(i,j)} + \frac{T(i,j+1) - T(i,j)}{RV(i,j+1)} \tag{1}$$

Figure B-1. Symmetrical Section and Nodal Arrangement

This rate was stored and subsequently used to determine the temperature of the node at time t + Δt by

$$T'(i,j) = T(i,j) + \frac{q(i,j)\Delta t}{C(i,j)} \tag{2}$$

Before proceeding in time the computation was iterated by computing q'(i,j) using equation (1) and the new temperatures found by equation (2). Then the average of q(i,j) and q'(i,j) was used in equation (2) to predict more accurate T'(i,j) values. This procedure was repeated at each time step.

For each node in the PCM, an accumulative record was maintained of the stored energy. When the nodal temperature reached the fusion temperature, it was held constant until sufficient energy had been absorbed or rejected to account for the latent heat of fusion. For each time step during the phase change, a fraction of the node which had changed phase was calculated based on the accumulated energy. The fraction was then used in predicting the location of the fusion front.

Appropriate modifications of equations (1) and (2) were made for nodes located on or near a boundary. The only unique deviation of the above procedure used so far was in connection with determining the unspecified fin temperatures. Since the thermal capacitance of a node on the fin was several orders of magnitude lower than that of a node in the PCM, steady state relations were used to compute the instantaneous unspecified fin temperatures. This can be relaxed at the expense of more computer time. The increase in computer time is a consequence of the small time step demanded by the stability requirement associated with an extremely small capacitance.

In an attempt to include convection in the melting cases, the technique involved computation of a modified or effective thermal con-

ductivity of the liquid. Correlations reported in Reference (15) were used to determine the effective conductivity. It should be mentioned that these relations were correlated for cases involving fixed boundaries. The procedure required keeping track of the liquid and computing a new thermal resistance in the liquid at each time step.

The program facilitated computation of temperatures, heat transfer rates, fusion front location and other related quantities. The program was checked out and run for several cases. A portion of the results for two example cases are given below.

## DISCUSSION OF RESULTS AND CONCLUSIONS

Numerical results included several quantities of interest such as temperatures, heat transfer rates, net rate of phase change and fusion front location. So far, all runs were for a 0.75-inch wide cell. Various parameters were changed to evaluate their influence on the predictions. Node size is a quantity of particular interest in this regard. For presentation here, comparisons are only given between the predicted fusion front location at the center of the cell and the measured value for an example melting case and an example freezing case.

Figure B-3 gives the comparisons for the selected freezing case. In the case of freezing, it was difficult to experimentally identify an interface. The solidification process is characterized by dendritic formations. When observing the film of a freezing run, a dark area appeared and progressed through the liquid. This, however, was later followed by a chalky appearing region. The dramatic difference between measurements corresponding to the edges of these two regions is depicted in Figure B-3. Numerical predictions agree more closely with the edge of the chalky region. It is not necessarily implied here, however, that
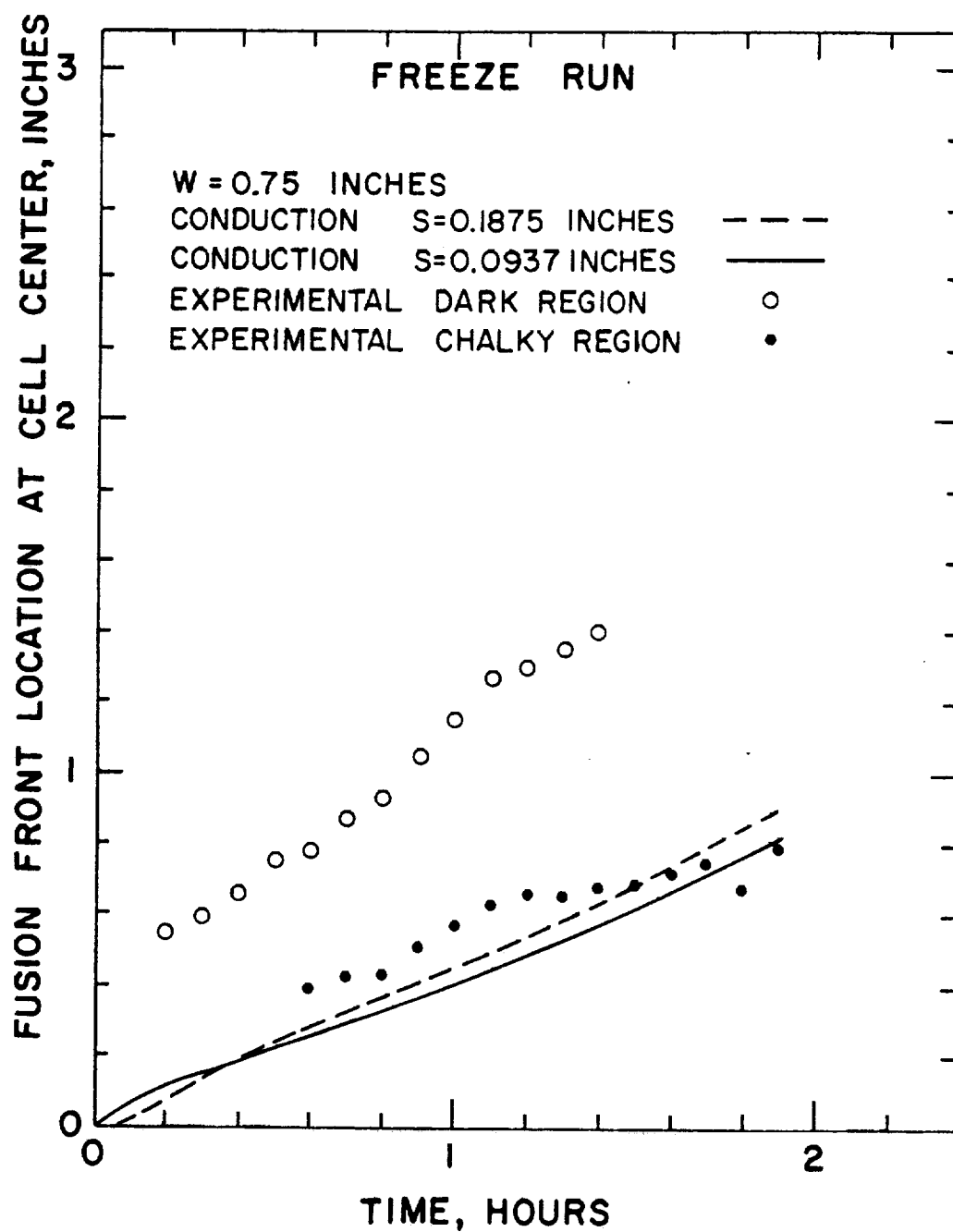
Figure B-3.  Comparison Between Predicted and Measured Fusion Front Location for an Example Freeze Run

the chalky region best represents the interface. Even though the freezing process should be conduction controlled, the presence of the dendritic formation should provide a much larger solid-liquid interfacial area than the planar value employed in the computations. This would cause the predictions to be low. Comparison of the predictions for two different node sizes indicates that the lower node size results in a slightly advanced prediction at early times and somewhat retarded values at larger times. The differences are not large.

Figure B-4 shows the comparisons for the selected melting run. Interfacial definition was quite good in the melting cases. The experimentally measured interfacial velocity was much larger than the conduction controlled prediction. Inclusion of convection through use of an effective liquid conductivity produced much improved agreement. This is particularly interesting since the correlations of Reference (15) which were used were obtained for steady cases involving fixed boundaries. Again, the node size doesn't significantly alter the conduction controlled predictions except during the early stages. The smaller node case predicted faster melting at the start. This is plausible since the time constant associated with a larger node would cause a delay in its response to a changed boundary temperature. The agreement between the trends of the data and those of the predictions when including convection is very promising. The curves appear to differ by a shift in time which may be due to the starting conditions associated with node size as discussed above.

The computer program developed can be used for further data evaluation. Runs should be made for smaller cell widths and the consequences of employing an effective thermal conductivity to account for convection should be explored.
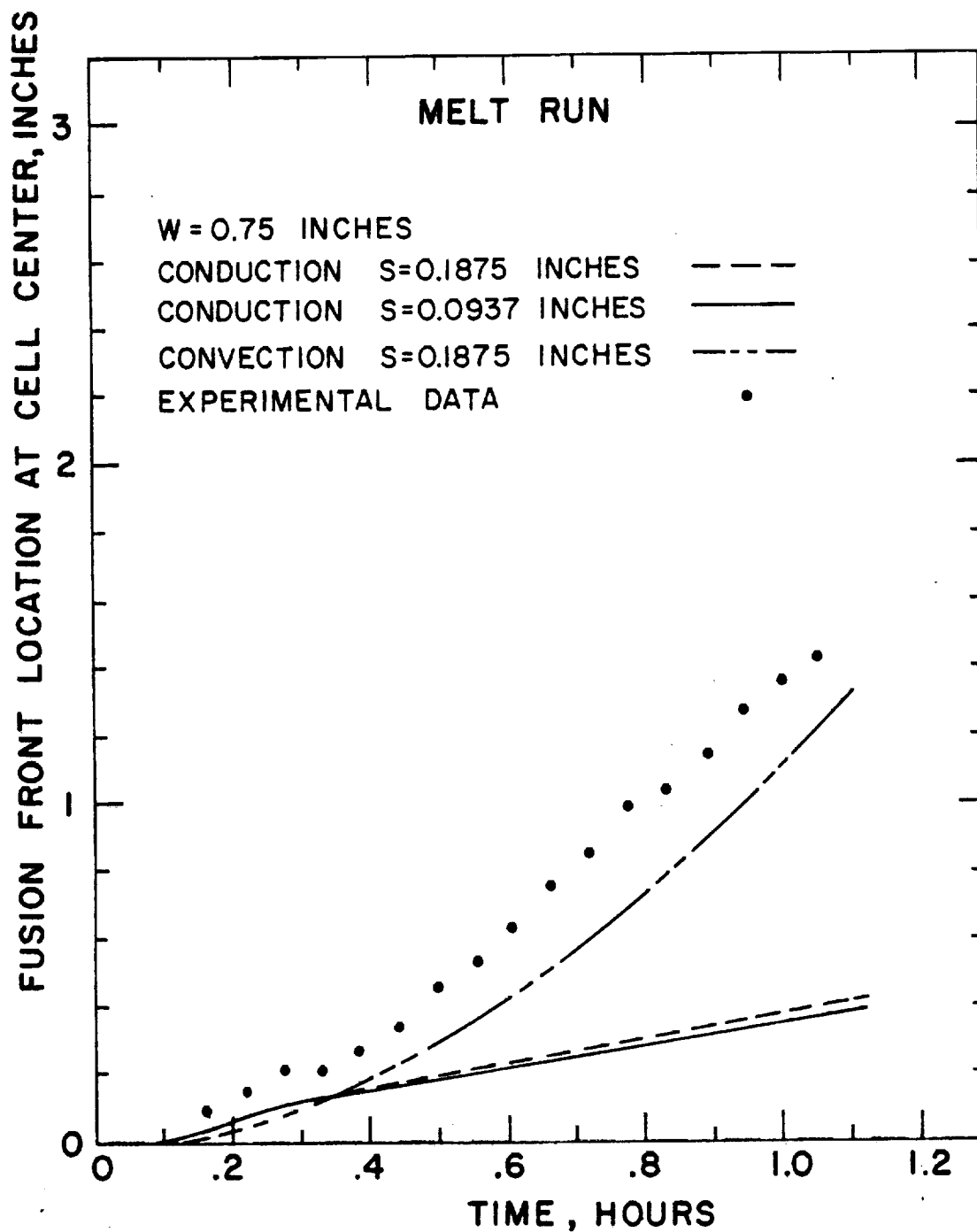
Figure B-4.   Comparison Between Predicted and Measured Fusion
             Front Location for an Example Melt Run

## PROPOSALS FOR FUTURE STUDIES

There are several avenues of future endeavors which would serve to enhance the state-of-the-art of thermal capacitor technology. With regard to an extension of the summer's efforts, the computer program should be used to further evaluate the existing experimental data. Several questions which arose during the course of this work suggest the need for both additional experimental and analytical studies.

Some proposed experimental studies are:

- Further investigate the interfacial characteristics during solidification.

- Conduct a series of melting experiments that permits controlled heating from above and below. This should permit experimental extraction of convective effects.

- Examine the influence of various fin and honeycomb arrangements on overall performance. This should also be incorporated with the previous suggestion.

- Try to experimentally evaluate interfacial tension effects.

- Determine long-term use influence on the constancy of PCM characteristics.

Several fundamental analytical studies are:

- Predict convective currents present during a phase change process. Retrieve an effective thermal conductivity for design purposes. Examine relative time scales of the convective and interfacial motion.

- Study interfacial tension driven currents. Analytically predict patterns and their contribution to energy transfer. Determine whether Marangoni and Raleigh convection compliment or oppose each other.

- Study deterioration effects on long-term PCM usage.

In addition, with increasing concern about energy conservation, thought should be given to novel uses of the PCM concept. The author hopes to pursue his interest in this area at his university.

REFERENCES

1.  Telkes, M., "A Review of Solar House Heating," Heating and
        Ventilating, 46, September 1949, pp. 68-74.

2.  Altman, M., and D. P. Ross and H. Chang, "The Prediction of
        Transient Heat Transfer Performance of Thermal Energy
        Storage Devices," Chemical Engineering Progress Symposium
        Series, Am. Inst. Chem. Engrs., Vol. 61, No. 57, 1965,
        pp. 289-298.

3.  Fixler, S. Z., "Satellite Thermal Control Using Phase-Change
        Materials," J. Spacecraft, Vol. 3, No. 9, September 1966,
        pp. 1362-1368.

4.  Veselov, K. Ye, L. V. Kalisheva and M. L. Telepin, "Using Phase
        Transitions to Improve Thermostatic Control of Instruments,"
        NASA Technical Translation, NASA TT F-467.

5.  Shlosinger, A. P. and E. W. Bentilla, "Thermal Control by Use of
        Fusible Materials," Interim Report, Northrop Corporation,
        NSL65-16, Contract NAS8-11163, 1965.

6.  Bentilla, E. W., K. F. Sterrett and L. E. Karre, "Thermal Control
        by Use of Fusible Materials," Final Report, Northrop Corporation
        NSL65-16-1, Contract NAS8-11163, 1966.

7.  Grodzka, P. G. and C. Fan, "Thermal Control by Freezing and
        Melting," Interim Report on Space Thermal Control Study,
        Lockheed Missiles and Space Company, LMSC/HREC A791342,
        Contract NAS8-21123, March 1968.

8.  Grodzka, P. G., "Space Thermal Control by Freezing and Melting,"
        Second Interim Report on Space Thermal Control Study, Lockheed
        Missiles and Space Company, LMSC/HREC D148619, Contract NAS8-
        21123, May 1969.

9.  Grodzka, P. C. and M. J. Hoover, "Thermal Control and Heat
        Storage by Melting and Freezing," Interim Report on Space
        Thermal Control Development, Lockheed Missiles and Space
        Company, LMSC/HREC D162884, Contract NAS8-25183, March 1971.

10. Tien, C. and Y. C. Yen, "Approximate Solution of a Melting
        Problem with Natural Convection," Chemical Engineering
        Progress Symposium Series, Vol. 62, No. 64, 1966,
        pp. 166-172.

11. Boger, D. V. and J. W. Westwater, "Effect of Buoyancy on the
        Melting and Freezing Process," J. Heat Transfer, February
        1967, pp. 81-89.

12. Golden, J. O. and F. J. Stermole, "Research in Phase Change
        Thermal Control Technology," Total Program Summary Report
        (21 Nov., 1968 - 31 Dec., 1969), NASA Contract NAS8-30511
        for MSFC.

13. Humphries, W. R., "Description of Thermal Capacitance Performance Study," S&E-ASTN-PLA, Marshall Space Flight Center, July 1969.

14. Stafford, J. L. and M. G. Grote, "Thermal Capacitor, Liquid Coolant-to-Phase Change Material Heat Exchanger, for the NASA Skylab I Airlock Module," AIAA Paper No. 71-429, Presented at the 6th AIAA Thermophysics Conference, Tullahoma, Tennessee, April 26-28, 1971.

15. O'Toole, J. L. and P. L. Silveston, "Correlations of Convective Heat Transfer in Confined Horizontal Layers," Chemical Engineering Progress Symposium Series, Vol. 57, No. 32, 1961, pp. 81-86.

C. BIOGRAPHICAL SKETCH

GRIGGS, EDWIN I. - Assistant Professor of Mechanical Engineering, Tennessee
Technological University

| Education: | | |
|---|---|---|
| | Ph.D. (M.E.) - Purdue University | 1970 |
| | M.S.M.E. - Mississippi State University | 1962 |
| | B.S.M.E. - Mississippi State University | 1961 |

Experience: Assistant Professor of Mechanical Engineering,
    Tennessee Technological University, Cookeville,
    Tennessee     1969-Present

NASA-ASEE Summer Faculty Fellow, George C. Marshall
    Space Flight Center, Huntsville, Alabama     1971 Summer

Consulting Assistant (part-time) for Design and
    Manufacturing Corporation, Connersville,
    Indiana (Lafayette, Indiana Research Lab)     1967-1968

Research Assistant, School of Mechanical
    Engineering, Purdue University, Lafayette,
    Indiana     1966-1969

Graduate Instructor, School of Mechanical
    Engineering, Purdue University, Lafayette,
    Indiana     1964-1968

Instructor, Department of Mechanical Engineering,
    Tennessee Technological University, Cookeville,
    Tennessee     1962-1964

Co-Operative Engineering Student with Union
    Carbide at Paducah, Kentucky     1957-1960

Societies: Pi Tau Sigma
    Tau Beta Pi
    Phi Kappa Phi
    Eta Epsilon Sigma
    Sigma Xi
    American Society of Mechanical Engineers
    American Society for Engineering Education
    Tennessee Education Association

Research Interests: Heat and Mass Transfer; Fluid Mechanics--Two Phase
    Systems; Acoustical Effects on Transport Phenomena;
    Effects of Time-Varying Pressures on Two Phase
    Systems

Recent Publications and Reports:

    "Acoustically Augmented Convective Drying," AIChE Sonochemical
    Engineering Symposium, May 17-20, 1970, San Juan, Puerto Rico,
    Paper No. 33h, with G. W. Simmons, A. E. Hribar, and K. R.
    Purdy.

    "Transient Phenomena During Collapse of a Pressurized Vapor
    Film," (with J. L. Carson, R. J. Schoenhals, and E. R. F.
    Winter). Paper Cs2.5. Fourth International Heat Transfer
    Conference, Versailles/Paris, August 31-September 4, 1970.

Recent Publications and Reports:

"Transient Liquid-Vapor Phenomena During Collapse of a
Pressurized Vapor Film," Ph.D. Thesis, Purdue Univeristy,
1970.

"Acoustic Velocities in Two-Phase Mixtures of Some Cryogenic
Fluids," (with E. R. F. Winter and R. J. Schoenhals). Improved
Fluids Dynamics Similarity, Analysis and Verification--Final
Report (Part IV), Submitted to NASA George C. Marshall
Space Flight Center, Huntsville, Alabama, under Contract
Number NAS 8-20222, July, 1968.

"Effects of Longitudinal Vibration on Discharge of Liquids
From Propellant Tanks," (with R. J. Schoenhals and E. R. F.
Winter), Proceedings of the 1967 Heat Transfer and Fluid
Mechanics Institute, Stanford University Press, 1967.

"Measurement of the Specific Heat of Solids at High Tempera-
tures," M. S. Thesis, Mississippi State University, August,
1962.